
STOCHASTIC MULTISCALE MODELING OF POLYCRYSTALLINE MATERIALS

Bin Wen

Presentation for Thesis Defense (B-Exam)

Data: Aug 13, 2012

Materials Process Design and Control Laboratory
Sibley School of Mechanical and Aerospace Engineering
169 Frank H. T. Rhodes Hall
Cornell University
Ithaca, NY 14853-3801
Email: bw336@cornell.edu
URL: <http://mpdc.mae.cornell.edu/>



Report Documentation Page

Form Approved
OMB No. 0704-0188

Public reporting burden for the collection of information is estimated to average 1 hour per response, including the time for reviewing instructions, searching existing data sources, gathering and maintaining the data needed, and completing and reviewing the collection of information. Send comments regarding this burden estimate or any other aspect of this collection of information, including suggestions for reducing this burden, to Washington Headquarters Services, Directorate for Information Operations and Reports, 1215 Jefferson Davis Highway, Suite 1204, Arlington VA 22202-4302. Respondents should be aware that notwithstanding any other provision of law, no person shall be subject to a penalty for failing to comply with a collection of information if it does not display a currently valid OMB control number.

1. REPORT DATE 13 AUG 2012		2. REPORT TYPE		3. DATES COVERED 00-00-2012 to 00-00-2012	
4. TITLE AND SUBTITLE Stochastic Multiscale Modeling of Polycrystalline Materials				5a. CONTRACT NUMBER	
				5b. GRANT NUMBER	
				5c. PROGRAM ELEMENT NUMBER	
6. AUTHOR(S)				5d. PROJECT NUMBER	
				5e. TASK NUMBER	
				5f. WORK UNIT NUMBER	
7. PERFORMING ORGANIZATION NAME(S) AND ADDRESS(ES) Cornell University, Sibley School of Mechanical and Aerospace Engineering, 169 Frank H. T. Rhodes Hall, Ithaca, NY, 14853-3801				8. PERFORMING ORGANIZATION REPORT NUMBER	
9. SPONSORING/MONITORING AGENCY NAME(S) AND ADDRESS(ES)				10. SPONSOR/MONITOR'S ACRONYM(S)	
				11. SPONSOR/MONITOR'S REPORT NUMBER(S)	
12. DISTRIBUTION/AVAILABILITY STATEMENT Approved for public release; distribution unlimited					
13. SUPPLEMENTARY NOTES					
14. ABSTRACT					
15. SUBJECT TERMS					
16. SECURITY CLASSIFICATION OF:			17. LIMITATION OF ABSTRACT	18. NUMBER OF PAGES	19a. NAME OF RESPONSIBLE PERSON
a. REPORT unclassified	b. ABSTRACT unclassified	c. THIS PAGE unclassified			

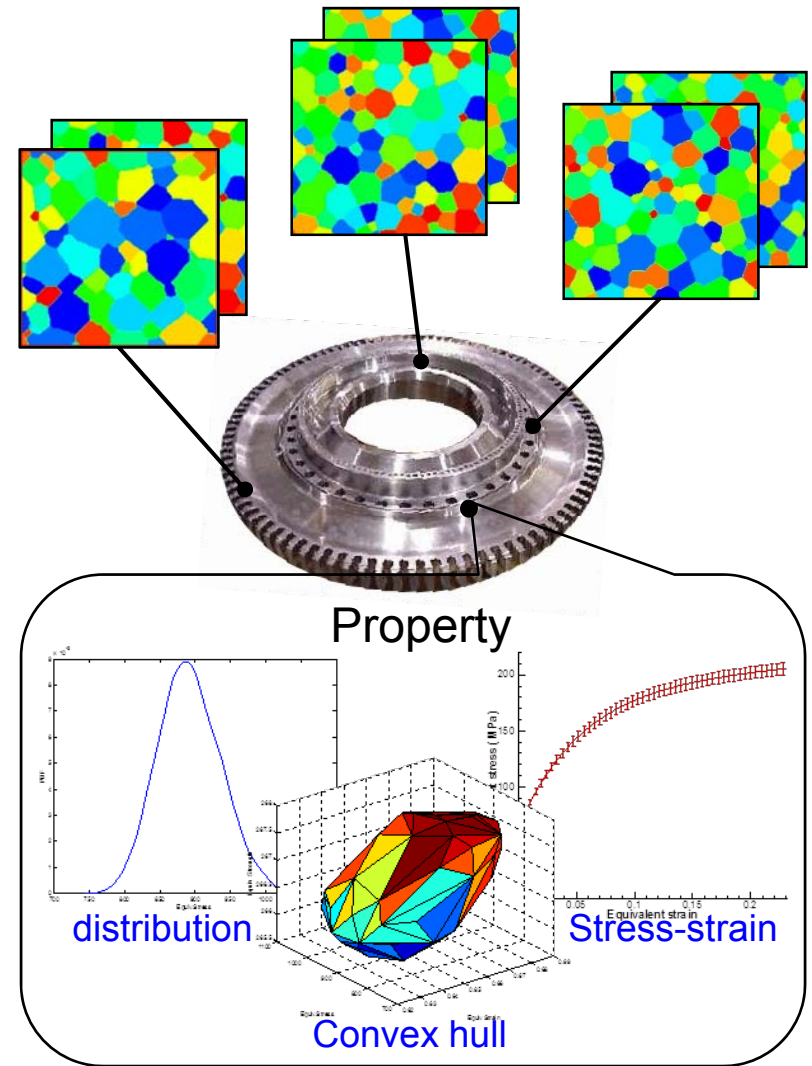
Outline

- ❑ Introduction and motivation
- ❑ Uncertainty quantification at a single material point
 - Investigating mechanical response variability of single-phase polycrystalline microstructures
 - Investigating variability of fatigue indicator parameters of two-phase nickel-based superalloy microstructures
- ❑ Uncertainty quantification of multiscale deformation process
- ❑ An efficient image-based method for modeling the elasto-viscoplastic behavior of realistic polycrystalline microstructures
- ❑ Conclusion and future research



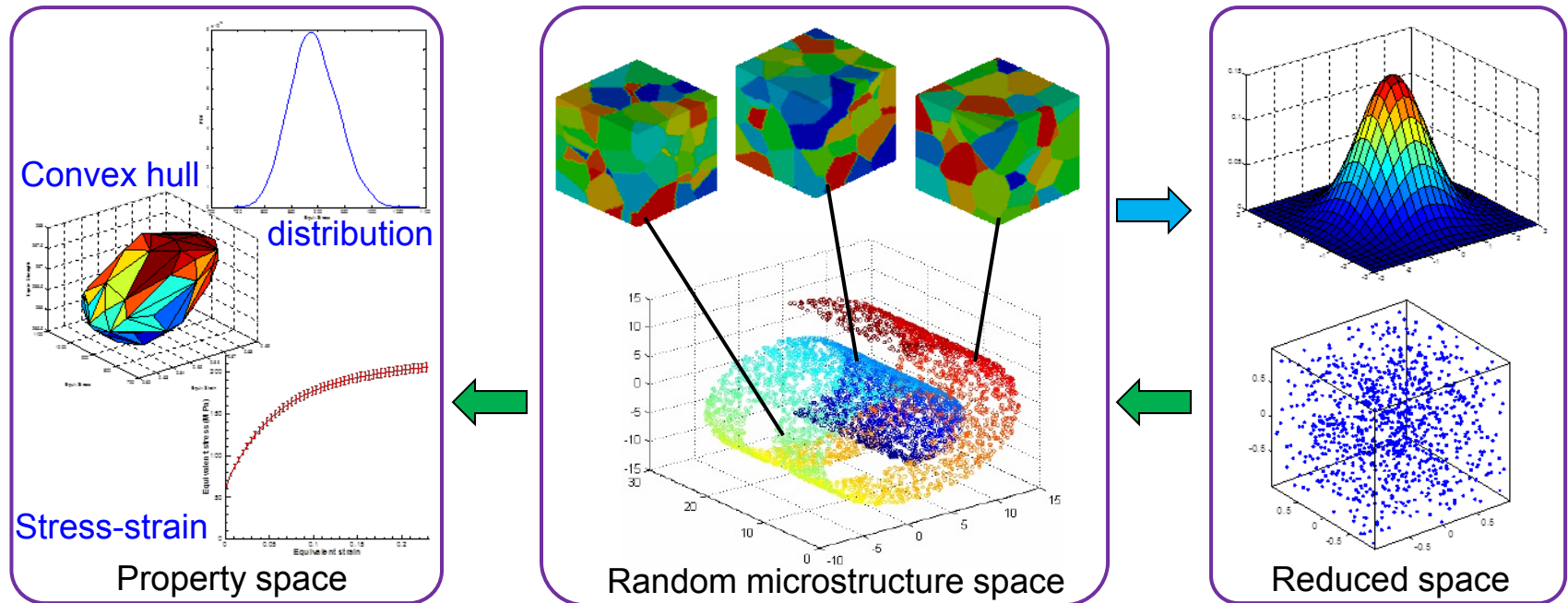
Motivation

- ❑ Microstructure and properties:
 - Material properties are sensitive to microscale structure.
 - Microstructure are inherently random but correlated.
 - Microstructure variation induces property variability.
- ❑ Importance of uncertainty analysis:
 - Assess product and process reliability.
 - Estimate confidence level in model predictions.
 - Identify key sources of randomness.
 - Provide robust design solutions.
- ❑ Focus: Polycrystalline materials
- ❑ Solution strategy:
 - Construct stochastic input model.
 - Solve the stochastic partial differential equations (SPDEs).



Primary Development

- ❑ Employ model reduction techniques to construct the reduced-order surrogate model of random microstructures based on given samples.
- ❑ Develop physics-based deterministic solvers to estimate mechanical properties/responses of polycrystalline materials based on the interrogation of microstructures.
- ❑ Investigate property/response variability of polycrystalline materials using efficient stochastic simulation methods.



Outline

- ❑ Introduction and motivation
- ❑ Uncertainty quantification at a single material point
 - Investigating mechanical response variability of single-phase polycrystalline microstructures
 - Investigating variability of fatigue indicator parameters of two-phase nickel-based superalloy microstructures
- ❑ Uncertainty quantification of multiscale deformation process
- ❑ An efficient image-based method for modeling the elasto-viscoplastic behavior of realistic polycrystalline microstructures
- ❑ Conclusion and future research



Problem Description

➤ Problem definition

Given:

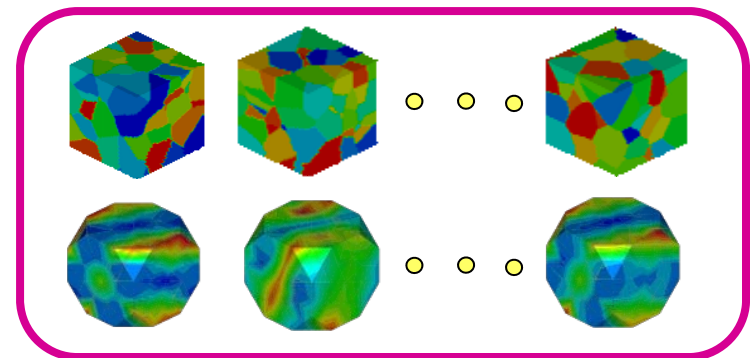
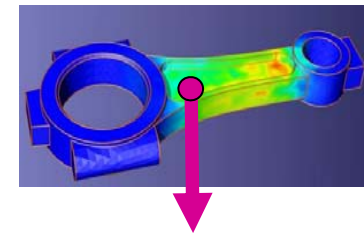
- Grain size snapshots constrained by moments (mean size, standard deviation, higher-order moments).
- Texture snapshots from random process.

Goal:

- The variability in material properties and responses

➤ Methodologies

- Model reduction to reduce the complexity of stochastic input
 - ✓ Nonlinear Model Reduction (isomap) to reduce grain size space
 - ✓ Karhunen-Loeve Expansion to reduce texture space
- Crystal plasticity Taylor model for property estimation.
- Adaptive sparse grid collocation to solve stochastic partial differential equations



(Z. Li, B. Wen and N. Zabaras, 2010)

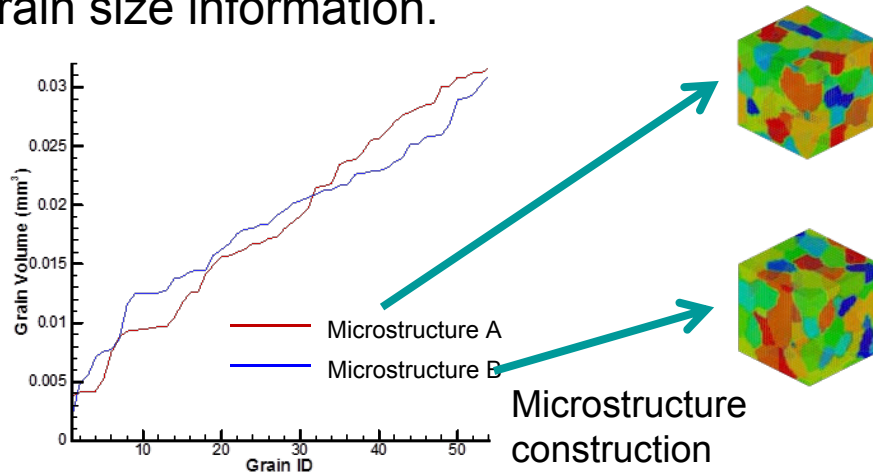
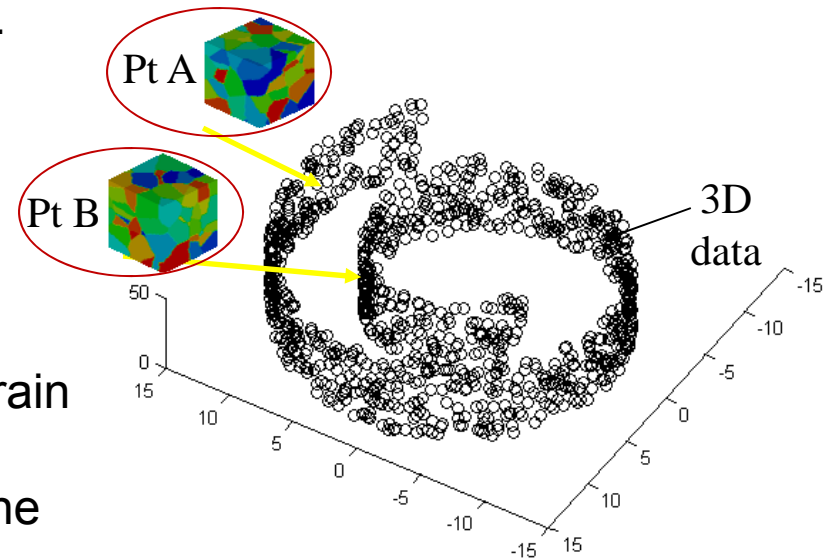


Microstructure Representation

Microstructures obtained from certain process satisfy some specific experimentally determined statistics of grain size distribution.

Each microstructure that satisfies the given statistics of the grain size distribution is a point that lies on a manifold embedded in a high-dimensional space.

For microstructures having the same mean grain size, a “sorted grain size vector”, whose dimension is invariant, can be used to carry the grain size information.



The difference between two microstructures is conveniently measured by Euclidean distance.

$$D(A, B) = \left(\sum_{i=1}^n (GS_i^A - GS_i^B)^2 \right)^{1/2}$$



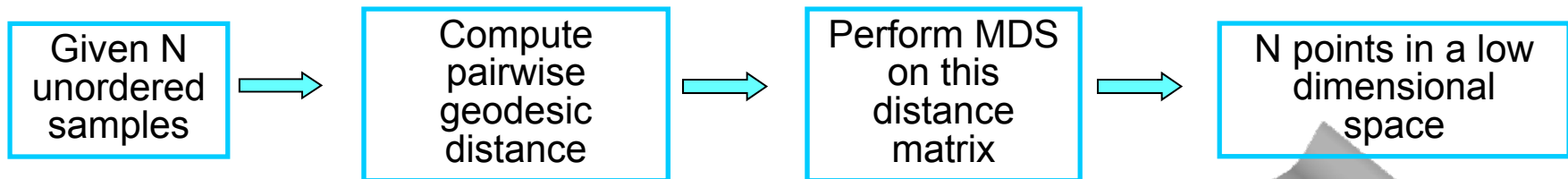
Nonlinear Model Reduction on Grain Size Feature

Given a set of N unordered points belonging to a manifold \mathcal{M} embedded in a high-dimensional space \mathbb{R}^n , find a low-dimensional region $\mathcal{A} \subset \mathbb{R}^d$ that parameterizes \mathcal{M} , where $d \ll n$.

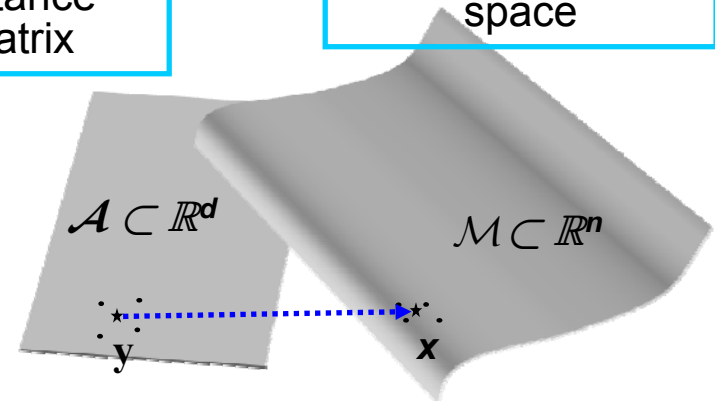
- 1) Geometry can be preserved if the distances between the points are preserved – Isometric mapping.
- 2) The geometry of the manifold is reflected in the geodesic distance between point.

Algorithm:

- 1) Compute the low-dimensional representation of a set of N unordered sample points belonging to a high-dimensional space



- 2) For an arbitrary point $\mathbf{y} \in \mathcal{A}$ must find the corresponding point $\mathbf{x} \in \mathcal{M}$. Compute the mapping from $\mathcal{A} \rightarrow \mathcal{M}$ based on k-nearest neighbors.



(B. Ganapathysubramanian and N. Zabaras, 2008)

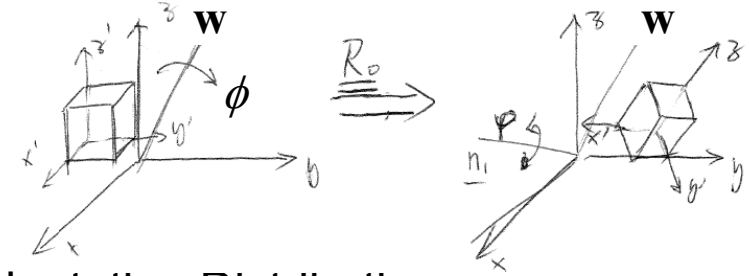


Texture Modeling

The properties of a polycrystalline microstructure are highly dependent on its texture: orientation distribution of grains.

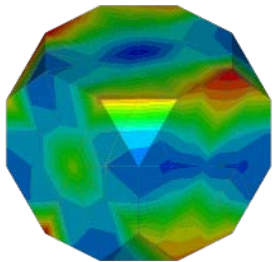
Orientation representation: Rodrigues parameters

$$r_1 = w_1 \tan \frac{\phi}{2}, \quad r_2 = w_2 \tan \frac{\phi}{2}, \quad r_3 = w_3 \tan \frac{\phi}{2}$$

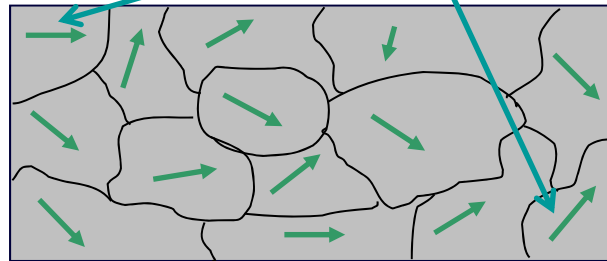


Texture representation: Grain orientation vector, Orientation Distribution Function (ODF)

A discrete form: $\tau(\mathbf{r}) = \{r_1^1, r_2^1, r_3^1, \dots, r_1^n, r_2^n, r_3^n\}$



ODF in RF fundamental zone of FCC crystal



12 slip systems in FCC

$$\mathbf{m}_{local}^{\alpha} : \langle 110 \rangle$$

$$\mathbf{n}_{local}^{\alpha} : \{111\}$$

Orientation dependence of slip system (anisotropy in crystalline materials)

$$\mathbf{m}^{j,\alpha} = \mathbf{R}^j \mathbf{m}_{local}^{\alpha}$$

$$\mathbf{n}^{j,\alpha} = \mathbf{R}^j \mathbf{n}_{local}^{\alpha}$$

$$\text{where } \mathbf{R}^j = \frac{1}{1 + \mathbf{r}^j \cdot \mathbf{r}^j} \left(\mathbf{I} (1 - \mathbf{r}^j \cdot \mathbf{r}^j) + 2(\mathbf{r}^j \otimes \mathbf{r}^j - \mathbf{I} \times \mathbf{r}^j) \right)$$



Generation of Initial Texture Samples

Initial texture samples can be obtained by a sequence of random processing simulations with various deformation rate

$$\mathbf{L} = \omega_1 \begin{bmatrix} 1 & 0 & 0 \\ 0 & -0.5 & 0 \\ 0 & 0 & -0.5 \end{bmatrix} + \omega_2 \begin{bmatrix} 0 & 0 & 0 \\ 0 & 1 & 0 \\ 0 & 0 & -1 \end{bmatrix} + \omega_3 \begin{bmatrix} 0 & 1 & 0 \\ 1 & 0 & 0 \\ 0 & 0 & 0 \end{bmatrix} + \omega_4 \begin{bmatrix} 0 & 0 & 1 \\ 0 & 0 & 0 \\ 1 & 0 & 0 \end{bmatrix} +$$
$$\omega_5 \begin{bmatrix} 0 & 0 & 0 \\ 0 & 0 & 1 \\ 0 & 1 & 0 \end{bmatrix} + \omega_6 \begin{bmatrix} 0 & -1 & 0 \\ 1 & 0 & 0 \\ 0 & 0 & 0 \end{bmatrix} + \omega_7 \begin{bmatrix} 0 & 0 & -1 \\ 0 & 0 & 0 \\ 1 & 0 & 0 \end{bmatrix} + \omega_8 \begin{bmatrix} 0 & 0 & 0 \\ 0 & 0 & -1 \\ 0 & 1 & 0 \end{bmatrix}$$

$\omega_1, \omega_2, \dots, \omega_8$ are random coefficients corresponding to tension/compression, plain strain compression, shear and rotation.

The slip systems are updated during deformation as

$$\mathbf{m}_t^\alpha = \mathbf{F}^e(t) \mathbf{m}_0^\alpha$$

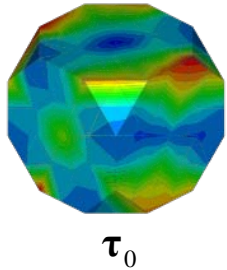
$$\mathbf{n}_t^\alpha = \mathbf{F}^{e-T}(t) \mathbf{n}_0^\alpha$$

Therefore the new orientations can be recovered from the rotation part of the elastic deformation gradient.



Karhunen-Loeve Expansion on Texture Samples

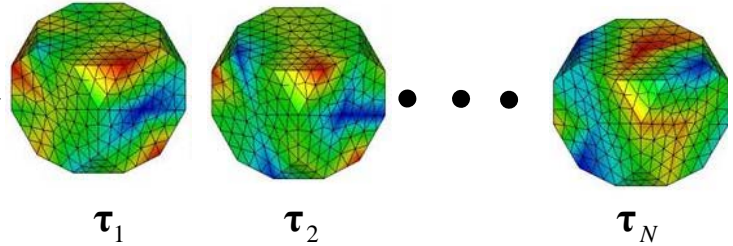
Deterministic texture



Random process
controlled by
 $\{\omega_1, \omega_2, \dots, \omega_8\}$



Initial texture samples



Given N texture examples, construct covariance matrix of these samples

$$\tilde{C} = \frac{1}{N-1} \sum_{i=1}^N (\tau_i - \bar{\tau})^T (\tau_i - \bar{\tau}), \quad \bar{\tau} = \frac{1}{N} \sum_{i=1}^N \tau_i$$

The truncated Karhunen-Loeve Expansion of a random vector τ is

$$\tau(\mathbf{r}, \omega) = \bar{\tau}(\mathbf{r}, \omega) + \sum_{i=1}^d \sqrt{\lambda_i} \phi_i(\mathbf{r}) \eta_i(\omega)$$

where ϕ_i, λ_i are the i th eigenvector and eigenvalue of \tilde{C} , respectively. $\{\eta_i(\omega)\}$ are a set of uncorrelated random variables satisfying

$$E(\eta_i(\omega)) = 0, \quad E(\eta_i(\omega)\eta_j(\omega)) = \delta_{ij}, \quad i, j = 1, \dots, d$$

Texture random field thus transformed to low-dimensional space $\eta \in \mathbb{R}^d$



Maximum Entropy Estimation of the Distribution of η

To sample new texture, we can sample η instead, and then transform it back to the texture space. The distribution of η is needed.

Maximum Entropy Estimation (MaxEnt): *amongst the probability distributions that satisfy our incomplete information about the system, the probability distribution that maximizes entropy is the least-biased estimate that can be made. In agreement with everything that is known but carefully avoids anything that is unknown.*

The form of MaxEnt distribution is

$$p^*(x) = \frac{e^{-\sum_{n=1}^N \lambda_n f(x)}}{Z}, \quad Z = \int e^{-\sum_{n=1}^N \lambda_n f(x)} dx$$

which maximize the entropy

$$H(p) = -\sum_{i=1}^M p(x_i) \log(p(x_i))$$

and satisfies constraints

$$E(f_n(\mathbf{x})) = M_n, \quad n = 1, 2, \dots$$

When the uncorrelated constraints are satisfied, the MaxEnt distribution is a standard Gaussian distribution

$$\eta \sim N(\mathbf{0}, \mathbf{I})$$



Inverse CDF Transformation

Uncorrelated Gaussian random variables are independent in current case. To employ Sparse Grid Collocation method, Gaussian distribution needs to be transformed to a uniform hypercube $[0, 1]^d$.

The cumulative distribution function (CDF) for standard Gaussian is

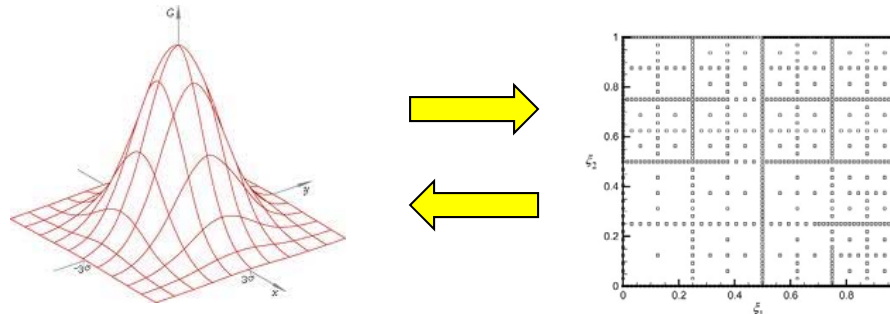
$$\Phi_{\eta_i}(\eta_i) = \frac{1}{2} \left[1 + \operatorname{erf} \left(\frac{\eta_i}{\sqrt{2}} \right) \right]$$

which is uniformly distributed in $[0, 1]$.

Given a point in the hypercube $\zeta \in [0, 1]^d$, we can also find a corresponding point in the original distribution by

$$\eta_i = \Phi^{-1}(\zeta_i), \quad i = 1, \dots, d$$

This process transforms a node in sparse grid back to a point in Gaussian distribution, and it can be further recovered to a texture realization



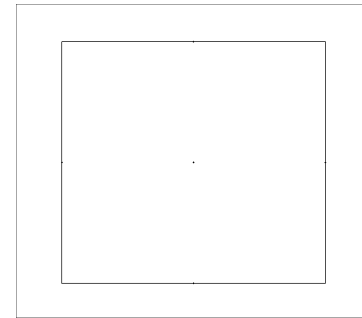
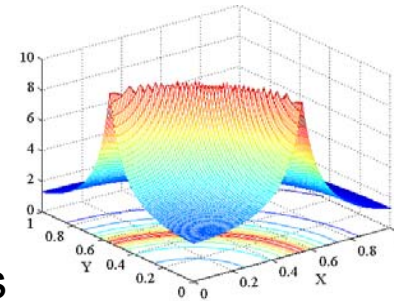
Adaptive Sparse Grid Collocation

Sparse grid collocation is an effective method to solve SPDEs. It approximates the multi-dimensional stochastic space using interpolating functions on a set of collocation points. The collocation method collapses the multi-dimensional problem to solving M (M is the number of collocation points) deterministic problems.

The interested function can be approximated by

$$u(x, \xi(\omega)) = \sum_{|i| \leq q} \sum_j \omega_j^i(x) a_j^i(\xi(\omega))$$

\downarrow \downarrow \downarrow
 Stochastic process Hierarchical surplus Multi-linear basis functions

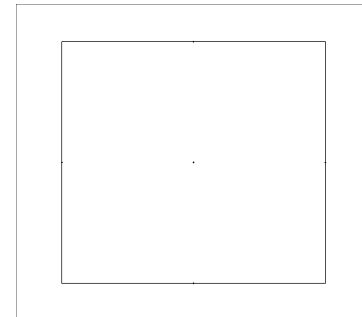
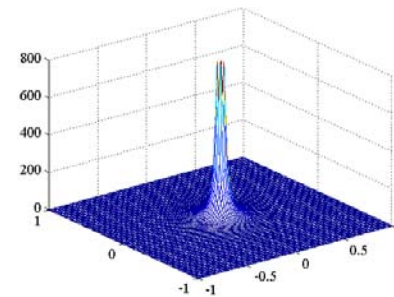


The mean of the random solution is evaluated as

$$E(u(t)) = \sum_{|i| \leq q} \sum_j \omega_j^i(x) \cdot \int_L a_j^i(\xi) d\xi$$

In the context of adaptivity, new support nodes are added to the hypercube only if the error indicator is larger than a threshold ε :

$$\gamma_j^i = \frac{\left\| \omega_j^i(x) \cdot \int_L a_j^i(\xi) d\xi \right\|_{L_2}}{\left\| E_{\|i\|=d-1} \right\|_{L_2}} > \varepsilon$$



(X. Ma and N. Zabarar, 2009)



Deterministic Solver

Material: FCC nickel

Deterministic solver: rate-independent crystal plasticity with Taylor homogenization.

Decomposition of deformation gradient: $\mathbf{F} \equiv \mathbf{F}^e \mathbf{F}^p$

Hardening law: $\kappa - \kappa_0 = \alpha \mu b \sqrt{\rho}$

where dislocation density changing rate $\dot{\rho} = \sum_{\kappa} \left\{ \frac{1}{L_g b} + k_1 \sqrt{\rho} - k_2 \rho \right\} |\dot{\gamma}^{\alpha}|$

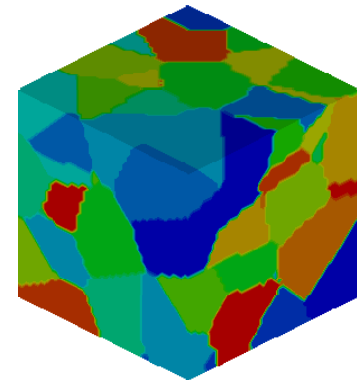
If the resolved shear stress is larger than the slip resistance $\tau^{\alpha} > \kappa^{\alpha}$, the slip system is active.

Upon calculating the incremental shear strain, elastic and plastic deformation gradient can be updated and Cauchy stress is computed

$$\mathbf{T} = \mathbf{F}^e \{ [\det \mathbf{F}^e]^{-1} \mathbf{T}^* \} \mathbf{F}^{eT} \quad \text{with} \quad \mathbf{T}^* = \mathbf{C}^e \mathbf{E}^e$$

Homogenized effective stress and strain

$$\bar{\sigma}_{eff} = \sqrt{\frac{3}{2} \bar{\mathbf{T}} : \bar{\mathbf{T}}}, \quad \text{where} \quad \bar{\mathbf{T}} = \langle \mathbf{T} \rangle = \frac{1}{V} \int_V \mathbf{T} dV$$
$$\bar{\boldsymbol{\varepsilon}}_{eff} = \int_0^t \sqrt{\frac{2}{3} \bar{\mathbf{D}} : \bar{\mathbf{D}}} dt, \quad \bar{\mathbf{D}} = \langle \mathbf{D} \rangle = \frac{1}{V} \int_V \mathbf{D} dV$$



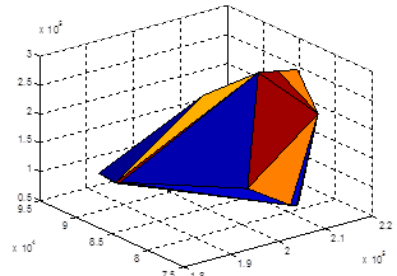
(L. Anand and M. Kothari, 1996; A. Acharya and A.J. Beaudoin, 2000)



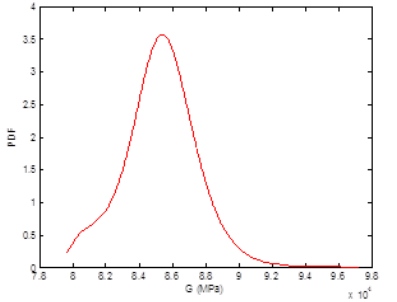
Investigating Property Variability Due to Microstructure Uncertainties

Property variability

Property convex hull



END



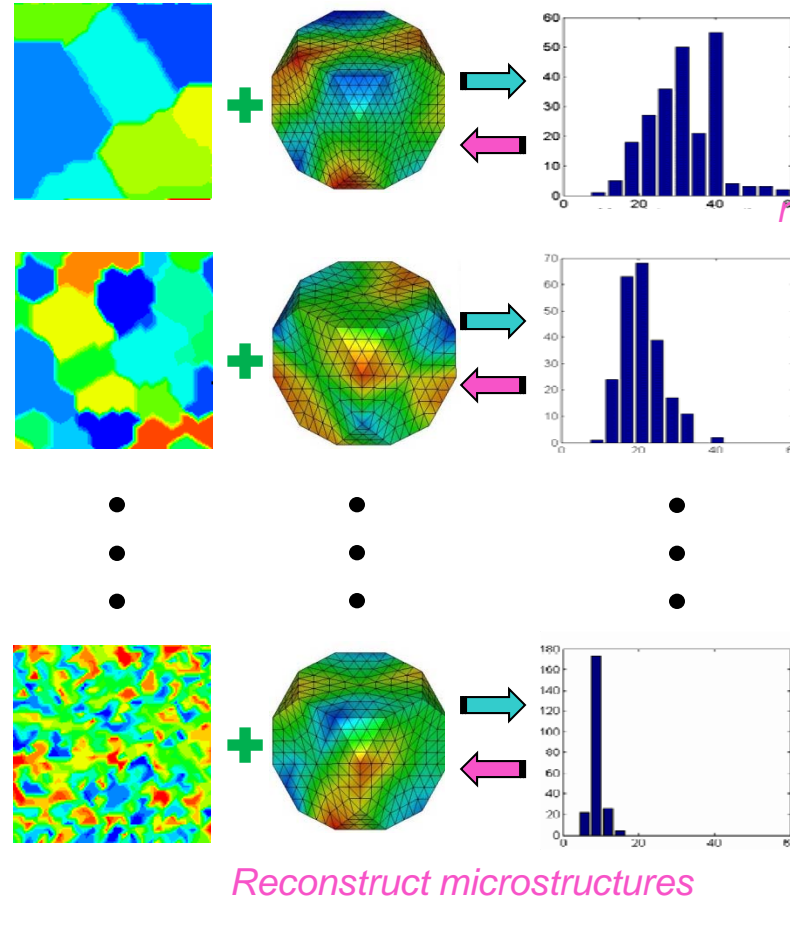
Property distribution

Obtain Properties

Solve SPEDs

Microstructure space

START: Extract microstructural features

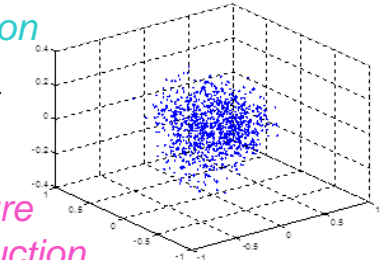


Database

Low-dimensional space

Model reduction

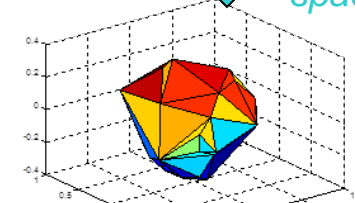
Low-D points



Feature reconstruction

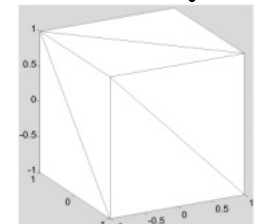
Interpolation

Construct low-D space



Sample from hypercube

Low-D space
Map to hypercube



Unit hypercube

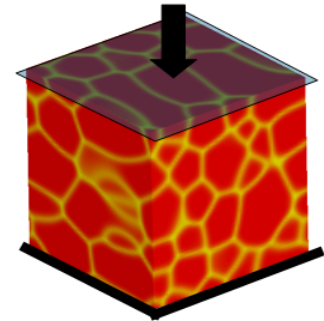


Numerical Examples

Microstructure domain: 1mm x 1mm x 1mm cube containing 54 grains.

Examine the effective stress variability of polycrystalline microstructures satisfying different constraints subjected to compression.

$$\mathbf{L} = 0.002 \text{ sec}^{-1} \begin{bmatrix} 0.5 & 0 & 0 \\ 0 & 0.5 & 0 \\ 0 & 0 & -1 \end{bmatrix}$$



Grain size sample constraints:

- (1) Mean volume 0.0185 mm^3
- (2) 2nd moment $3.704 \times 10^{-4} \text{ mm}^6$
- (3) 3rd moment $8.637 \times 10^{-6} \text{ mm}^9$

Texture generation:

$$(a) \mathbf{L} = \omega_1 \begin{bmatrix} 0 & 0 & 0 \\ 0 & 1 & 0 \\ 0 & 0 & -1 \end{bmatrix} + \omega_2 \begin{bmatrix} 0 & -1 & 0 \\ 1 & 0 & 0 \\ 0 & 0 & 0 \end{bmatrix}$$

$$(b) \mathbf{L} = \omega_1 \begin{bmatrix} 0.5 & 0 & 0 \\ 0 & 0.5 & 0 \\ 0 & 0 & -1 \end{bmatrix} + \omega_2 \begin{bmatrix} 0 & 0 & 0 \\ 0 & 1 & 0 \\ 0 & 0 & -1 \end{bmatrix} + \omega_3 \begin{bmatrix} 0 & -1 & 0 \\ 1 & 0 & 0 \\ 0 & 0 & 0 \end{bmatrix}$$

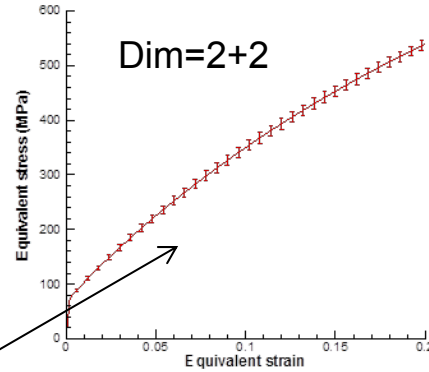
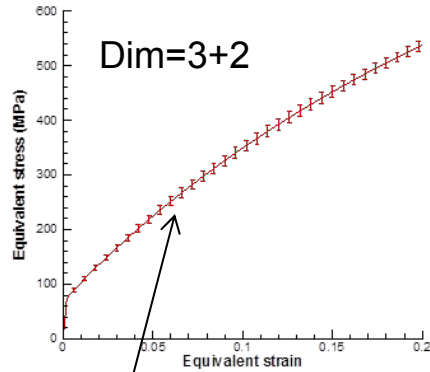
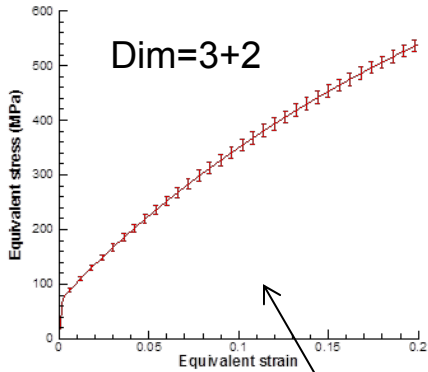
with $\omega_1, \omega_2 \sim [-0.002, 0.002] \text{ sec}^{-1}$

Run the simulation for 500 seconds.



Numerical Examples

Grain size effect

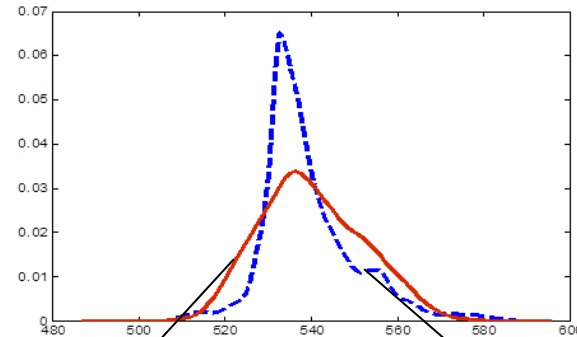
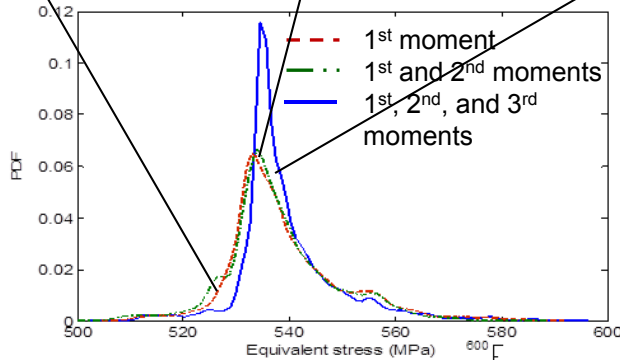


1st moment ((1)+(a))

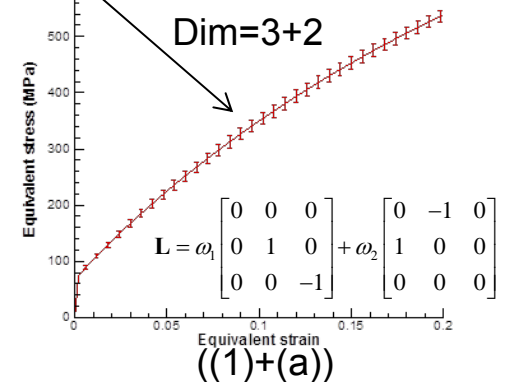
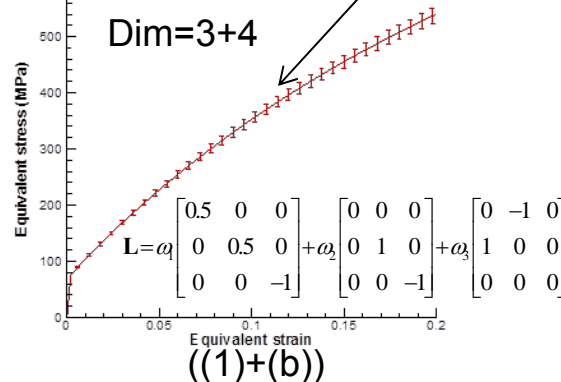
1st and 2nd moments ((2)+(a))

1st, 2nd, and 3rd moments ((3)+(a))

Effective stress distribution at strain 0.2

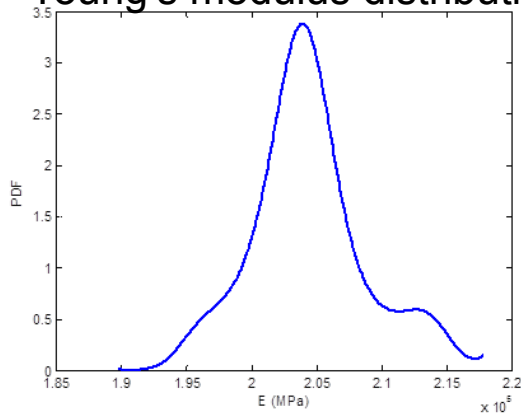


Texture effect

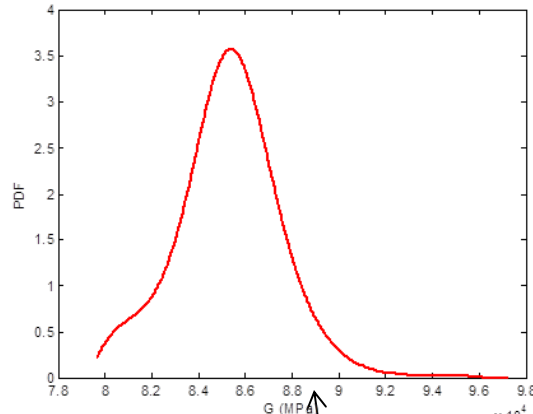


Elastic Properties Variability

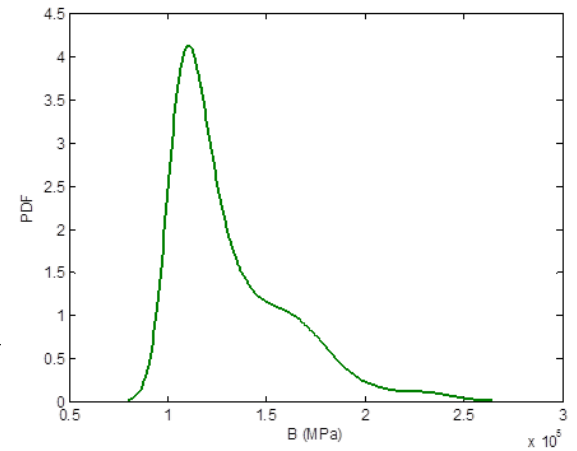
Young's modulus distribution



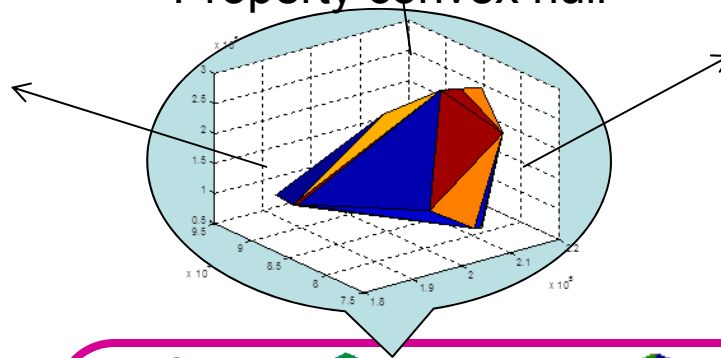
Shear modulus distribution



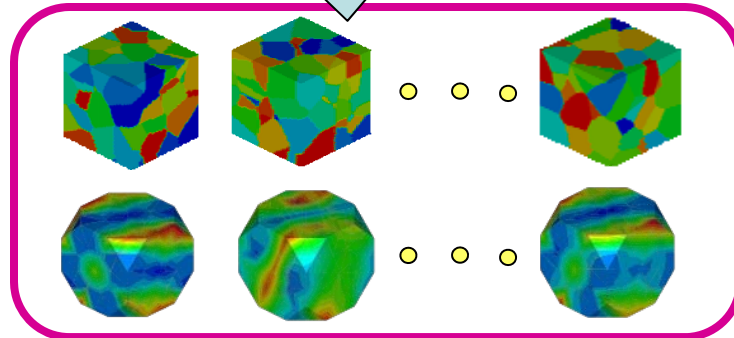
Bulk modulus distribution



Property convex hull



10000 samples
(1)+(a)



Outline

- ❑ Introduction and motivation
- ❑ Uncertainty quantification at a single material point
 - Investigating mechanical response variability of single-phase polycrystalline microstructures
 - Investigating variability of fatigue indicator parameters of two-phase nickel-based superalloy microstructures
- ❑ Uncertainty quantification of multiscale deformation process
- ❑ An efficient image-based method for modeling the elasto-viscoplastic behavior of realistic polycrystalline microstructures
- ❑ Conclusion and future research



Overview

- ❑ Nickel-based superalloys are widely used in components working in harsh environment, e.g. disks and blades of turbo engines.
- ❑ They have high resistance to creep and fatigue at high temperature.
- ❑ The performance of nickel-based superalloys depends on their underlying microstructures: grain topology, texture, and volume fraction of γ' phase.
- ❑ We are interested in the variability of fatigue properties of superalloy microstructures due to uncertainties in texture, grain size, and volume fraction of γ' .
- ❑ Principal component analysis (PCA) based model reduction techniques are adopted for reducing the complexity of the input space.



Problem Definition

➤ Problem definition

Given:

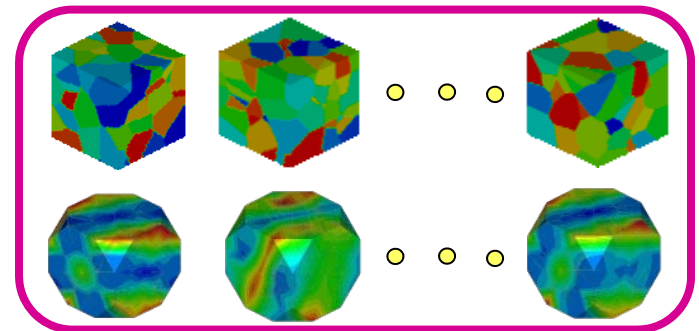
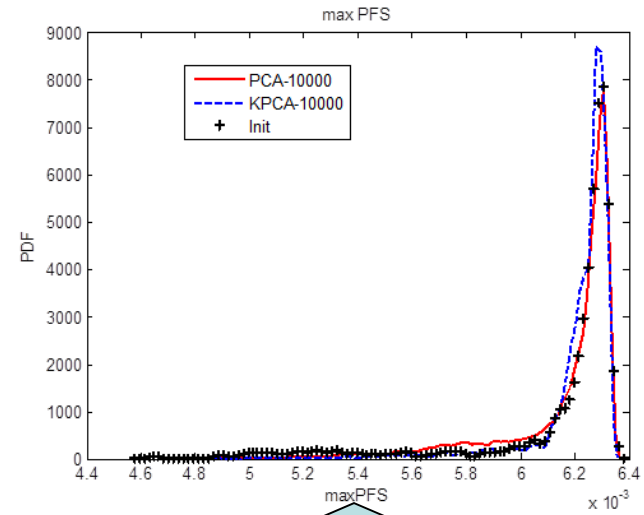
- Grain size snapshots constrained by the mean size and sampled from lognormal distribution.
- Texture snapshots from random process.
- Volume fraction of γ' precipitates.

Goal:

- The variability of fatigue resistance due to microstructure uncertainties.
- Find the feature(s) dominate the variability of fatigue resistance

➤ Methodologies

- PCA and KPCA model reduction to reduce the complexity of stochastic input.
- PCE to map reduced coordinates to a known distribution.
- Adaptive sparse grid and Monte Carlo collocation to solve stochastic partial differential equations



(Bin Wen and N. Zabaras, 2012)



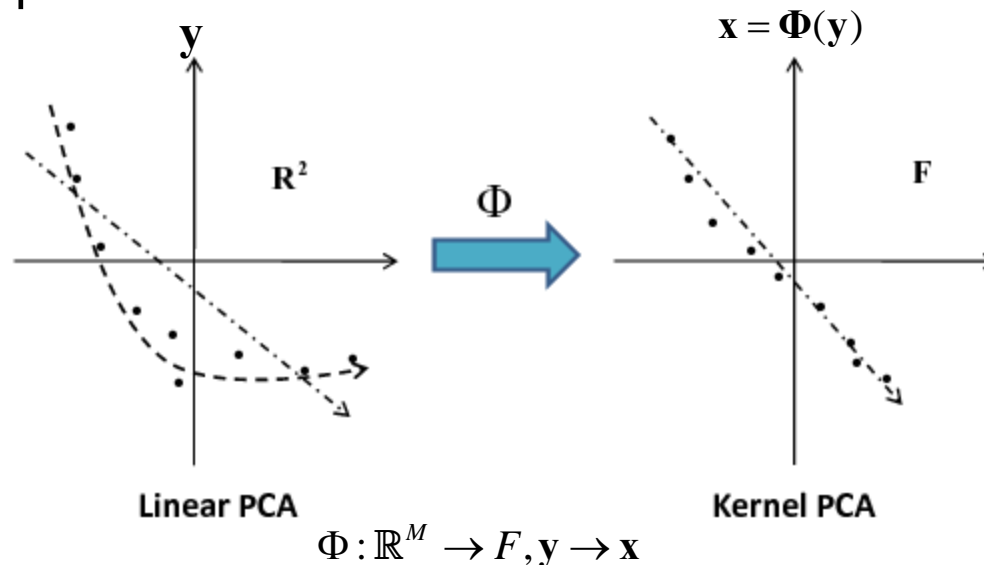
Stochastic Input Space

- ❑ A probability space (Ω, F, P) with sample space Ω , corresponding to all microstructures resulted from certain random process, $F \subset 2^\Omega$, being the σ -algebra of subsets in Ω , and $P: F \rightarrow [0,1]$, as the probability measure.
- ❑ Each sample $\omega \in \Omega$ is a random microstructure which can be described by a discretized representation $\mathbf{y}(\omega) = (y_1, \dots, y_M)^T : \Omega \rightarrow \mathbf{Y} \in \mathbb{R}^M$
- ❑ The input space information is only given as a set of samples $\mathbf{y}_i, i = 1, \dots, N$
- ❑ The variability of microstructure sensitive property $A = A(\mathbf{y})$ of the given input space is interested.
- ❑ It is necessary to construct the input space that has the same statistical properties with the given samples. Since the input space is high-dimensional, model reduction is adopted to construct a low-dimensional surrogate space.



PCA/KPCA

- ❑ In general, the components of stochastic input $y \in \mathbb{R}^M$ are not linearly related.
- ❑ Direct linear PCA attempting to fit a linear surface such that reconstruction error is minimized is not very appropriate to find the surrogate space.
- ❑ Solution: nonlinearly map the given samples to a feature space F , where PCA performs well.



- ❑ If PCA, $\Phi(y) = y$

(B. Schölkopf, A. Smola and K.-R. Müller, 1998; X. Ma and N. Zabaras, 2011)



PCA/KPCA Formulation

Covariance matrix in the feature space:

$$\mathbf{C} = \frac{1}{N} \sum_{i=1}^N \tilde{\Phi}(\mathbf{y}_i) \tilde{\Phi}(\mathbf{y}_i)^T \quad \tilde{\Phi} = \Phi(\mathbf{y}) - \bar{\Phi}$$

Eigenvalue problem: $\mathbf{C}\mathbf{V} = \lambda\mathbf{V}$

KL expansion:
$$\Phi(\mathbf{y}) = \sum_{i=1}^{M_F} \sqrt{\lambda_i} \mathbf{V}_i \eta_i + \bar{\Phi} = \sum_{i=1}^{M_F} z_i \mathbf{V}_i + \bar{\Phi}$$

Multiply with $\tilde{\Phi}_i$ and reform the eigenvalue problem:

$$\tilde{\mathbf{K}}\mathbf{U} = \tilde{\Lambda}\mathbf{U} \quad \text{where} \quad \tilde{\mathbf{K}} : \tilde{K}_{ij} = (\tilde{\Phi}(\mathbf{y}_i) \cdot \tilde{\Phi}(\mathbf{y}_j))$$

$$\mathbf{U} = [\mathbf{a}_1, \dots, \mathbf{a}_N]$$

$$\tilde{\Lambda} = \text{diag}(\tilde{\lambda}_1, \dots, \tilde{\lambda}_N)$$

The eigenbasis of the covariance matrix \mathbf{C} is projected to the given samples by

$$\mathbf{V}_i = \sum_{j=1}^N \tilde{\alpha}_{ij} \tilde{\Phi}(\mathbf{y}_j) = \sum_{j=1}^N \frac{\alpha_{ij}}{\sqrt{\tilde{\lambda}_i}} \tilde{\Phi}(\mathbf{y}_j)$$



PCA/KPCA Formulation

Any sample in F: $\Phi(\mathbf{y}) = \sum_{i=1}^N z_i \mathbf{V}_i + \bar{\Phi} \approx \sum_{i=1}^r z_i \mathbf{V}_i + \bar{\Phi} = \sum_{i=1}^r \beta_i \Phi(\mathbf{y}_i)$

where $\boldsymbol{\beta} = \mathbf{AZ} + \frac{1}{N}\mathbf{1}$ $\mathbf{A} = \mathbf{H}\tilde{\mathbf{U}}_r = \left(\mathbf{I} - \frac{1}{N}\mathbf{1}\mathbf{1}^T \right) [\tilde{\boldsymbol{\alpha}}_1, \dots, \tilde{\boldsymbol{\alpha}}_r]$ $\mathbf{Z} = [z_1, \dots, z_r]^T$

Reduced representation:

$$z_i = \mathbf{V}_i \cdot \tilde{\Phi}(\mathbf{y}) = \sum_{j=1}^N \tilde{\alpha}_{ij} (\tilde{\Phi}(\mathbf{y}) \cdot \tilde{\Phi}(\mathbf{y}_j)) = \sum_{j=1}^N \tilde{\alpha}_{ij} \tilde{k}(\mathbf{y}, \mathbf{y}_j) = \tilde{\boldsymbol{\alpha}}_i^T \tilde{\mathbf{k}}_y = \tilde{\boldsymbol{\alpha}}_i^T \mathbf{H}\mathbf{k}_y - \frac{1}{N} \tilde{\boldsymbol{\alpha}}_i^T \mathbf{H}\mathbf{K}\mathbf{1},$$

Gaussian Kernel: $K_{ij} = k(\mathbf{y}_i, \mathbf{y}_j) = \exp\left(-\frac{\|\mathbf{y}_i - \mathbf{y}_j\|^2}{2\sigma^2}\right)$

In PCA $k(\mathbf{y}_i, \mathbf{y}_j) = \mathbf{y}_i \cdot \mathbf{y}_j$

Only the dot products of vectors in the feature space are required, while the explicit calculation of the map is not necessary.

Construct reduced-order space by initial samples \mathbf{z}_i

Random sample ξ in the reduce space (constructed by \mathbf{z}_i), we can obtain its corresponding high-dimensional counterpart.



Polynomial Chaos Expansion (PCE)

Map the reduced space to a known distribution.

$$\xi_i = \sum_{j=0}^p \gamma_{ij} \psi_j(\eta_i), \quad i = 1, \dots, r$$

Each independent random variable ξ_i can be expanded on to an one-dimensional polynomial chaos basis ψ_j of degree p .

Gaussian-Hermite PCs

$$\gamma_{ij} = \frac{E[\xi_i \psi_j(\eta_i)]}{E[(\psi_j(\eta_i))^2]} = \frac{1}{\sqrt{2\pi} j!} \int_{-\infty}^{\infty} \xi_i \psi_j(\eta_i) e^{-\frac{\eta_i^2}{2}} d\eta_i, \quad i = 1, \dots, r, \quad j = 0, \dots, p$$

Uniform-Legendre PCs

$$\gamma_{ij} = \frac{E[\xi_i \psi_j(\eta_i)]}{E[(\psi_j(\eta_i))^2]} = \frac{2j+1}{2} \int_{-1}^1 \xi_i \psi_j(\eta_i) d\eta_i, \quad i = 1, \dots, r, \quad j = 0, \dots, p$$

To compute the integral, a map between ξ_i and η_i is needed.

Mapping through CDF

$$\xi_i = \Gamma_i(\eta_i), \quad \Gamma_i \equiv F_{\xi_i}^{-1} \circ F_{\eta_i}$$

where F_{ξ_i} and F_{η_i} are the CDFs of the two random variables, respectively.

(D. Xiu and G.E. Karniadakis, 2002; G. Stefanou, A. Nouy and A. Clement, 2009)



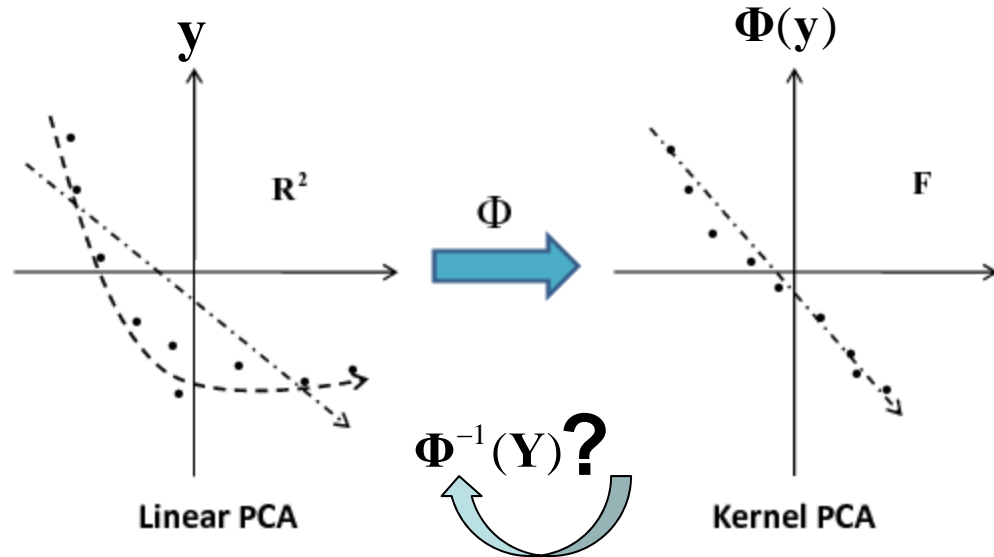
Pre-imaging

- Sample η , and find the input realization \mathbf{y} , approximately.

Draw random sample η

Map to ξ **PCE**

Construct high-D representation $\Phi(\mathbf{y})$ **PCA/KPCA**



Recover microstructure feature \mathbf{y} **Pre-imaging**

$$\tilde{d}_i^2 = 1 + \boldsymbol{\beta}^T \mathbf{K} \boldsymbol{\beta} - 2\boldsymbol{\beta}^T \mathbf{k}_{y_i}$$

K-nearest neighbor: $\mathbf{y} \approx \hat{\mathbf{y}} = \frac{\sum_{i=1}^K \frac{1}{d_i} \mathbf{y}_i}{\sum_{i=1}^K \frac{1}{d_i}}$

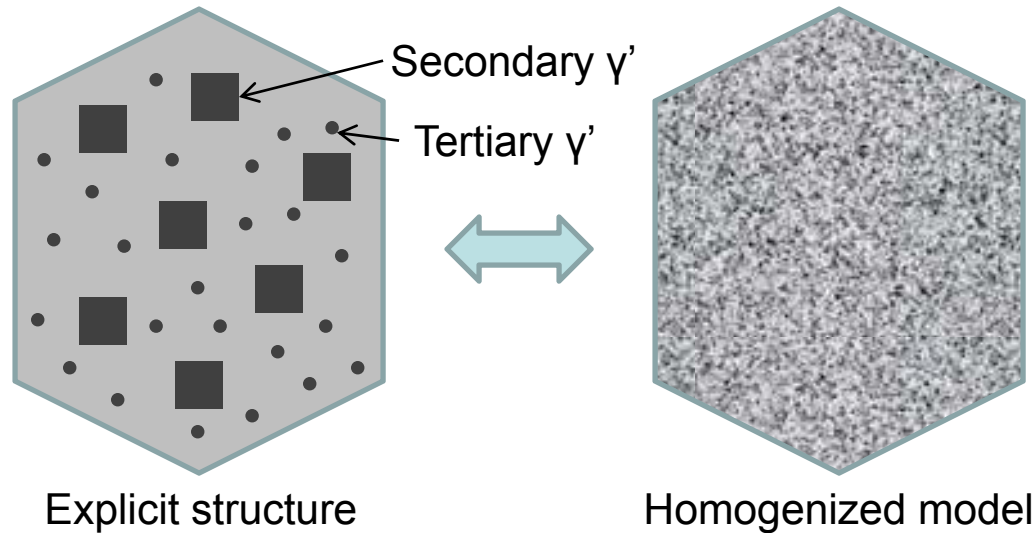
Gauss kernel:

$$\begin{aligned} d_i^2(\hat{\mathbf{y}}, \mathbf{y}_i) &= \|\hat{\mathbf{y}} - \mathbf{y}_i\|^2 = -2\sigma^2 \ln\left(1 - 0.5\hat{d}_i^2(\Phi(\hat{\mathbf{y}}), \Phi(\mathbf{y}_i))\right) \\ &\approx -2\sigma^2 \ln\left(1 - 0.5\tilde{d}_i^2(\Phi(\mathbf{y}), \Phi(\mathbf{y}_i))\right) \end{aligned}$$



Crystal Plasticity Constitutive Model

- ❑ The superalloy microstructure is modeled as a homogenized single crystal with effective properties.



- ❑ Taylor model: all grains have the same deformation. No realistic microstructure is required. Computationally efficient.
- ❑ Finite element model: the boundary nodes have the same deformation while heterogeneous deformation is allowed within the microstructure. Realistic microstructure. More accurate but less efficient.



Homogenized Constitutive Model

- ❑ The model is for polycrystalline IN100. All grains are assumed to be the mixture of γ matrix and γ' precipitates. The same set of constitutive equations apply to all grains.
- ❑ Three types of γ' precipitates: primary, secondary, and tertiary.
- ❑ The effect of γ' precipitates is taken into consideration as constitutive parameters (volume fraction, mean particle size, etc.).
- ❑ Rate dependent flow rule:

$$\dot{\gamma}^{(\alpha)} = \left[\dot{\gamma}_0^{(\alpha)} \left\langle \frac{|\tau^{(\alpha)} - \chi^{(\alpha)}| - \kappa^{(\alpha)}}{D^{(\alpha)}} \right\rangle^{n_1} + \dot{\gamma}_1^{(\alpha)} \left\langle \frac{|\tau^{(\alpha)} - \chi^{(\alpha)}|}{D^{(\alpha)}} \right\rangle^{n_2} \right] \text{sgn}(\tau^{(\alpha)} - \chi^{(\alpha)})$$

- ❑ Hardening law: $\kappa_{\lambda}^{(\alpha)} = \kappa_{0,\lambda}^{(\alpha)} + \alpha_t \mu_{mix} b \sqrt{\rho_{\lambda}^{(\alpha)}}$

where $\alpha_t = \langle 0.1 - 0.68 f'_{p1} + 1.1 f'^2_{p1} \rangle$

$$\mu_{mix} = (f_{p1} + f_{p2} + f_{p3}) \mu_{\gamma'} + f_{\gamma} \mu_{\gamma}$$

$$f'_{p1} = \frac{f_{p1}}{f_{p1} + f_{\gamma}}, f'_{p2} = \frac{f_{p2}}{f_{p2} + f_{\gamma}}, f'_{p3} = \frac{f_{p3}}{f_{p3} + f_{\gamma}}$$

$$\lambda = \begin{cases} oct & \text{octahedral slip system} \\ cub & \text{cube slip system} \end{cases}$$

$$\kappa_{0,oct}^{(\alpha)} = \left[(\tau_{0,oct}^{(\alpha)})^{n_k} + \psi_{oct}^{n_k} \right]^{\frac{1}{n_k}} + (f_{p1} + f_{p2}) \tau_{ns}^{(\alpha)}$$

$$\kappa_{0,cub}^{(\alpha)} = \left[(\tau_{0,cub}^{(\alpha)})^{n_k} + \psi_{cub}^{n_k} \right]^{\frac{1}{n_k}}$$

$$\psi_{\lambda} = c_{p1} \sqrt{w \frac{f'_{p1}}{d_1}} + c_{p2} \sqrt{w \frac{f'_{p2}}{d_2}} + c_{p3} \sqrt{w f'_{p3} d_3} + c_{gr} d_{gr}^{-0.5}$$

γ' hardening

Grain size
effect

$$w = \frac{\Gamma_{APB}}{\Gamma_{APB-ref}}$$

(C.P. Przybyla and D.L. McDowell, 2010)



Homogenized Constitutive Model

- Dislocation density evolution:

$$\dot{\rho}_{\lambda}^{(\alpha)} = h_0 \left\{ \frac{k_{\delta}}{bd_{\delta eff}} + k_{1,\lambda} \sqrt{\rho_{\lambda}^{(\alpha)}} - k_{2,\lambda} \rho_{\lambda}^{(\alpha)} \right\} |\dot{\gamma}^{(\alpha)}| \quad d_{\delta eff} \approx \left(\frac{2}{d_{2\delta}} \right)^{-1}$$

- Back stress evolution:

$$\dot{\chi}_{\lambda}^{(\alpha)} = C_{\chi} \left(\eta \mu_{mix} b \sqrt{\rho_{\lambda}^{(\alpha)}} \operatorname{sgn}(\tau^{(\alpha)} - \chi_{\lambda}^{(\alpha)}) - \chi_{\lambda}^{(\alpha)} \right) |\dot{\gamma}^{(\alpha)}|$$

$$C_{\chi} = 123.93 - 433.98 f_{p2}' + 384.06 f_{p2}'^2 \quad \eta = \frac{\eta_{0,\lambda} Z_0}{Z_0 + k_{1,\lambda} \sqrt{\rho_{\lambda}^{(\alpha)}}}$$

- Fatigue indicator parameters (FIPs) are employed to measure the fatigue properties of nickel-based superalloy.

- Cumulative plastic strain per cycle $P_{cyc} = \int_{cyc} \sqrt{\frac{2}{3}} \dot{p} dt = \int_{cyc} \sqrt{\frac{2}{3}} \mathbf{D}^p : \mathbf{D}^p dt$

- Cumulative net plastic shear strain $P_r = \max \left(\int_{cyc} \dot{\epsilon}_{ij}^p n_i t_j dt \right)$

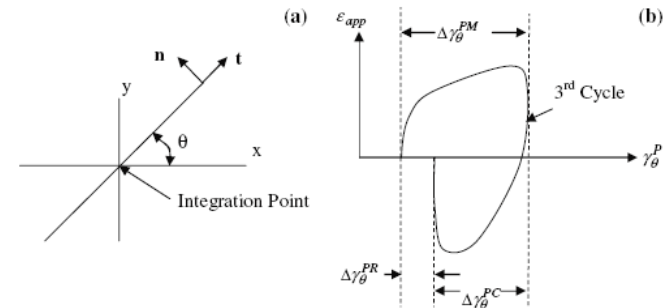
- The Fatemi-Socie parameter $P_{FS} = \frac{\Delta \gamma_{max}^p}{2} \left[1 + k^* \frac{\sigma_n^{max}}{\sigma_y} \right]$

- Maximum range of cyclic plastic shear strain $P_{mps} = \frac{\Delta \gamma_{max}^p}{2}$

(M. Shenoy, J. Zhang, and D.L. McDowell, 2007)

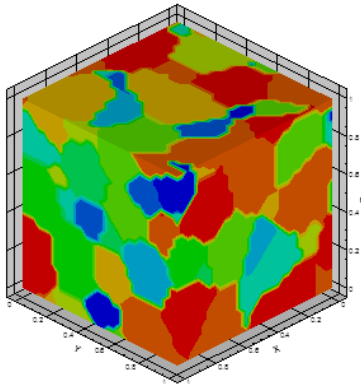
maximum range of cyclic plastic shear strain

$$\Delta \gamma_{max}^p = \max_{\theta} \left(\left| \max_{cyc} (\gamma_{\theta}^p) - \min_{cyc} (\gamma_{\theta}^p) \right| \right)$$

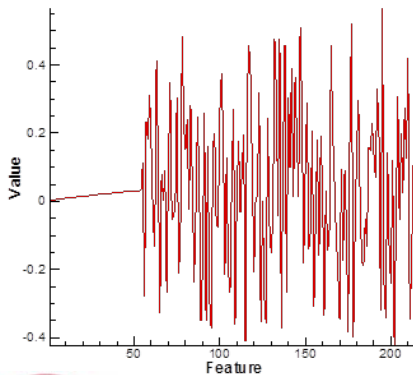
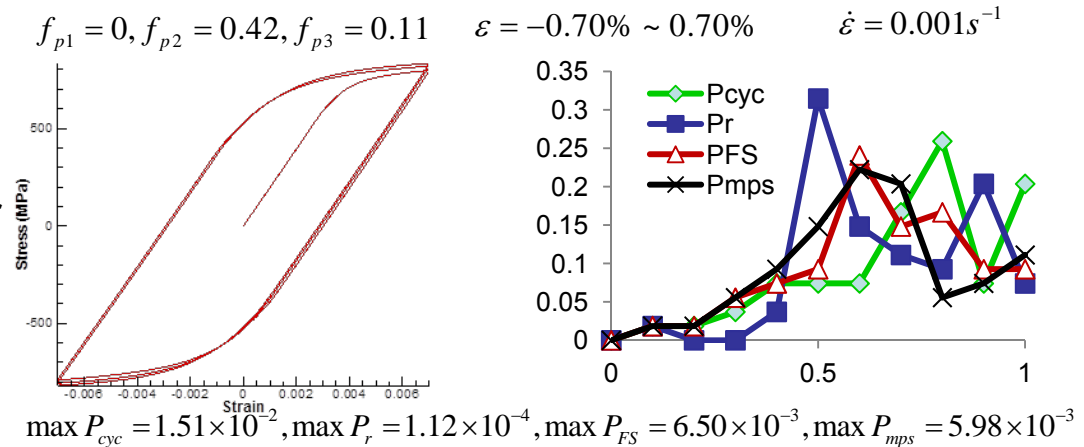


Numerical Example: Taylor Model vs. FEM

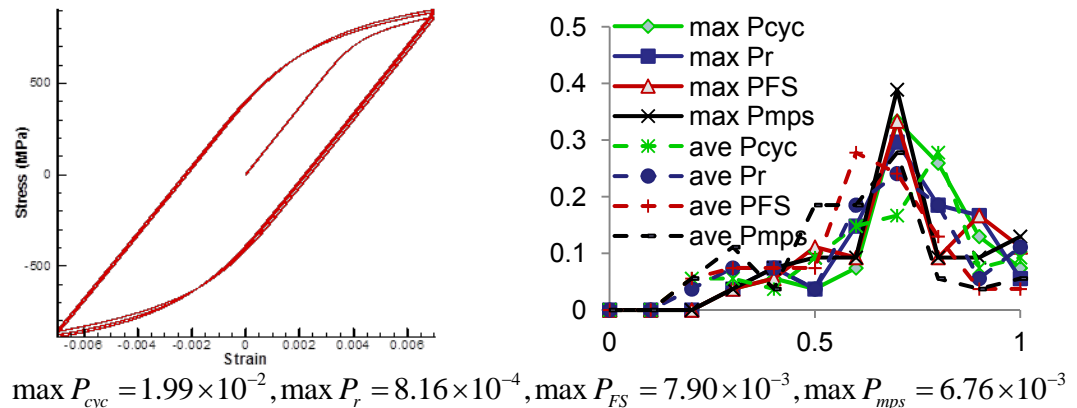
- ❑ Polycrystalline microstructures with homogenized grains implemented in the Taylor model and FEM.
- ❑ Initial input samples: 1000 randomly generated microstructures composed of 54 grains represented by grain size and texture features.



Taylor



FEM



Generation of Initial Samples

□ Initial texture: obtained by a sequence of random processing simulations with various deformation rate

$$\mathbf{L} = \omega_1 \begin{bmatrix} 1 & 0 & 0 \\ 0 & -0.5 & 0 \\ 0 & 0 & -0.5 \end{bmatrix} + \omega_2 \begin{bmatrix} 0 & 0 & 0 \\ 0 & 1 & 0 \\ 0 & 0 & -1 \end{bmatrix} + \omega_3 \begin{bmatrix} 0 & -1 & 0 \\ 1 & 0 & 0 \\ 0 & 0 & 0 \end{bmatrix}$$

$\omega_1, \omega_2, \omega_3$ are random coefficients corresponding to tension/compression, rotation, and shear, respectively.

The slip systems are updated during deformation as

$$\begin{aligned} \mathbf{m}_t^\alpha &= \mathbf{F}^e(t) \mathbf{m}_0^\alpha \\ \mathbf{n}_t^\alpha &= \mathbf{F}^{e-T}(t) \mathbf{n}_0^\alpha \end{aligned}$$

□ Initial grain sizes: obtained by sampling in a lognormal distribution. The mean grain size is fixed at 0.0265 mm.

$$p(d_{gr}) = \frac{1}{d_{gr} \sqrt{2\pi\sigma^2}} \exp\left(-\frac{\ln(d_{gr}) - \mu}{2\sigma^2}\right) \quad \begin{aligned} \bar{d}_{gr} &= \exp(\mu + \sigma^2 / 2) = 0.0265 \\ \sigma &= 0.025 \end{aligned}$$

□ The above process is only for generating data having inherent correlation. After that, the only accessible information of the input is the data. No knowledge of how they are generated is assumed.

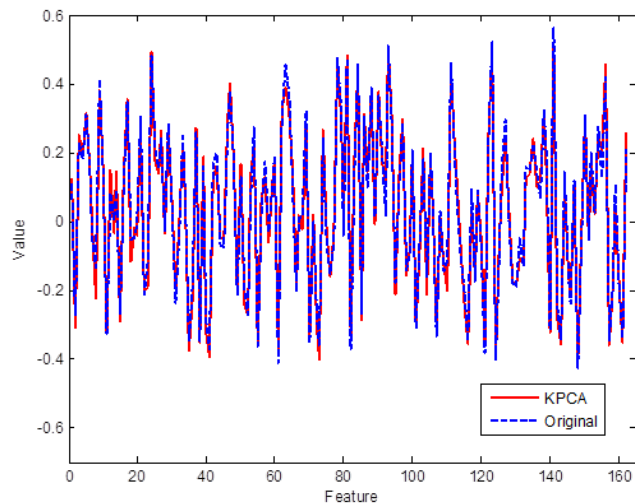
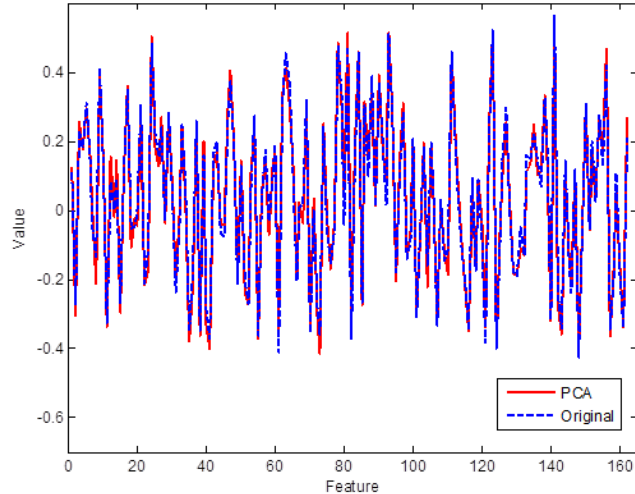


PCA/KPCA on Texture

$$f_{p1} = 0, f_{p2} = 0.42, f_{p3} = 0.11$$

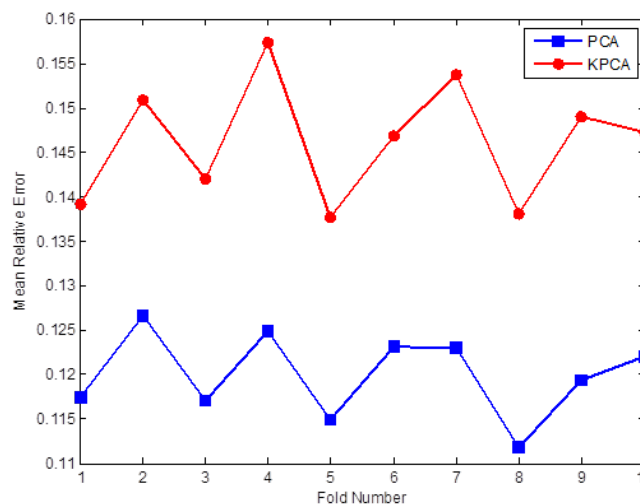
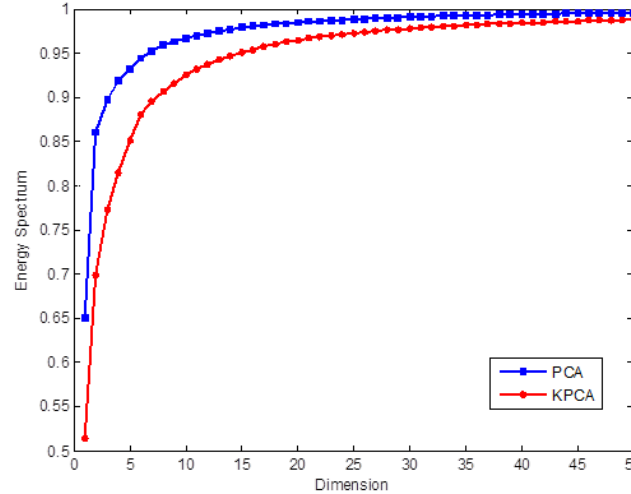
$$\varepsilon = -0.7\% \sim 0.7\%$$

$$\dot{\varepsilon} = 0.001s^{-1}$$



Reconstruct features

(reduced from 162-dim to 4dim)



4 components in PCA:91.8%

4 components in KPCA:81.5%

Energy spectrum

$$Energy = \frac{\sum_{i=1}^r \lambda_i}{\sum_{j=1}^N \lambda_j}$$

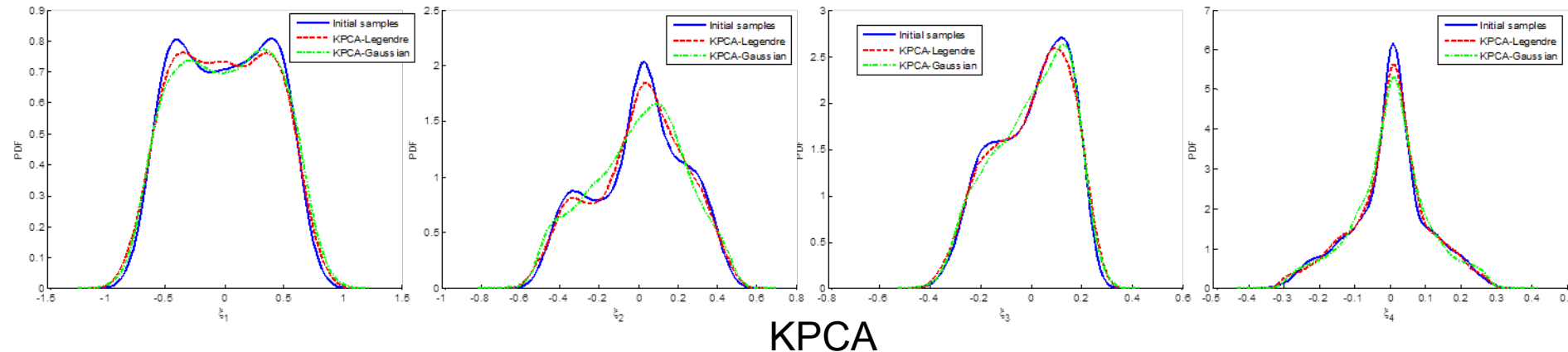
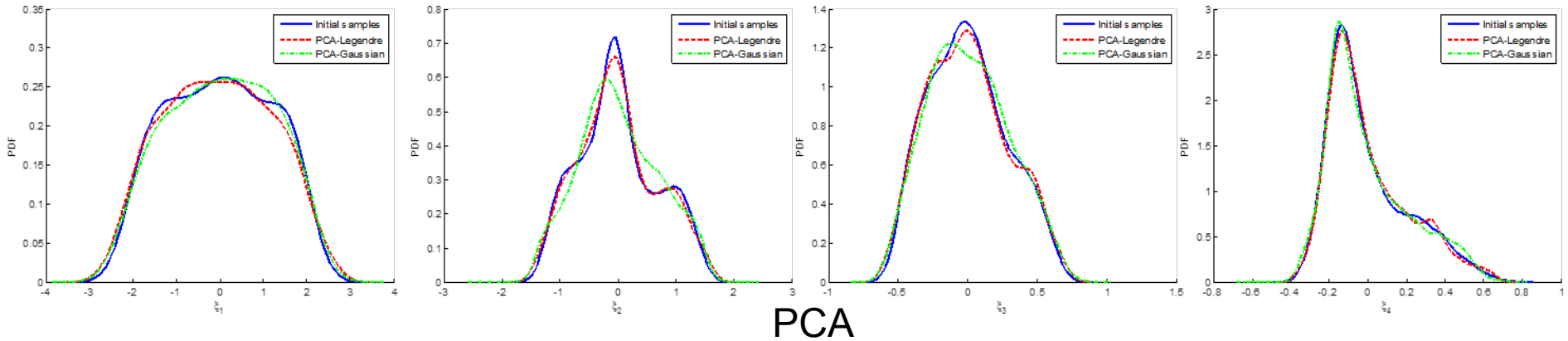
10-old cross validation

$$Err = \frac{1}{N_{test}} \sum_{i=1}^{N_{test}} \frac{\|y_i - \hat{y}_i\|}{\|y_i\|}$$



PC expansion on reduced random variables

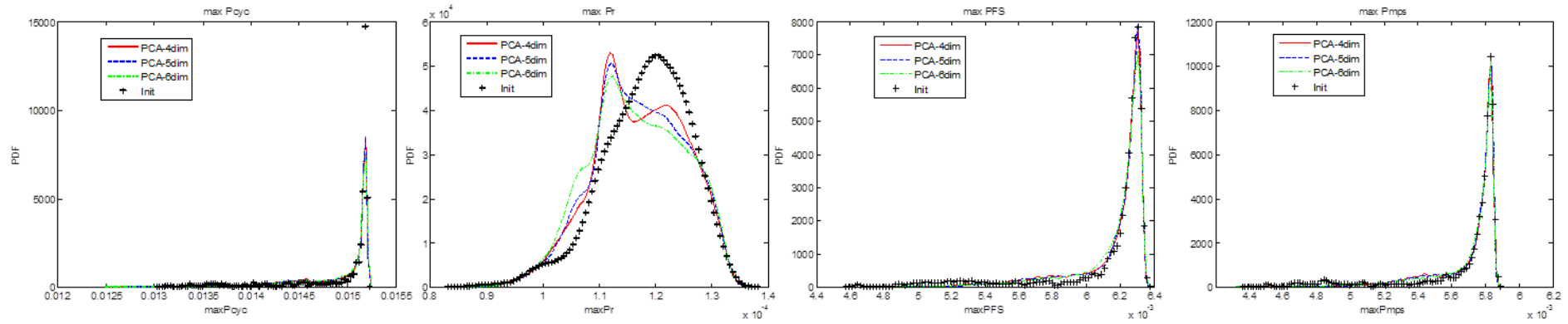
$$\xi_i = \sum_{j=0}^p \gamma_{ij} \psi_j(\eta_i), \quad i = 1, \dots, r$$



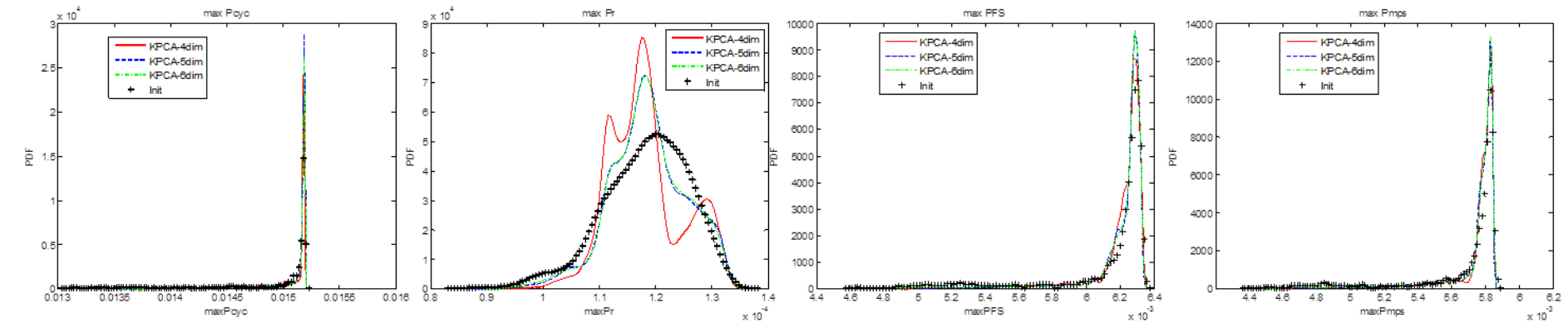
Uniform-Legendre PCs give better representation of the reduced random variables



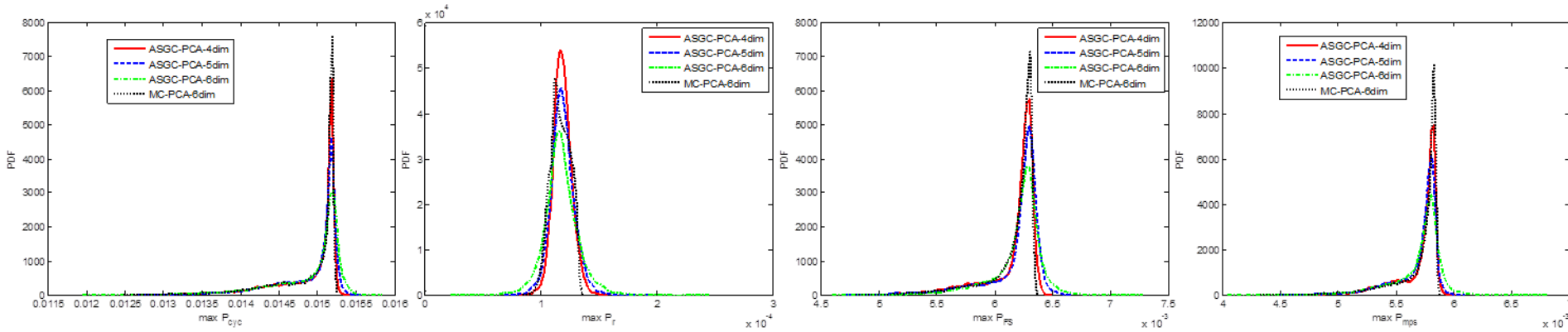
MC-PCA



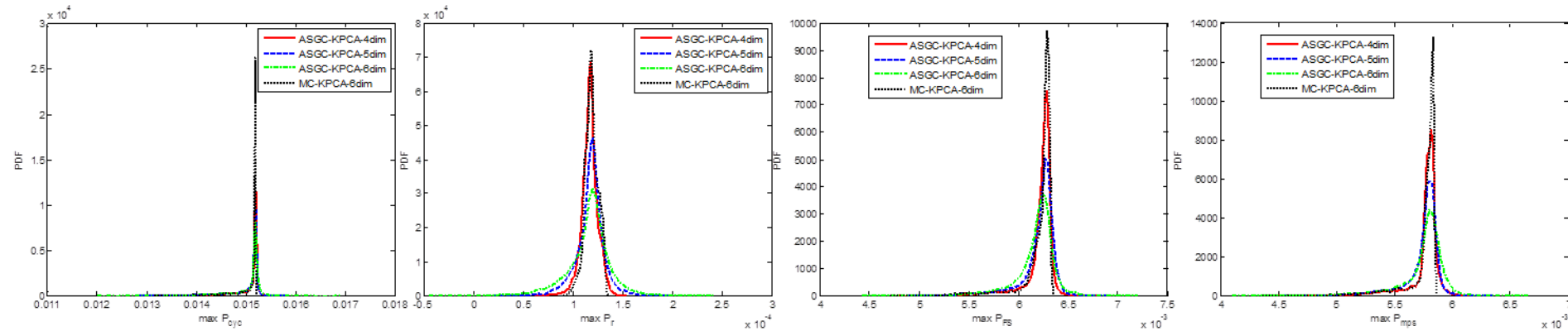
MC-KPCA



ASGC-PCA



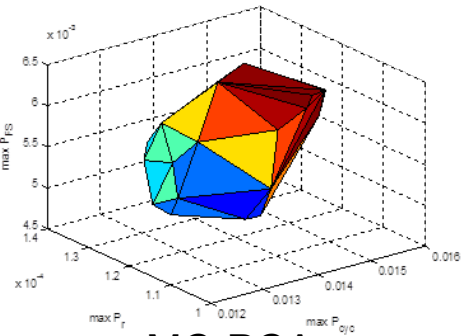
ASGC-KPCA



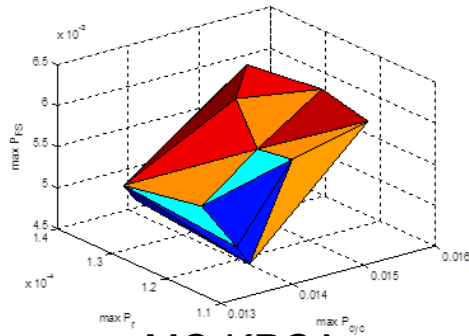
ASGC: level 8, converge to err=0.0001



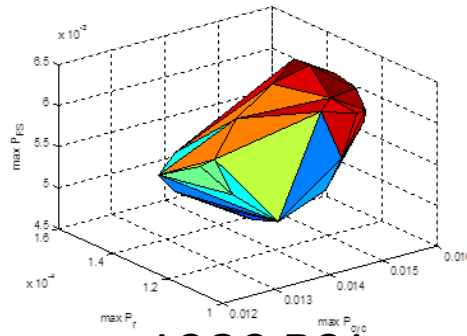
Convex Hull



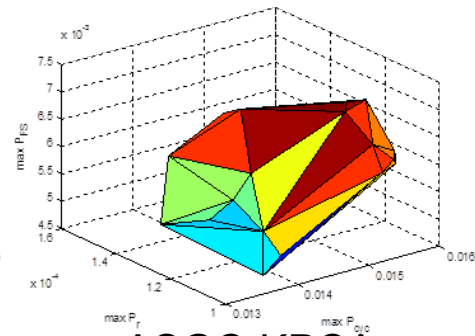
MC-PCA



MC-KPCA

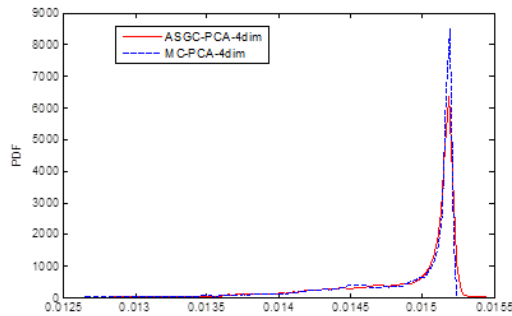


ASGC-PCA

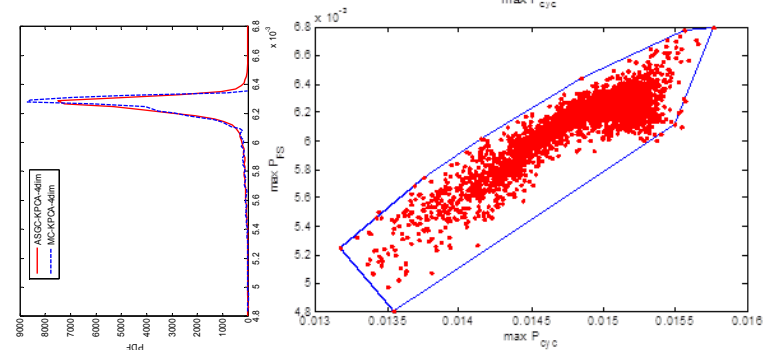
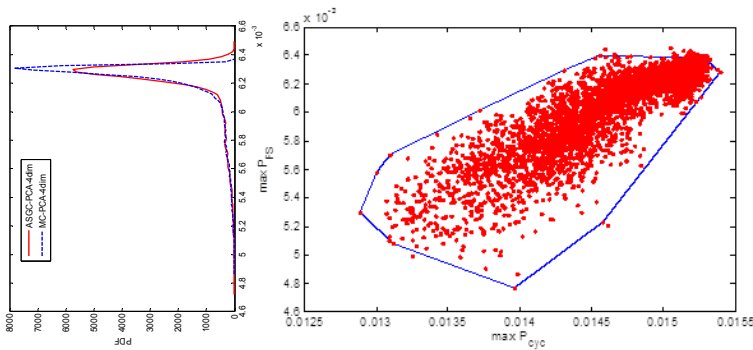
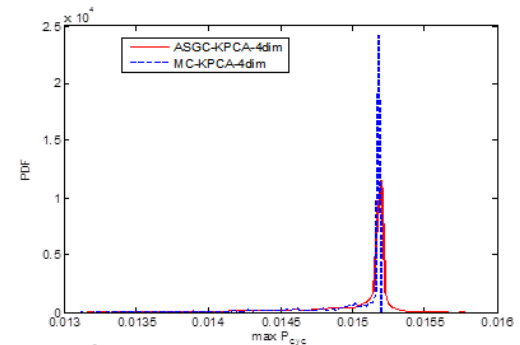


ASGC-KPCA

PCA



KPCA

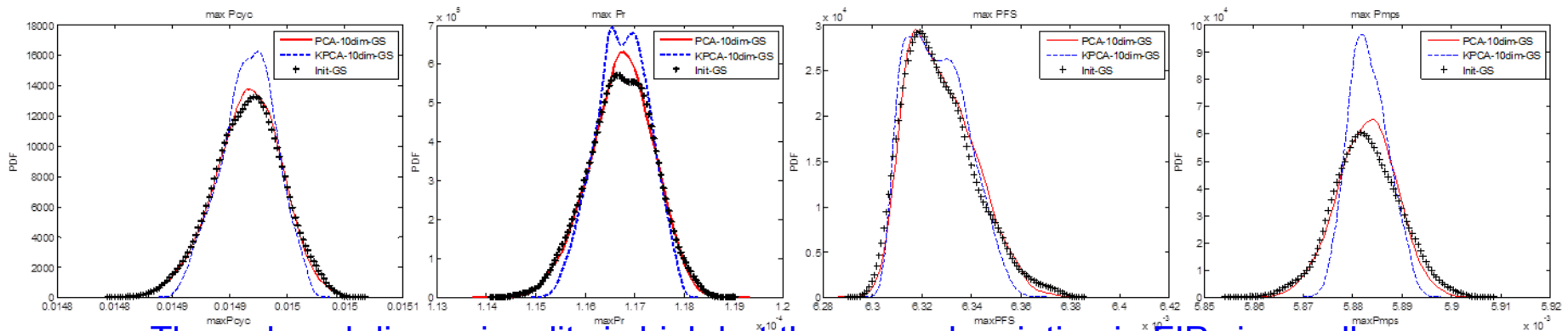


Some of the tails predicted by ASGC are not captured by MC.



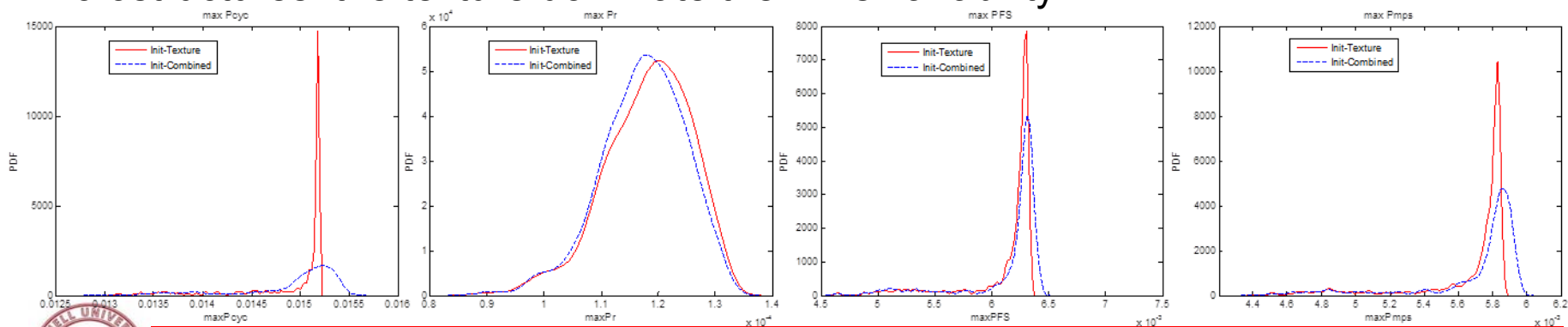
Grain Size Variation

- ❑ Fix texture and volume fractions of γ' particles, while vary the grain sizes (sampled from the lognormal distribution).
- ❑ The reduced dimensionality is taken to be 10, which captures 91.2% of the total energy by PCA, and 89.2% of the total energy by KPCA.



The reduced dimensionality is high but the caused variation in FIPs is small.

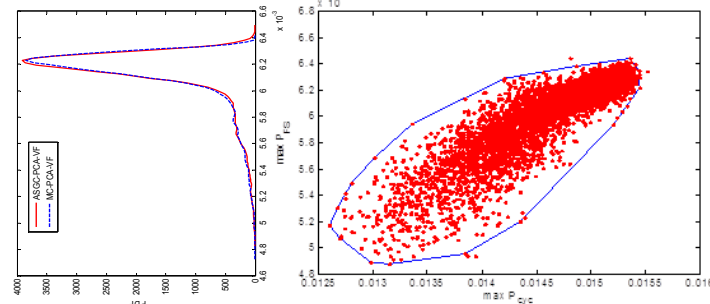
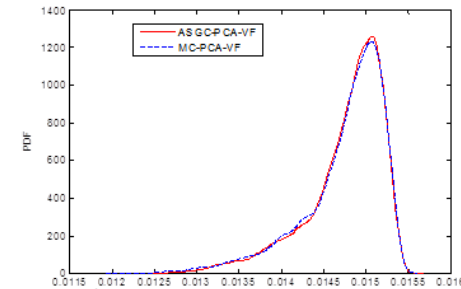
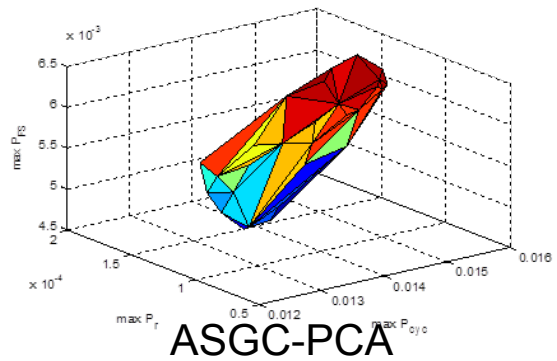
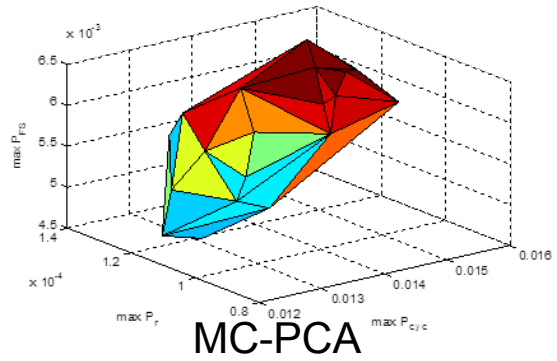
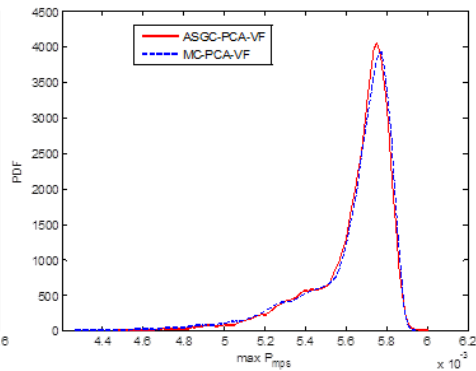
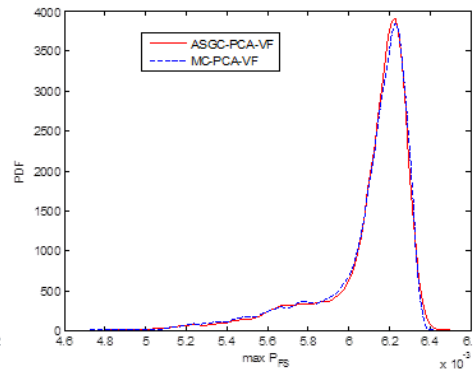
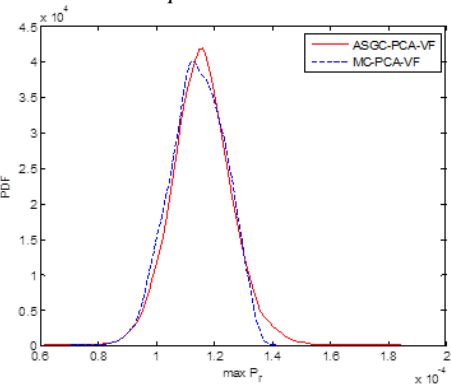
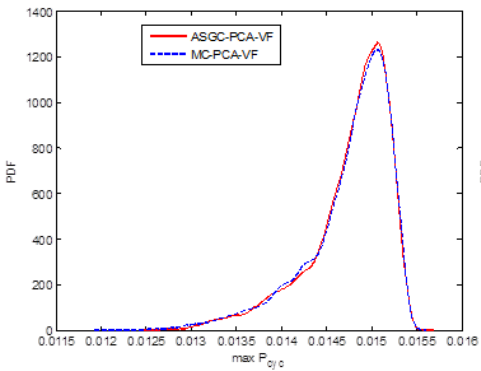
- ❑ Distributions of maximum FIPs extracted from the 1000 initial sample microstructures: the texture dominate the FIPs variability.



Combined Volume Fraction and Texture Variation

$$f_{p1} = 0, f_{p2} \sim U(0.3, 0.5), f_{p3} \sim U(0.11, 0.14)$$

Texture dim=4



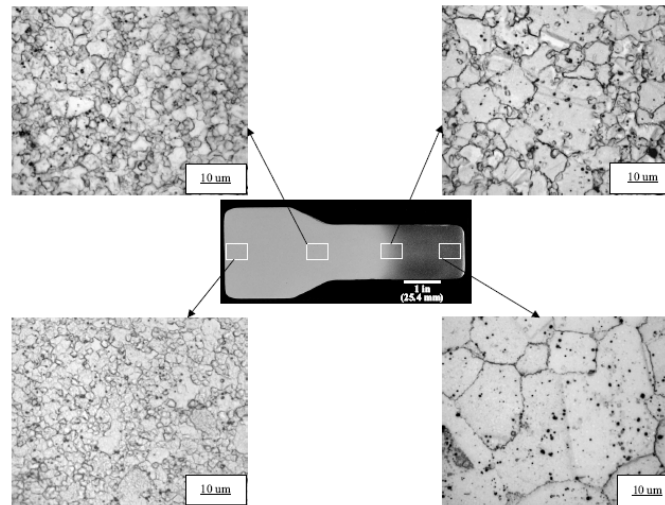
Outline

- ❑ Introduction and motivation
- ❑ Uncertainty quantification at a single material point
 - Investigating mechanical response variability of single-phase polycrystalline microstructures
 - Investigating variability of fatigue indicator parameters of two-phase nickel-based superalloy microstructures
- ❑ **Uncertainty quantification of multiscale deformation process**
- ❑ An efficient image-based method for modeling the elasto-viscoplastic behavior of realistic polycrystalline microstructures
- ❑ Conclusion and future research



Multiscale Model Reduction

- ❑ **Motivation:** Microstructure features are **location specific**. Traditional construction of reduced-order stochastic models for one point cannot see the microstructure correlation between points in the macroscale. The location dependence causes the “curse of dimensionality” in stochastic multiscale simulations.
- ❑ **Goal:** Consider the correlation of microstructures between different points. Separate random variables from coordinates. Dramatically reduce the dimensionality of the stochastic multiscale input.



Grain structures
of a nickel-base
superalloy turbine
disk having dual-
microstructures

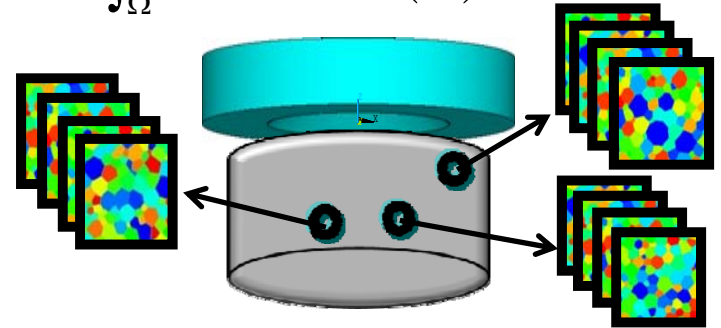
(B. Wen and N. Zabaras, 2012)



Bi-orthogonal Decomposition

- Start from realizations of the microstructure random field (\mathbf{A}) varying in both micro (\mathbf{s}) and macro-scale (\mathbf{x}): $\mathbf{A}(\mathbf{x}, \mathbf{s}, \omega) : X \times S \times \Omega \rightarrow \mathbb{R}$
- Project \mathbf{A} to a set of bi-orthogonal bases

$$\begin{aligned} \mathbf{A}(\mathbf{x}, \mathbf{s}, \omega) &= \bar{\mathbf{A}}(\mathbf{x}, \mathbf{s}) + \tilde{\mathbf{A}}(\mathbf{x}, \mathbf{s}, \omega) & \bar{\mathbf{A}}(\mathbf{x}, \mathbf{s}) &:= \int_{\Omega} \mathbf{A}(\mathbf{x}, \mathbf{s}, \omega) p(\omega) d\omega \\ &= \bar{\mathbf{A}}(\mathbf{x}, \mathbf{s}) + \sum_{i=1}^{\infty} \sqrt{\rho_i} \Psi_i(\mathbf{s}) \Phi_i(\mathbf{x}, \omega) \\ &\approx \bar{\mathbf{A}}(\mathbf{x}, \mathbf{s}) + \sum_{i=1}^d \sqrt{\rho_i} \Psi_i(\mathbf{s}) \Phi_i(\mathbf{x}, \omega) \end{aligned}$$



- The inner product in the microstructure domain is denoted as

$$(\Psi_i, \Psi_j) := \int_S \Psi_i(\mathbf{s}) \Psi_j(\mathbf{s}) ds$$

- The inner product in the spatial domain is defined as

$$\{\Phi_i, \Phi_j\} := \int_X \langle \Phi_i(\mathbf{x}, \omega) \cdot \Phi_j(\mathbf{x}, \omega) \rangle d\mathbf{x}$$

- The orthogonality conditions:

$$(\Psi_i, \Psi_j) = \delta_{ij} \quad \{\Phi_i, \Phi_j\} = \delta_{ij}$$

(D. Venturi, X. Wan and G.M. Karniadakis, 2008; B. Kouchmeshky and N. Zabarar, 2010)



Bi-orthogonal Decomposition

- By minimizing the distance between the Karhunen-Loeve expansion and the random field, the microscale basis can be computed by

$$\Psi_i(\mathbf{s}) = \frac{1}{\sqrt{\rho_i}} \{ \tilde{\mathbf{A}}, \Phi_i \}$$

- The macroscale basis is obtained through orthogonality condition

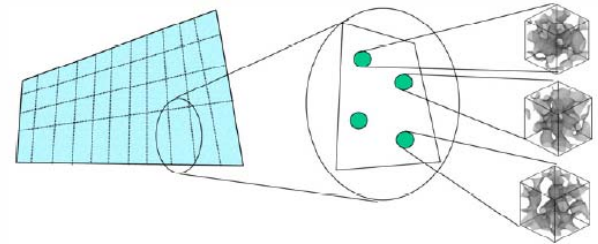
$$\Phi_i(\mathbf{x}, \omega) = \frac{1}{\sqrt{\rho_i}} \int_S \tilde{\mathbf{A}}(\mathbf{x}, \mathbf{s}, \omega) \Psi_i(\mathbf{s}) ds$$

- The eigenvalue problem in K-L expansion can be defined as

$$\rho_i \Psi_i(\mathbf{s}) = \int_S C(\mathbf{s}, \mathbf{s}') \Psi_i(\mathbf{s}') ds'$$

- The covariance matrix is

$$C(\mathbf{s}, \mathbf{s}') = \{ \tilde{\mathbf{A}}(\mathbf{x}, \mathbf{s}, \omega), \tilde{\mathbf{A}}(\mathbf{x}, \mathbf{s}', \omega) \}$$



Or in discrete form:
$$C(\mathbf{s}, \mathbf{s}') = \frac{1}{n_r} \sum_{j=1}^{n_r} \sum_{i_n=1}^{n_{el}} \sum_{i_m=1}^{n_{int}} \tilde{\mathbf{A}}_j(\mathbf{x}_{i_m}, \mathbf{s}, \xi_j) \tilde{\mathbf{A}}_j^T(\mathbf{x}_{i_m}, \mathbf{s}', \xi_j) \hat{W}_{i_m} |J_{i_n}|$$

if realizations of the random field are given as $\mathbf{A}_i(\mathbf{x}, \mathbf{s}, \omega_i)$, where $i = 1, \dots, n_r$



Second Level KLE

- The random field $\mathbf{A}(\mathbf{x}, \mathbf{s}, \omega)$ is decomposed into a set of microscale modes $\Psi_i(\mathbf{s})$ and spatial-random coupled modes $\Phi_i(\mathbf{x}, \omega)$.
- $\Phi_i(\mathbf{x}, \omega)$ is still high-dimensional. By assuming **independence** of these macromodes, the random variable can be further separated from spatial modes via a second level KLE

$$\Phi_i(\mathbf{x}, \omega) \approx \bar{\Phi}_i(\mathbf{x}) + \sum_{j=1}^{r_i} \sqrt{\lambda_i^j} \psi_i^j(\mathbf{x}) \phi_i^j(\omega) \quad i=1, \dots, d$$

- λ_i^j and ψ_i^j are eigenvalues and eigenvectors, respectively, of the covariance matrix

$$\tilde{C}_i = \frac{1}{N-1} \sum_{k=1}^N (\Phi_i^k - \bar{\Phi}_i)^T (\Phi_i^k - \bar{\Phi}_i)$$

- The dimensionality of the reduced representation of the i th macromode Φ_i is r_i . The total dimensionality r of the reduced space of feature $\mathbf{A}(\mathbf{x}, \mathbf{s}, \omega)$ is then the sum of all r_i .

$$r = \sum_i^d r_i$$



Polynomial Chaos Expansion

- After performing the second level KLE on macro modes $\Phi_i(\mathbf{x}, \omega)$, we separate the randomness from spatial coordinates. The random term $\varphi_i^j(\omega)$ can be mapped to well-shaped distribution by polynomial chaos expansion (PCE):

$$\varphi_i^j(\omega) = \sum_k \gamma_i^{jk} \Upsilon_i^k(\zeta_i^j(\omega))$$

The choice of polynomial Υ_i^k of random variable ζ_i^j that follows well-shaped distribution (e.g. Gaussian or Uniform) depends on the specific distribution of ζ_i^j .

- In the current work, we choose ζ_i^j to be uniformly distributed between -1 and 1. Therefore, Υ_i^k are Legendre polynomials. The coefficients of the PCE can be computed by

$$\gamma_i^{jk} = \frac{\langle \varphi_i^j(\zeta_i^j) \Upsilon_i^k(\zeta_i^j) \rangle}{\langle (\Upsilon_i^k(\zeta_i^j))^2 \rangle} = \frac{2k+1}{2} \int_{-1}^1 \varphi_i^j(\zeta_i^j) \Upsilon_i^k(\zeta_i^j) d\zeta_i^j$$

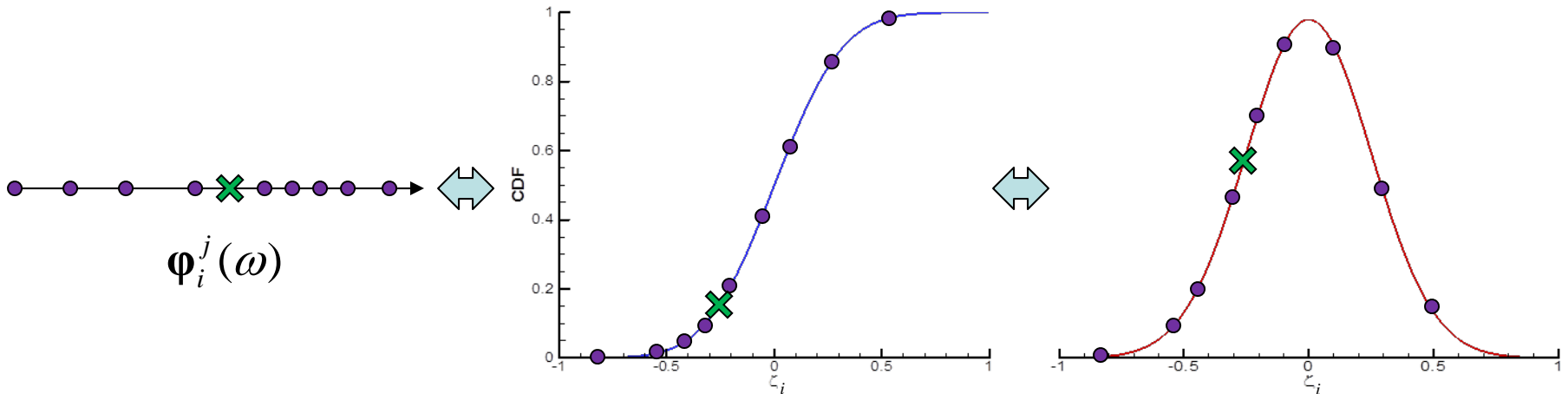
$$i = 1, \dots, d; \quad j = 1, \dots, r_i; \quad k = 0, \dots, p$$



Non-intrusive Mapping

- $\Phi_i^j(\omega)$ is non-linearly mapped to ζ_i^j through cumulative density function (CDF) and based on the given realizations:

$$\Phi_i^j(\omega) = \Gamma_i^j(\zeta_i^j), \Gamma_i^j = F_{\Phi_i^j}^{-1} \circ F_{\zeta_i^j}$$

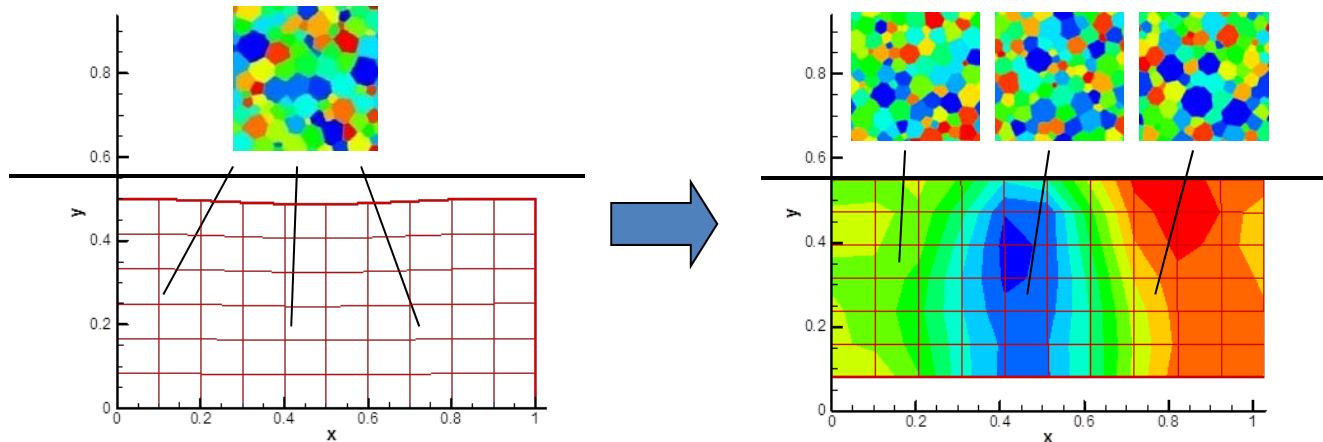


- Two assumptions were made during this Bi-orthogonal KLE-second level KLE-PCE process:
 - Assumption 1: the random variable ω is independent from microscale and macroscale coordinates (\mathbf{x} and \mathbf{s}).
 - Assumption 2: $\Phi_i, i = 1, \dots, d$ are independent from each other.



Initial Samples

- ❑ The input to the stochastic simulation is a set of ingot samples whose microstructures at different points are random but correlated.
- ❑ The input ingots are resulted from pre-processes.
- ❑ To obtain the random input ingots having correlated microstructures, we generate them through a random deformation process.
 - A set of workpieces whose surfaces are randomly curved are pushed against a flat die.
 - The microstructures at all points of all the initial ingots are assumed to be identical.
 - The resulted microstructures at different points of different ingots are distinct due to the random shape of the initial ingots.



Initial Surface

- The surface of initial workpieces are described by a degree 6 Bezier curve

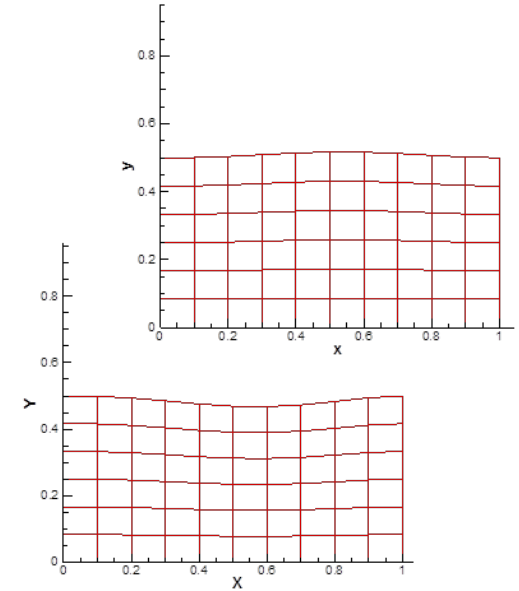
$$R_{\beta}(a, \omega) = 0.5 \left(1 + \sum_{i=0}^6 \beta_i(\omega) \varphi_i(a) \right)$$

$$\varphi_0(a) = (1-a)^6 \quad \varphi_4(a) = 15a^4(1-a)^2$$

$$\varphi_1(a) = 6a(1-a)^5 \quad \varphi_5(a) = 6a^5(1-a)$$

$$\varphi_2(a) = 15a^2(1-a)^4 \quad \varphi_6(a) = a^6$$

$$\varphi_3(a) = 20a^3(1-a)^3 \quad a = x/L$$

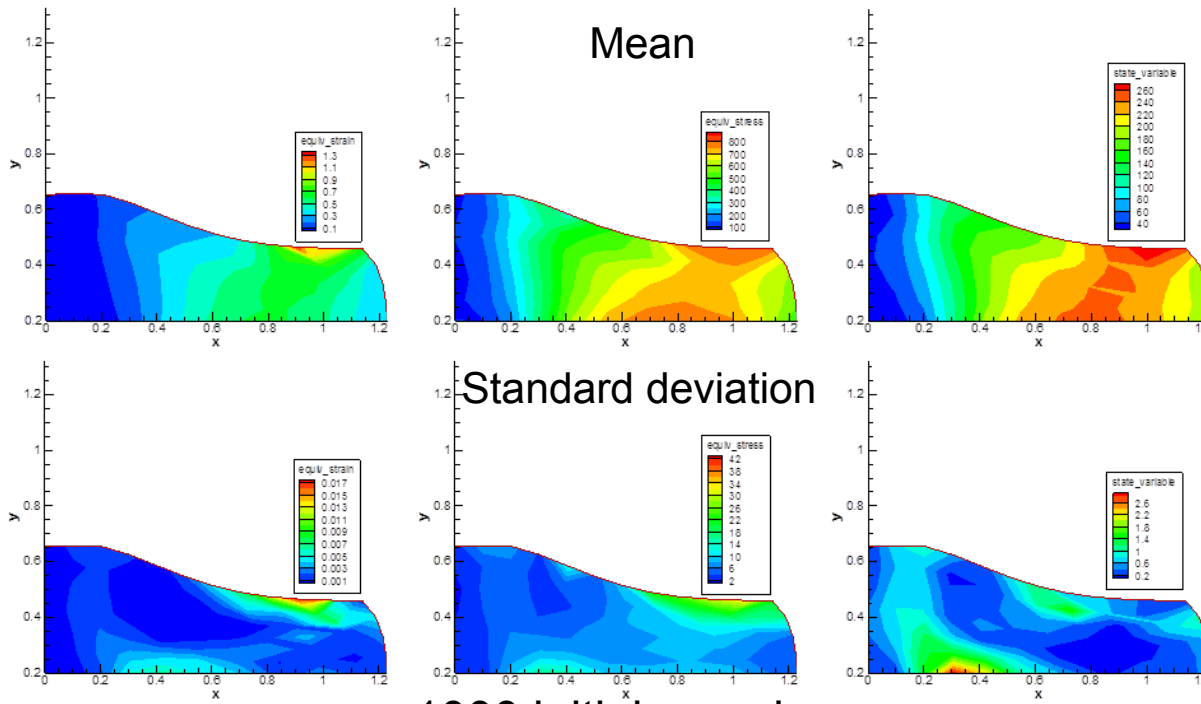


- β_i are selected to be uniformly distributed in $(-0.1, 0.1)$.
- 1000 initial samples are generated. The resulted microstructures (or more precisely, texture) are the input to the stochastic simulation.

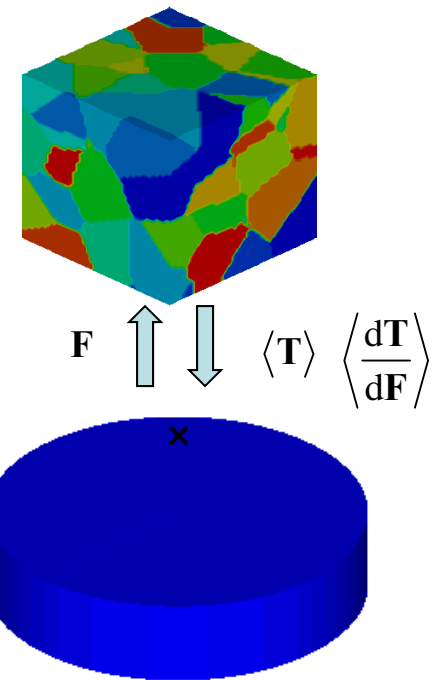


Deterministic Solver

- ❑ Each Gauss point in the macroscale is linked to a microstructure.
- ❑ The deformation of the microstructure is controlled by the local deformation gradient in the macroscale via Taylor hypothesis.
- ❑ The mechanical properties of the point is evaluated on the microstructure by crystal plasticity constitutive and homogenized.
- ❑ Homogenization: $\langle \mathbf{T} \rangle = \frac{1}{V} \int_{\mathcal{B}_{n+1}} \mathbf{T} dV$



1000 initial samples



Stochastic Input

- ❑ Mesh of the macroscale workpiece: 10x6 quadrilateral elements.
- ❑ Microstructure representation: grain sizes and orientations of 20 grains.
- ❑ Uncertainty source **A**: random textures

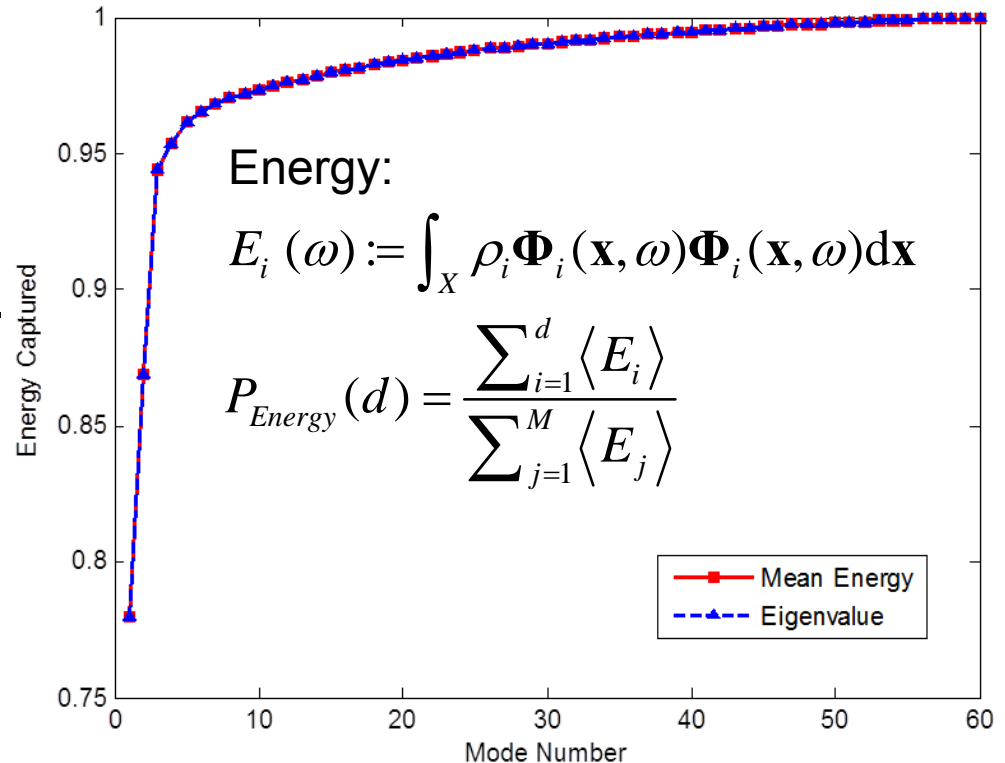
❑ The total dimensionality of the stochastic input:

$$10 \times 6 \times 4 \times 20 \times 3 = 14400.$$

❑ The first 3 macro modes are preserved which captures around 95% of the total energy.

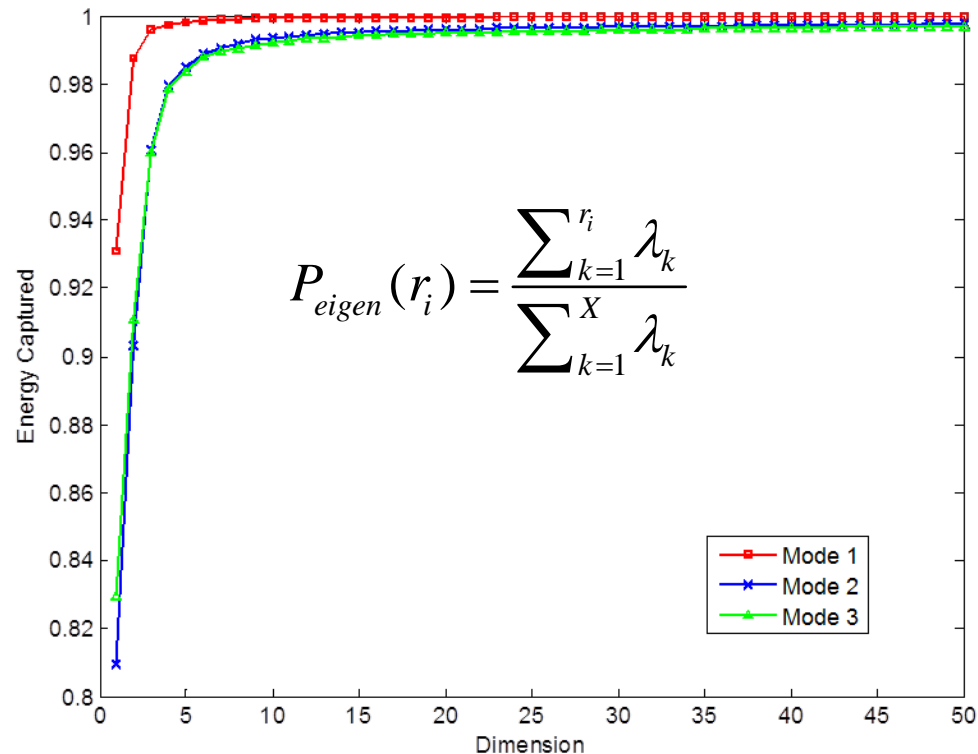
$$\tilde{\mathbf{A}}(\mathbf{x}, \mathbf{s}, \omega) \approx \sum_{i=1}^3 \sqrt{\rho_i} \Psi_i(\mathbf{s}) \Phi_i(\mathbf{x}, \omega)$$

❑ The expectation of macro modes energy is identical to the corresponding eigenvalue.



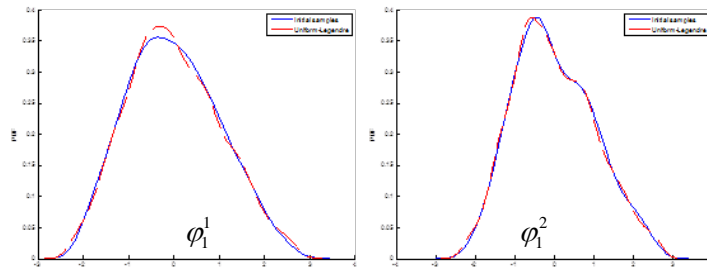
The Second Level KLE

- ❑ The macro modes are further decomposed by the second level KLE.
- ❑ Each decomposition preserves more than 95% of the total energy of the macro mode. The dimensionality of reduced macro modes are $r_1 = 2$, $r_2 = 3$, $r_3 = 3$, respectively. The dimensionality of the reduced space of the microstructure feature is therefore $r = r_1 + r_2 + r_3 = 8$.

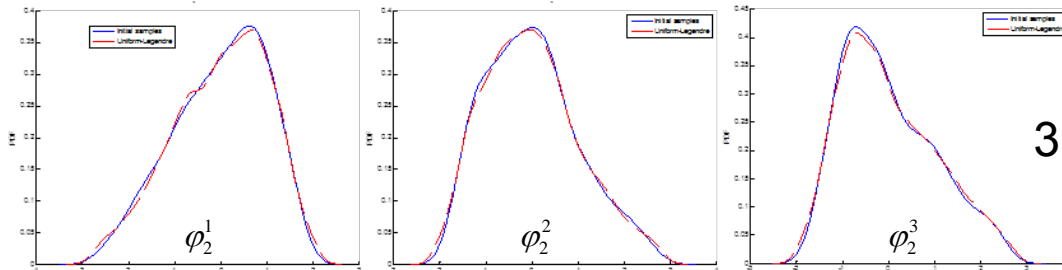


PDFs of Reduced Representations

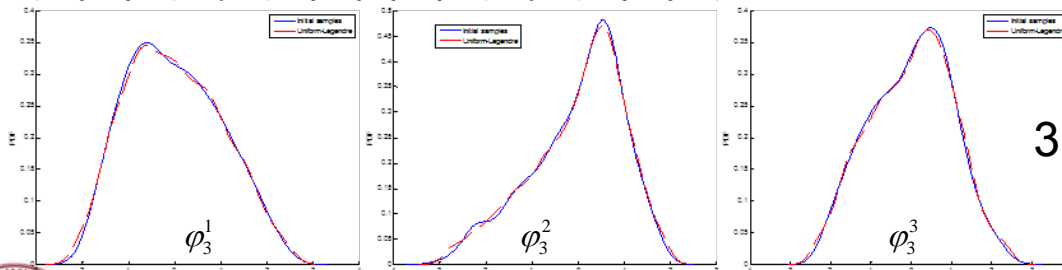
- ❑ The PDFs of reduced microstructure representations φ_i^j obtained from the model reduction on the given 1000 samples are constructed by kernel density.
- ❑ The PDFs of reconstructed φ_i^j through PCE using 10000 random samples from the uniform distribution $U(-1,1)$ are also plotted.



2 components of macro mode 1



3 components of macro mode 2

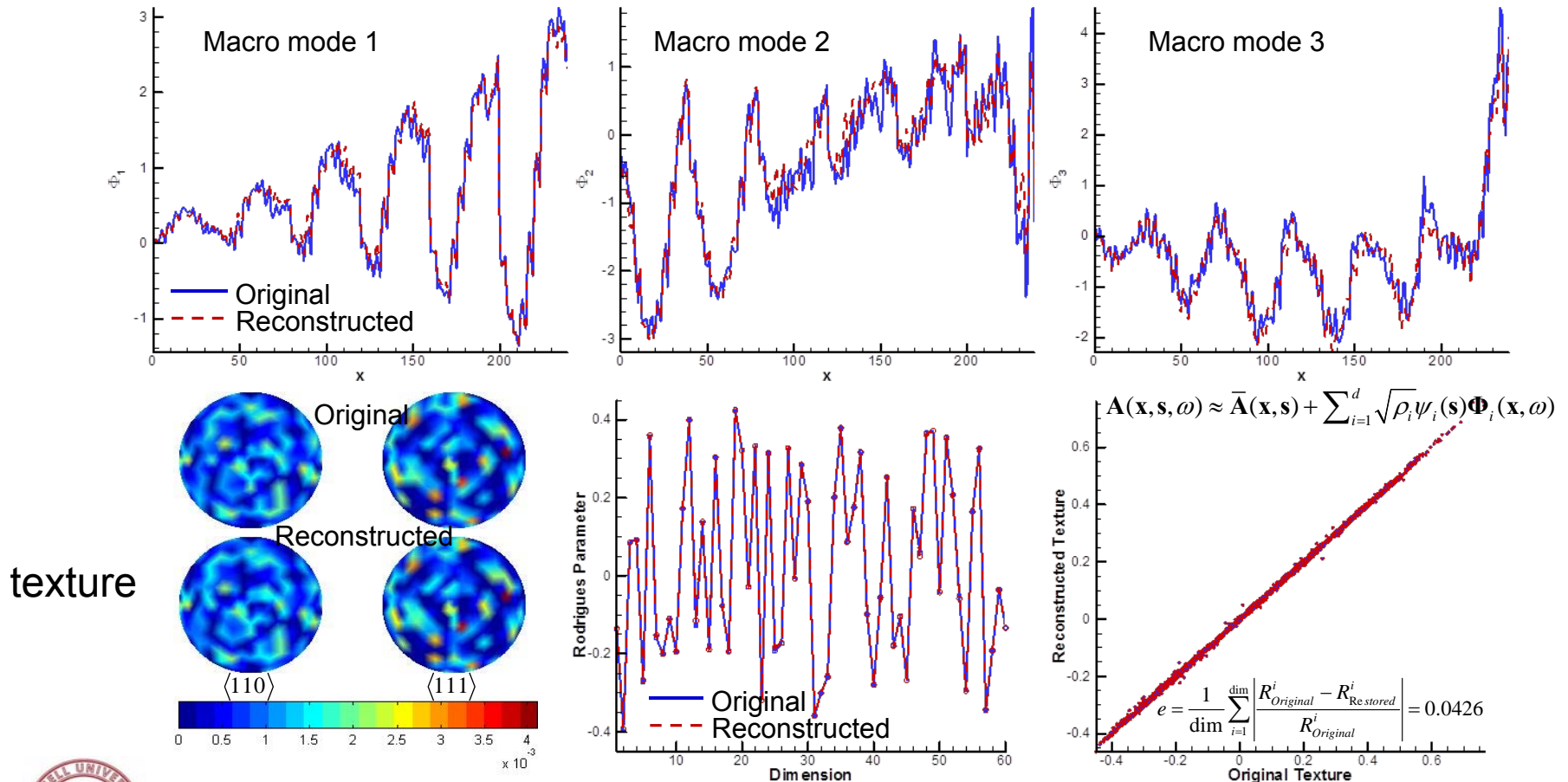


3 components of macro mode 3

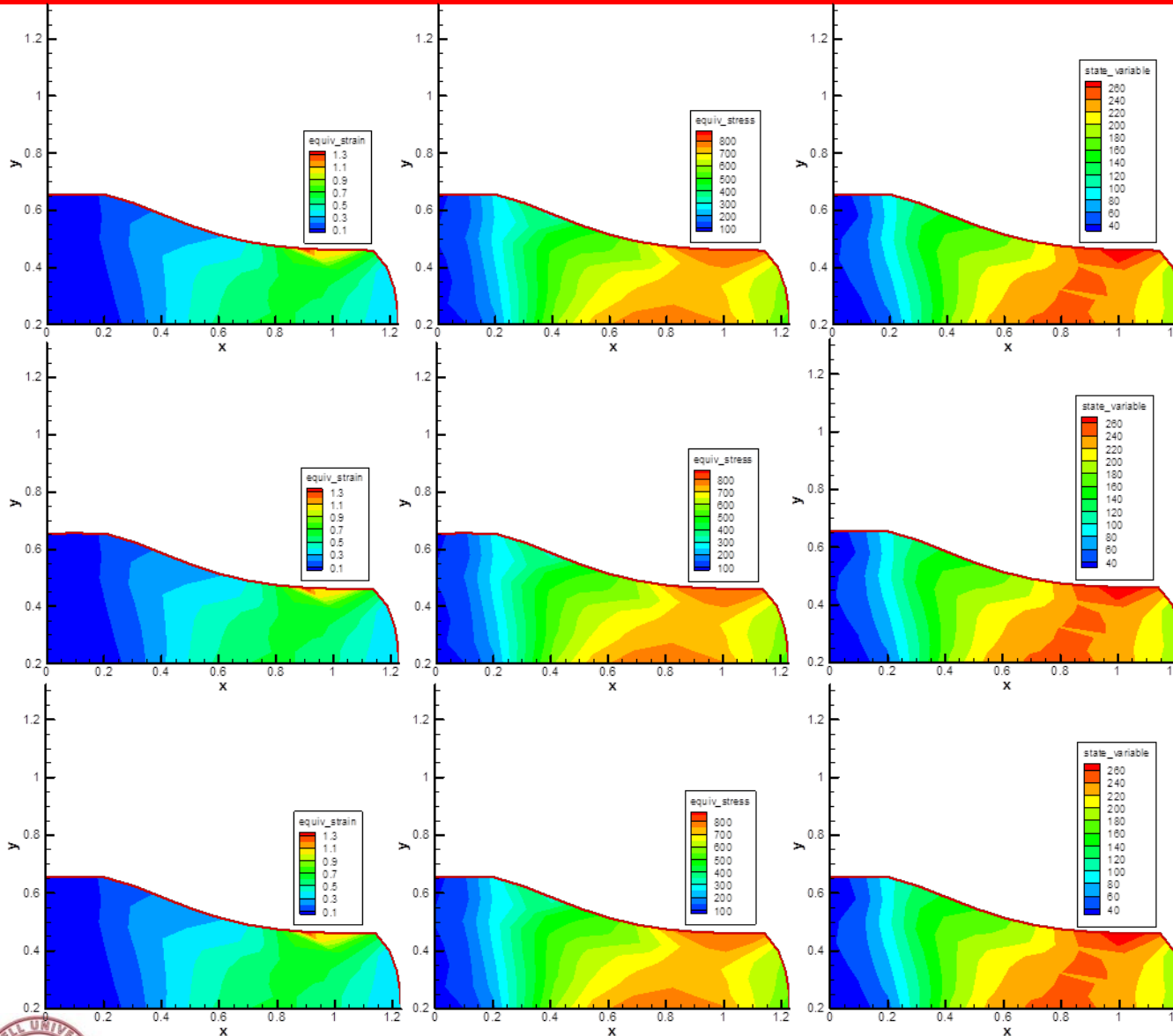


Reconstruction vs. Test Sample

- Take an arbitrary microstructure realization and project it to the reduced surrogate space. We can reconstruct the microstructure using its reduced representation.
- The first step is to reconstruct its macro modes through PCE-KLE.



Reconstructed Mean



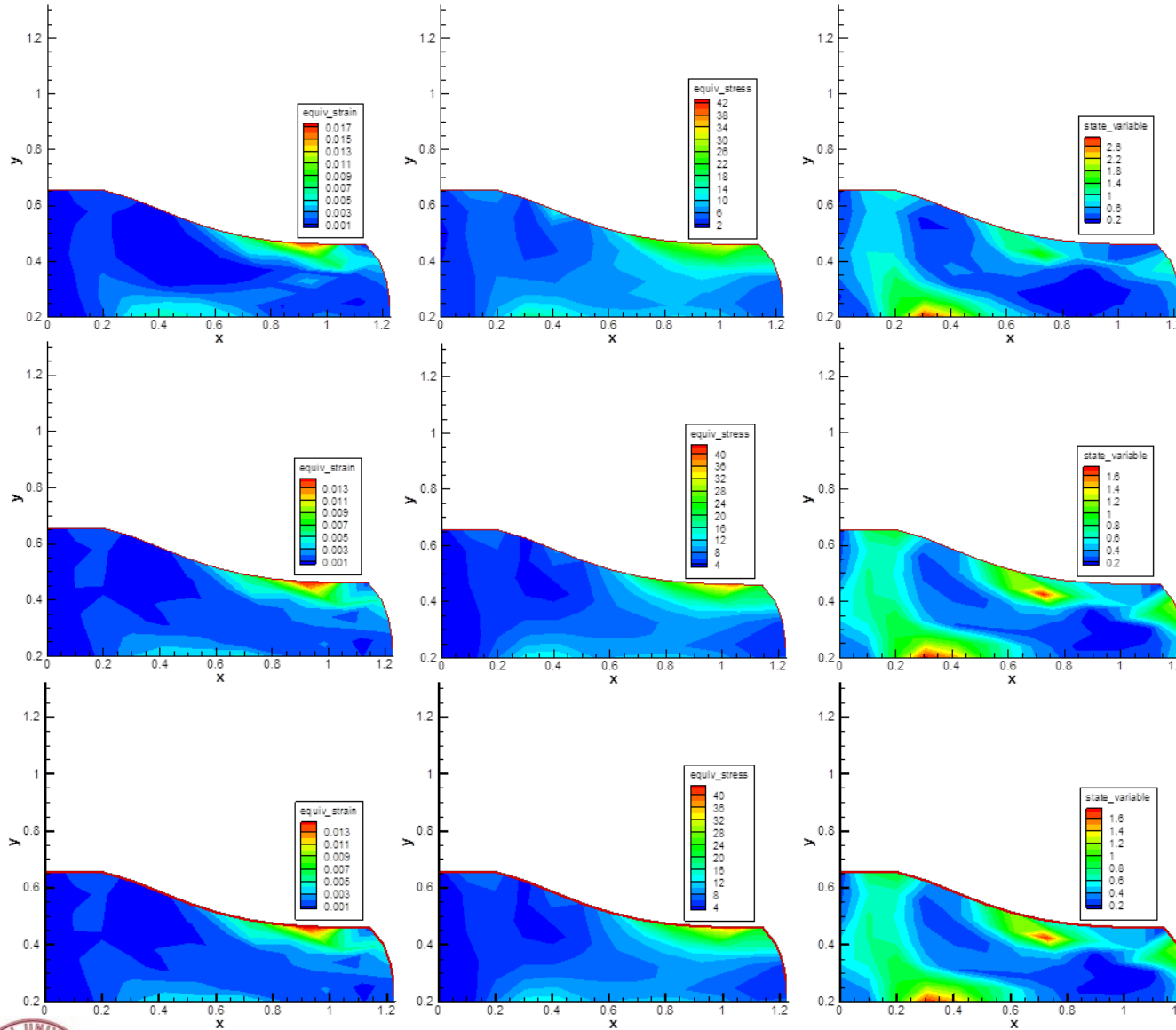
Initial samples

4032 MC
reconstructed
samples

8064 MC
reconstructed
samples



Reconstructed STD



Initial samples

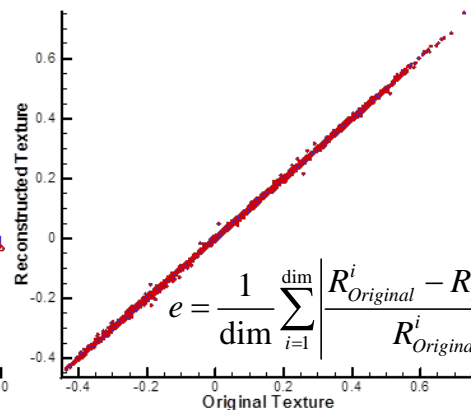
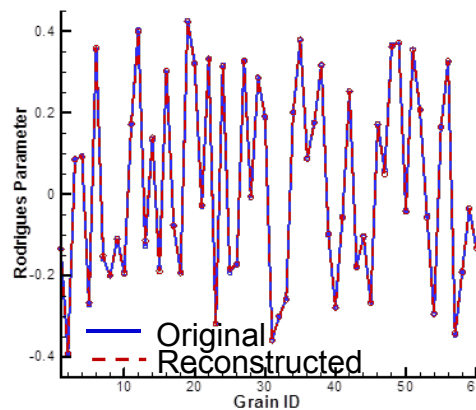
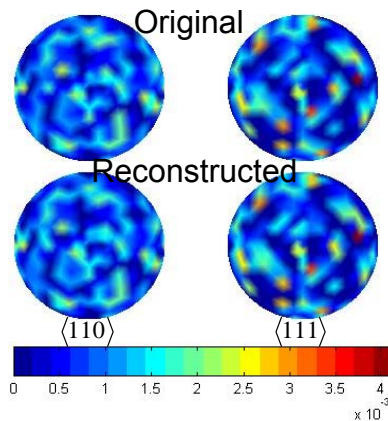
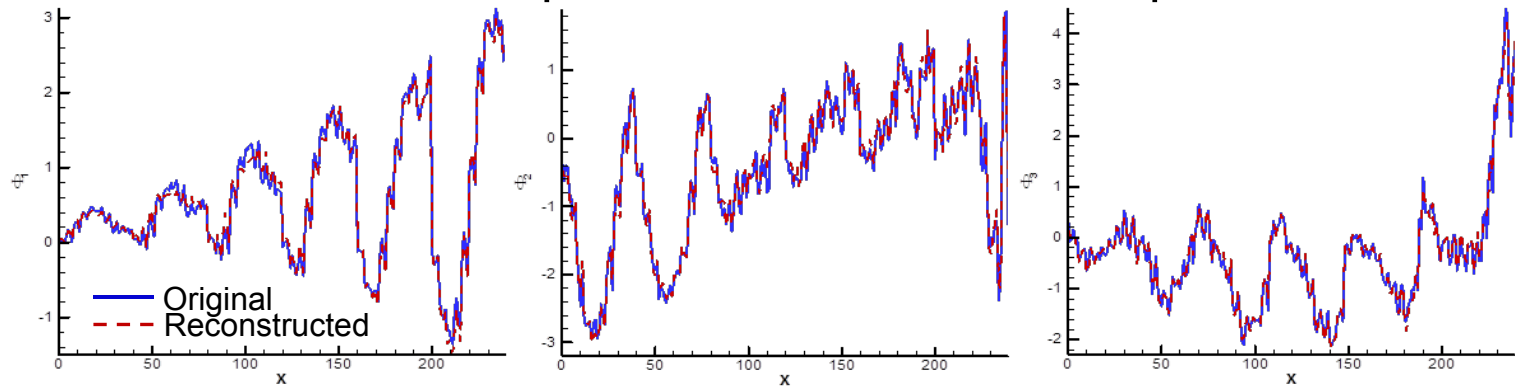
4032 MC
reconstructed
samples

8064 MC
reconstructed
samples



Increase Dimensionality of the Reduced Space

- Next, we increase the dimensionality of the reduced space to 18, so that the reduced representations capture 99% of the total energy of each macro mode: $r = r_1 + r_2 + r_3 = 3 + 7 + 8 = 18$
- The reconstructed macro modes of a single texture realization is more “realistic” than the previous 8 dimensional representation.



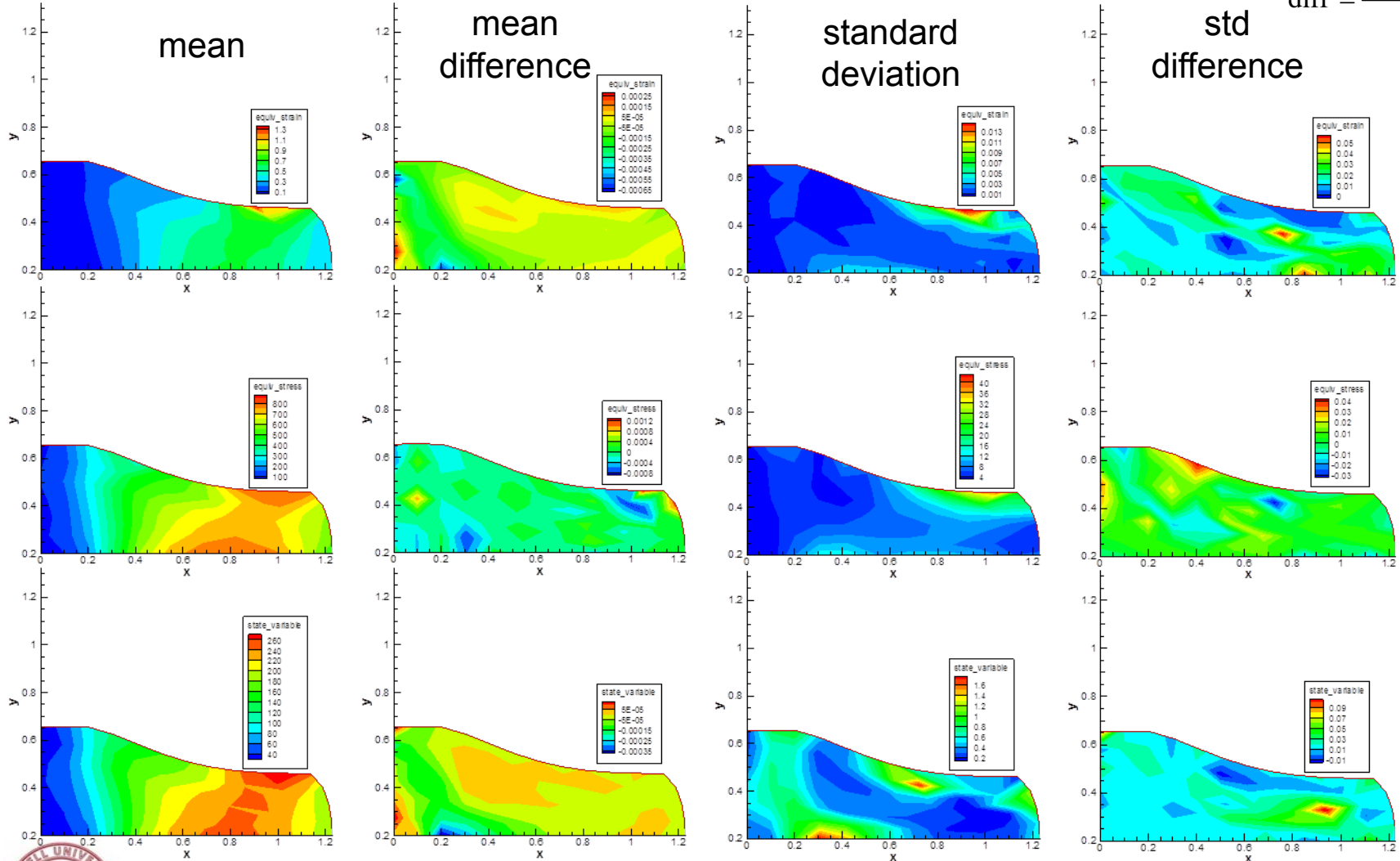
$$e = \frac{1}{\dim} \sum_{i=1}^{\dim} \left| \frac{R_{Original}^i - R_{Reconstructed}^i}{R_{Original}^i} \right| = 0.0398$$



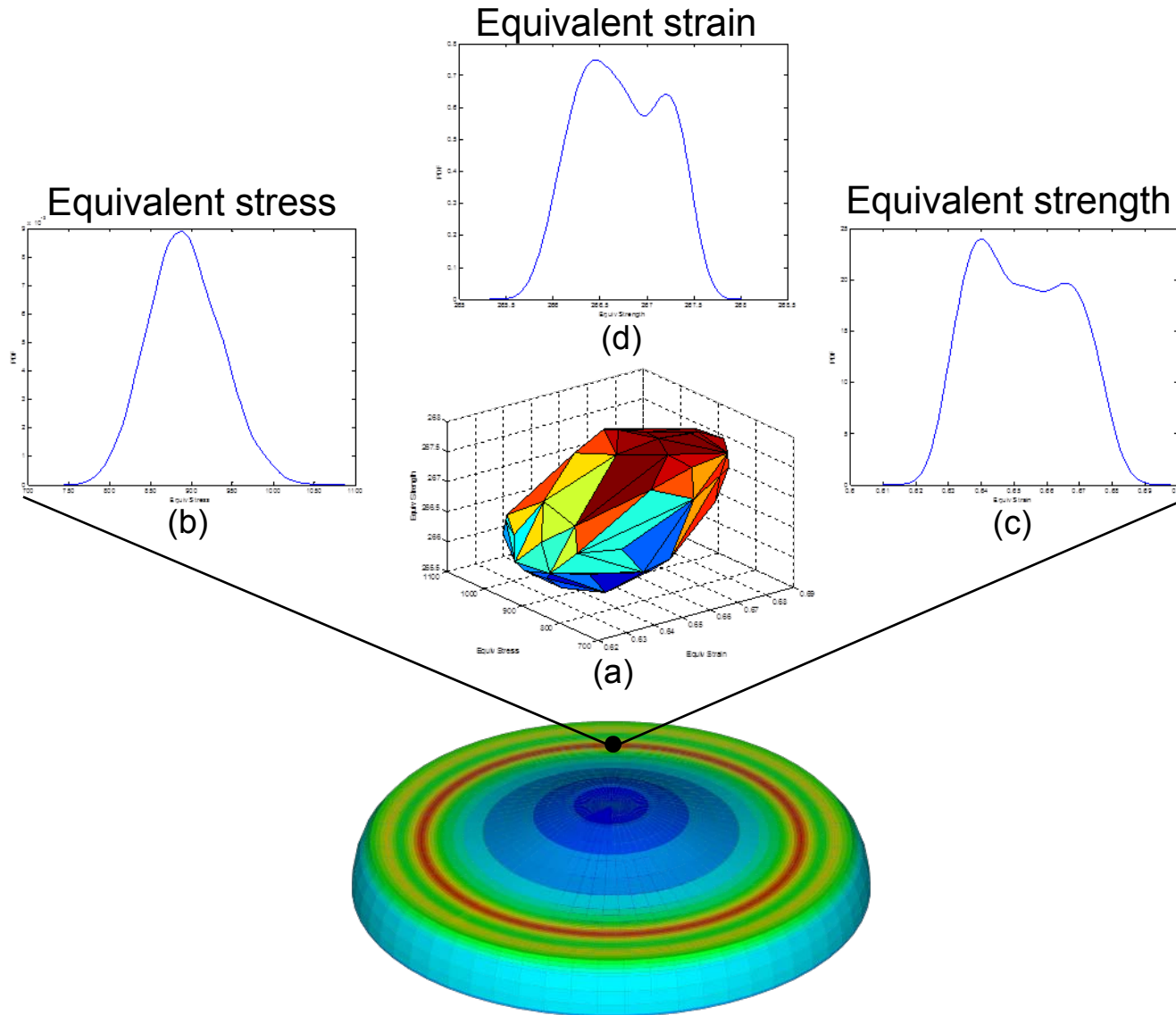
Convergence with Increasing Dimensionality

Increase the dimensionality of the reduced space to 18 (3+7+8), which captures 99% of the total energy of each macro mode.

$$\text{diff} = \frac{P_{18\text{dim}} - P_{8\text{dim}}}{P_{18\text{dim}}}$$



Statistics of One Point



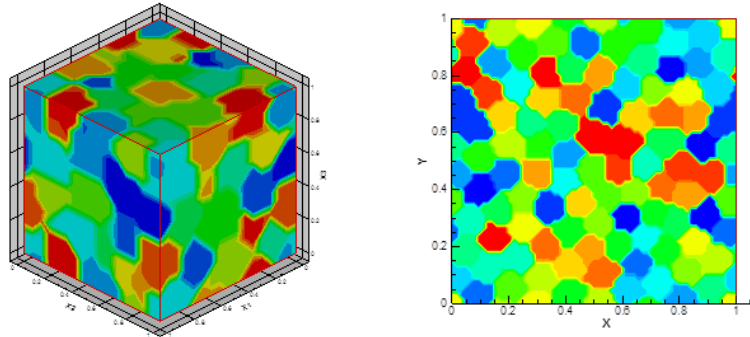
Outline

- ❑ Introduction and motivation
- ❑ Uncertainty quantification at a single material point
 - Investigating mechanical response variability of single-phase polycrystalline microstructures
 - Investigating variability of fatigue indicator parameters of two-phase nickel-based superalloy microstructures
- ❑ Uncertainty quantification of multiscale deformation process
- ❑ An efficient image-based method for modeling the elasto-viscoplastic behavior of realistic polycrystalline microstructures
- ❑ Conclusion and future research



Problem Definition

- ❑ **Goal:** Accurately and efficiently investigate effective and local mechanical properties/response of polycrystalline materials based on realistic microstructure image.



- ❑ **Solution strategy:** Green function method in combination with fast Fourier transform solving governing equations.
- ❑ **Merit:** no complex meshing, no inversion of huge matrix, consider both intergranular and intragranular interactions, take image as input.
- ❑ **New:** elasto-viscoplastic constitutive, application to fatigue properties, multigrid strategy.
- ❑ Local mechanical response of a heterogeneous medium can be calculated as a *convolution integral* between a linear **homogeneous reference** medium Green function and the **actual heterogeneous field**.
- ❑ Fast Fourier transform is introduced to reduce convolution integrals in real space to simple products in Fourier space.

(B. Wen and N. Zabaras, 2012)



Governing Equations

- ❑ The governing equations are equilibrium equations and boundary conditions. An separate formulation is proposed for solving crystal elasto-viscoplastic problems, where elastic and plastic responses are computed separately.
- ❑ Elastic problem:
 - Equilibrium (stress rate divergence): $\dot{\sigma}_{ij,j} = 0$
 - Periodic boundary conditions.
- ❑ Elasto-plastic problem:
 - Equilibrium (stress divergence): $\sigma_{ij,j} = 0$
 - Periodic boundary conditions. Incompressibility: $\dot{\epsilon}_{kk} = 0$
- ❑ Solution strategy:
 - Solve the two sets equations for elastic and plastic responses separately.
 - Represent a local quantity by the mean plus fluctuation.
 - Reform the equilibrium equation using Green function method.
 - Transform reformed equations to Fourier space through FFT.
 - Update strain related quantities in Fourier space then transform them back to real space.
 - Update stress related quantities in real space following constitutive laws.



Elasticity: Green Function Method

- Stress rate and polarization fields:

$$\dot{\boldsymbol{\sigma}}(\mathbf{x}) = \mathbf{C}_0^e : \dot{\boldsymbol{\varepsilon}}^e(\mathbf{x}) + \boldsymbol{\varphi}^e(\mathbf{x}) \quad \mathbf{C}_0^e = \langle \mathbf{C}^e \rangle_h$$

$$\boldsymbol{\varphi}^e(\mathbf{x}) = \dot{\boldsymbol{\sigma}}(\mathbf{x}) - \mathbf{C}_0^e : \dot{\boldsymbol{\varepsilon}}^e(\mathbf{x}) = \tilde{\boldsymbol{\sigma}}(\mathbf{x}) - \mathbf{C}_0^e : \tilde{\boldsymbol{\varepsilon}}^e(\mathbf{x})$$

- Equilibrium equation: $\tilde{\boldsymbol{\sigma}}_{ij,j} = C_{0ijkl}^e \tilde{\boldsymbol{\varepsilon}}_{kl,j}^e + \varphi_{ij,j}^e = C_{0ijkl}^e \tilde{v}_{k,lj}^e + \varphi_{ij,j}^e = 0$

- Solve the equilibrium equations using Green function method:

Assume solutions: $\tilde{v}_i^e = -\int_{\mathbb{R}^3} G_{im}^e(\mathbf{x} - \mathbf{x}') f_m^e(\mathbf{x}') d\mathbf{x}' \quad f_m^e(\mathbf{x}) = \varphi_{mn,n}^e(\mathbf{x})$

Substitute solutions into equilibrium equations:

$$-C_{0ijkl}^e \int_{\mathbb{R}^3} G_{km,lj}^e(\mathbf{x} - \mathbf{x}') f_m^e(\mathbf{x}') d\mathbf{x}' + \int_{\mathbb{R}^3} \delta_{im} f_m^e(\mathbf{x}') \delta(\mathbf{x} - \mathbf{x}') d\mathbf{x}' = 0$$

$$\implies \int_{\mathbb{R}^3} \left[-C_{0ijkl}^e G_{km,lj}^e(\mathbf{x} - \mathbf{x}') + \delta_{im} \delta(\mathbf{x} - \mathbf{x}') \right] f_m^e(\mathbf{x}') d\mathbf{x}' = 0$$

If $f_m^e(\mathbf{x}')$ is arbitrary $-C_{0ijkl}^e G_{km,lj}^e(\mathbf{x} - \mathbf{x}') + \delta_{im} \delta(\mathbf{x} - \mathbf{x}') = 0$

As a result: $\tilde{v}_i^e = -\int_{\mathbb{R}^3} G_{im}^e(\mathbf{x} - \mathbf{x}') \varphi_{mj,j}^e(\mathbf{x}') d\mathbf{x}'$

$$\tilde{v}_{i,k}^e = -\int_{\mathbb{R}^3} G_{im,k}^e(\mathbf{x} - \mathbf{x}') \varphi_{mj,j}^e(\mathbf{x}') d\mathbf{x}'$$

(R.A. Lebensohn, 2001)



Elasticity: Green Function Method and FFT

Integrate by parts and assume boundary terms vanish



$$\tilde{v}_i^e = \int_{\mathbb{R}^3} G_{im,j}^e(\mathbf{x} - \mathbf{x}') \varphi_{mj}^e(\mathbf{x}') d\mathbf{x}'$$

$$\tilde{v}_{i,k}^e = \int_{\mathbb{R}^3} G_{im,kj}^e(\mathbf{x} - \mathbf{x}') \varphi_{mj}^e(\mathbf{x}') d\mathbf{x}'$$

□ Transform to Fourier space:

Governing equation in Fourier space:

$$\xi_l \xi_j C_{0ijkl}^e \hat{G}_{km}^e(\xi) = -\delta_{im}$$

Solutions in Fourier space:

$$FFT(\tilde{v}_i^e) = \hat{v}_i^e = i \xi_j \hat{G}_{im}^e(\xi) \hat{\varphi}_{mj}^e(\xi)$$

$$FFT(\tilde{v}_{i,k}^e) = \hat{v}_{i,k}^e = -\xi_k \xi_j \hat{G}_{im}^e(\xi) \hat{\varphi}_{mj}^e(\xi)$$

Green operator in Fourier space:

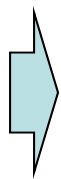
$$\hat{\Gamma}_{ijkl}^e(\xi) = -\xi_j \xi_l \hat{G}_{ik}^e(\xi) \Leftrightarrow G_{ik,jl}^e(\xi)$$

Define

$$A_{ik}^e = \xi_l \xi_j C_{0ijkl}^e$$



$$\hat{G}_{ij}^e(\xi) = -(A^{e-1})_{ij}$$



$$\hat{v}_{i,j}^e(\xi) = \hat{\Gamma}_{ijkl}^e(\xi) \hat{\varphi}_{kl}^e(\xi)$$

$$\forall \xi \neq 0 \text{ and } \hat{v}_{i,j}^e(\mathbf{0}) = 0$$

Velocity gradient fluctuation

$$\tilde{\mathcal{E}}_{ij}^e(\mathbf{x}) = 1/2 (\tilde{v}_{i,j}^e(\mathbf{x}) + \tilde{v}_{j,i}^e(\mathbf{x}))$$

$$\tilde{\omega}_{ij}^e(\mathbf{x}) = 1/2 (\tilde{v}_{i,j}^e(\mathbf{x}) - \tilde{v}_{j,i}^e(\mathbf{x}))$$

Strain rate and spin fluctuation



Viscoplasticity: Green Function and FFT Approach

- Stress and polarization fields:

$$\boldsymbol{\sigma}(\mathbf{x}) = \mathbf{C}_0^p : \dot{\boldsymbol{\varepsilon}}^p(\mathbf{x}) + \boldsymbol{\varphi}^p(\mathbf{x}) \quad \mathbf{C}_0^p = \langle \mathbf{M}^{p-1} \rangle_h$$

$$\boldsymbol{\varphi}^p(\mathbf{x}) = \boldsymbol{\sigma}(\mathbf{x}) - \mathbf{C}_0^p : \dot{\boldsymbol{\varepsilon}}^p(\mathbf{x}) = \tilde{\boldsymbol{\sigma}}(\mathbf{x}) - \mathbf{C}_0^p : \tilde{\dot{\boldsymbol{\varepsilon}}}^p(\mathbf{x})$$

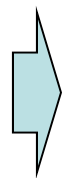
- Equilibrium equation: $\tilde{\boldsymbol{\sigma}}_{ij,j} = C_{0ijkl}^p \tilde{\dot{\boldsymbol{\varepsilon}}}_{kl,j}^p + \varphi_{ij,j}^p = C_{0ijkl}^p \tilde{v}_{k,lj}^p + \varphi_{ij,j}^p = 0$
- Equilibrium equation in Green function form:

$$-C_{0ijkl}^p G_{km,lj}^p(\mathbf{x} - \mathbf{x}') + \delta_{im} \delta(\mathbf{x} - \mathbf{x}') = 0$$

- Equilibrium equation in Fourier space:

$$\xi_l \xi_j C_{0ijkl}^p \hat{G}_{km}^p(\boldsymbol{\xi}) = -\delta_{im} \quad \hat{G}_{ij}^p(\boldsymbol{\xi}) = -\left(A_{ij}^p\right)^{-1} \quad A_{ik}^p = \xi_l \xi_j C_{0ijkl}^p$$

$$\text{Solution: } FFT(\tilde{v}_i^p) = \hat{v}_i^p = i \xi_j \hat{G}_{im}^p(\boldsymbol{\xi}) \hat{\varphi}_{mj}^p(\boldsymbol{\xi}) \quad FFT(\tilde{v}_{i,k}^p) = \hat{v}_{i,k}^p = -\xi_k \xi_j \hat{G}_{im}^p(\boldsymbol{\xi}) \hat{\varphi}_{mj}^p(\boldsymbol{\xi})$$



$$\hat{v}_{i,j}^p(\boldsymbol{\xi}) = \hat{\Gamma}_{ijkl}^p(\boldsymbol{\xi}) \hat{\varphi}_{kl}^p(\boldsymbol{\xi})$$

$$\forall \boldsymbol{\xi} \neq 0 \text{ and } \hat{v}_{i,j}^p(\mathbf{0}) = 0$$

Velocity gradient fluctuation

$$\tilde{\dot{\boldsymbol{\varepsilon}}}_{ij}^p(\mathbf{x}) = 1/2 \left(\tilde{v}_{i,j}^p(\mathbf{x}) + \tilde{v}_{j,i}^p(\mathbf{x}) \right)$$

$$\tilde{\dot{\boldsymbol{\omega}}}_{ij}^p(\mathbf{x}) = 1/2 \left(\tilde{v}_{i,j}^p(\mathbf{x}) - \tilde{v}_{j,i}^p(\mathbf{x}) \right)$$

Strain rate and spin fluctuation



Elasto-viscoplastic Solution

- The total velocity gradient combining both elastic and plastic parts at a single point is: $\nabla \mathbf{v}(\mathbf{x}) = \nabla \mathbf{V} + \nabla \tilde{\mathbf{v}}^e(\mathbf{x}) + \nabla \tilde{\mathbf{v}}^p(\mathbf{x})$

- Total strain rate: $\dot{\boldsymbol{\varepsilon}}_{ij}(\mathbf{x}) = 1/2(v_{i,j}(\mathbf{x}) + v_{j,i}(\mathbf{x}))$

- Elastic strain rate is computed following a Newton-Raphson process

$$\dot{\boldsymbol{\varepsilon}}_{i+1}^e(\mathbf{x}) = \dot{\boldsymbol{\varepsilon}}_i^e(\mathbf{x}) - \left[\frac{d\mathbf{F}}{d\dot{\boldsymbol{\varepsilon}}^e} \right]^{-1} \mathbf{F}_i(\dot{\boldsymbol{\varepsilon}}_i^e(\mathbf{x})) \quad \mathbf{F}(\dot{\boldsymbol{\varepsilon}}^e(\mathbf{x})) = \dot{\boldsymbol{\varepsilon}}^e(\mathbf{x}) + \dot{\boldsymbol{\varepsilon}}^p(\mathbf{x}) - \dot{\boldsymbol{\varepsilon}}(\mathbf{x}) = \mathbf{0}$$

$$\frac{d\mathbf{F}}{d\dot{\boldsymbol{\varepsilon}}^e} = \frac{d\dot{\boldsymbol{\varepsilon}}^e}{d\dot{\boldsymbol{\varepsilon}}^e} + \frac{d\dot{\boldsymbol{\varepsilon}}^p}{d\dot{\boldsymbol{\varepsilon}}^e} = \mathbf{I}_4 + \frac{d\dot{\boldsymbol{\varepsilon}}^p}{d\boldsymbol{\sigma}} \frac{d\boldsymbol{\sigma}}{d\dot{\boldsymbol{\varepsilon}}^e} = \mathbf{I}_4 + \mathbf{M}_t^p : dt\mathbf{I}_4 : \mathbf{C}^e$$

- Plastic strain rate: $\dot{\boldsymbol{\varepsilon}}^p(\mathbf{x}) = \dot{\boldsymbol{\varepsilon}}(\mathbf{x}) - \dot{\boldsymbol{\varepsilon}}^e(\mathbf{x}) \quad \dot{\boldsymbol{\varepsilon}}^p(\mathbf{x}) = \dot{\boldsymbol{\varepsilon}}^p(\mathbf{x}) - \frac{1}{3} \text{trace}(\dot{\boldsymbol{\varepsilon}}^p(\mathbf{x}))$

- Stress and stress rate: $\dot{\boldsymbol{\sigma}}(\mathbf{x}) = \mathbf{C}^e(\mathbf{x}) : \dot{\boldsymbol{\varepsilon}}^e(\mathbf{x}) \quad \boldsymbol{\sigma}(\mathbf{x}) = \mathbf{C}^p(\boldsymbol{\sigma}(\mathbf{x})) : \dot{\boldsymbol{\varepsilon}}^p(\mathbf{x})$

- Polarizations for the next iteration:

$$\boldsymbol{\varphi}^e(\mathbf{x}) = \dot{\boldsymbol{\sigma}}(\mathbf{x}) - \mathbf{C}_0^e : \dot{\boldsymbol{\varepsilon}}^e(\mathbf{x})$$

$$\boldsymbol{\varphi}^p(\mathbf{x}) = \boldsymbol{\sigma}(\mathbf{x}) - \mathbf{C}_0^p : \dot{\boldsymbol{\varepsilon}}^p(\mathbf{x})$$



Algorithm-Basic Formulation

- Basic formulation: based on the exact expression of Green function for linear elastic, homogeneous reference material.

For each time step, the iterative algorithm can be:

(1) At the beginning of the 1st iteration, give an initial guess to the total velocity gradient: ${}_{n+1}^0 \nabla \mathbf{v}(\mathbf{x}) = {}_n \nabla \mathbf{v}(\mathbf{x})$. Then compute initial elastic and plastic strain rates, ${}_{n+1}^0 \dot{\boldsymbol{\epsilon}}^e(\mathbf{x})$ and ${}_{n+1}^0 \dot{\boldsymbol{\epsilon}}^p(\mathbf{x})$, as well as stress ${}_{n+1}^0 \boldsymbol{\sigma}(\mathbf{x})$ and stress rate ${}_{n+1}^0 \dot{\boldsymbol{\sigma}}(\mathbf{x})$, using elasto-plastic constitutive relations.

(2) Compute the elastic and plastic polarization fields, ${}^i \boldsymbol{\Phi}^e(\mathbf{x})$ and ${}^i \boldsymbol{\Phi}^p(\mathbf{x})$, for the i th iteration.

(3) Transform the polarization fields to Fourier space via FFT:

$${}^i \hat{\boldsymbol{\Phi}}^e(\boldsymbol{\xi}) = FFT\left({}^i \boldsymbol{\Phi}^e(\mathbf{x})\right) \quad {}^i \hat{\boldsymbol{\Phi}}^p(\boldsymbol{\xi}) = FFT\left({}^i \boldsymbol{\Phi}^p(\mathbf{x})\right)$$

(4) Compute velocity gradient fluctuations in the Fourier space at the $(i+1)$ th iteration:

$${}_{n+1}^{i+1} \nabla \hat{\mathbf{v}}^e(\boldsymbol{\xi}) = sym\left(\hat{\boldsymbol{\Gamma}}^e(\boldsymbol{\xi}) : {}^i \hat{\boldsymbol{\Phi}}^e(\boldsymbol{\xi})\right); \quad \forall \boldsymbol{\xi} \neq 0, \quad \text{and} \quad {}_{n+1}^{i+1} \nabla \hat{\mathbf{v}}^e(\mathbf{0}) = 0$$

$${}_{n+1}^{i+1} \nabla \hat{\mathbf{v}}^p(\boldsymbol{\xi}) = sym\left(\hat{\boldsymbol{\Gamma}}^p(\boldsymbol{\xi}) : {}^i \hat{\boldsymbol{\Phi}}^p(\boldsymbol{\xi})\right); \quad \forall \boldsymbol{\xi} \neq 0, \quad \text{and} \quad {}_{n+1}^{i+1} \nabla \hat{\mathbf{v}}^p(\mathbf{0}) = 0$$

(5) Transform velocity gradient fluctuations back to the real space through inverse FFT:

$${}_{n+1}^{i+1} \nabla \tilde{\mathbf{v}}^e(\mathbf{x}) = FFT^{-1}\left({}_{n+1}^{i+1} \nabla \hat{\mathbf{v}}^e(\boldsymbol{\xi})\right) \quad {}_{n+1}^{i+1} \nabla \tilde{\mathbf{v}}^p(\mathbf{x}) = FFT^{-1}\left({}_{n+1}^{i+1} \nabla \hat{\mathbf{v}}^p(\boldsymbol{\xi})\right)$$

(6) Compute strain rate, strain, and stress fields using updated velocity gradient.

(7) Check the convergence $\delta = \left| \frac{{}^{i+1} e - {}^i e}{{}^i e} \right|$ $e = \frac{\left\langle \|\text{div}({}^{i+1} \boldsymbol{\sigma})\|^2 \right\rangle^{1/2}}{\left\| \langle {}^{i+1} \boldsymbol{\sigma} \rangle \right\|} = \frac{\left\langle \|\boldsymbol{\xi} \cdot {}^{i+1} \hat{\boldsymbol{\sigma}}(\boldsymbol{\xi})\|^2 \right\rangle^{1/2}}{\left\| \langle {}^{i+1} \hat{\boldsymbol{\sigma}}(\mathbf{0}) \rangle \right\|}$ Equilibrium error

If not converged, repeat steps (2) to (7).

(H. Moulinec and P. Suquet, 1998)



Microstructure Representation and Discretization

- ❑ The input to the CPFFT simulator is pixelized image with orientation parameters associated with each pixel (or voxel for 3D).
- ❑ Regular grids with $N_1 \times N_2$ (for 2D) pixels or $N_1 \times N_2 \times N_3$ (for 3D) voxels are the discretization of the image (bitmap image).
- ❑ The i th coordinate component of real points (pixel or voxel) in real space:

$$x_i = 0, \frac{L_i}{N_i}, 2\frac{L_i}{N_i}, \dots, (N_i - 1)\frac{L_i}{N_i} \quad L_i: \text{length of the microstructure in the } i\text{th direction}$$

$$N_i: \text{Number of points in the } i\text{th direction}$$

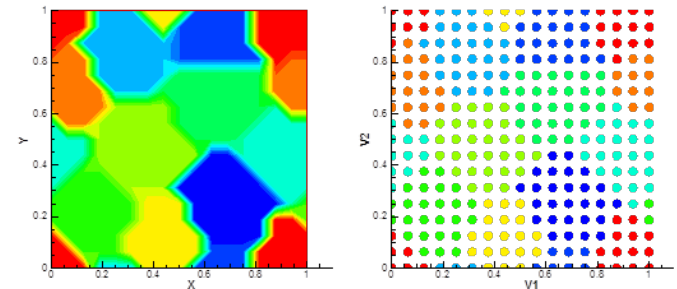
- ❑ The i th coordinate component of frequency points in Fourier space:

$$\xi_i^n = \left(-\frac{N_i}{2} + n \right) \frac{1}{L_i}, \quad n = 1, \dots, N_i \quad N_i: \text{even} \quad \xi_i^n = \left(-\frac{N_i + 1}{2} + n \right) \frac{1}{L_i}, \quad n = 1, \dots, N_i \quad N_i: \text{odd}$$

In order to take advantage of FFT, the point number in each direction should be taken to be the integer power of 2.

Input format

```
PT1: coord(1), coord(2), coord(3), orient(1), orient(2), orient(3)
PT2: coord(1), coord(2), coord(3), orient(1), orient(2), orient(3)
      ⋮
```



Geometric and Crystallographic Texture Evolution

- ❑ The material grid in the real space should be updated after deformation through:

$$\mathbf{x}_p(\mathbf{X}_p) = \mathbf{X}_p + (\mathbf{L} \cdot \mathbf{X}_p + \tilde{\mathbf{v}}(\mathbf{X}_p))dt$$

- ❑ The computational grid after deformation should stay regular:

$$\mathbf{x}_c(\mathbf{X}_c) = (\mathbf{I} + \mathbf{L}dt)\mathbf{X}_c$$

- ❑ For convenience, the deformed material grid is usually approximately assumed to be coincident with the regular computation grid (single-grid simplification):

$$\mathbf{x}_p = \mathbf{x}_c$$

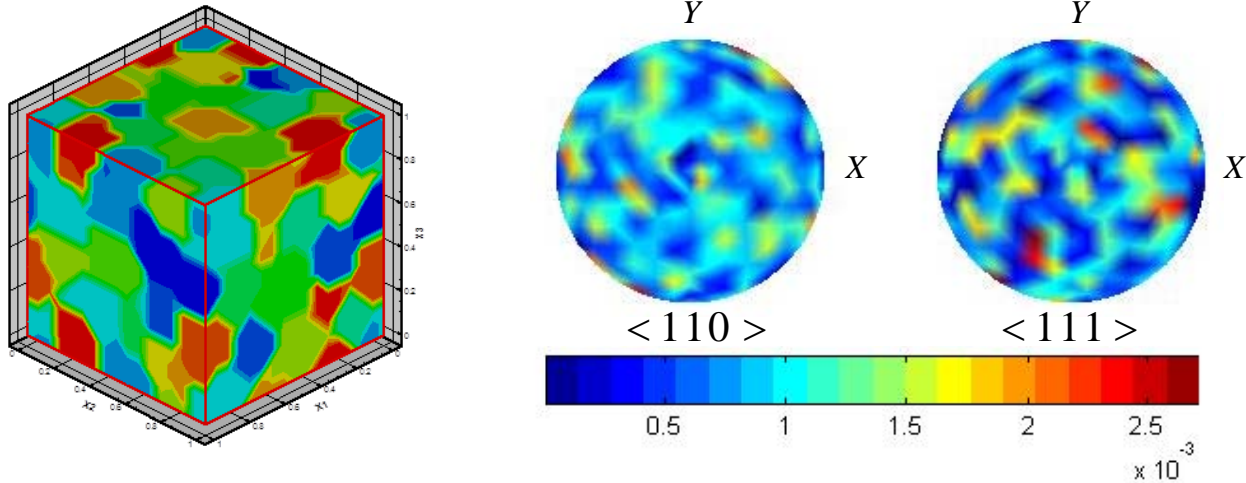
- ❑ The grain orientation is rotated according to the total spin tensor:

$$\boldsymbol{\omega}(\mathbf{x}) = \left[\dot{\boldsymbol{\Omega}} + \tilde{\boldsymbol{\omega}}(\mathbf{x}) - \dot{\boldsymbol{\omega}}^{slip}(\mathbf{x}) \right] dt \quad \dot{\boldsymbol{\omega}}^{slip}(\mathbf{x}) = \sum_{\alpha=1}^{N_s} \boldsymbol{\beta}^{\alpha}(\mathbf{x}) \dot{\gamma}^{\alpha}(\mathbf{x}), \quad \boldsymbol{\beta}^{\alpha}(\mathbf{x}) = \textit{antisym}(\mathbf{S}_0^{\alpha})$$



Plane Strain Example

- ❑ Example: A FCC aluminum microstructure containing 64 grains (with random orientation) discretized by 16x16x16 voxels for CPFET and 16x16x16 elements for CPFEM.
- ❑ Random initial texture.
- ❑ Elastic constants: C11=110GPa, C12=59GPa, and C44=26GPa.



- ❑ Material parameters: $\tau_0 = 47, \tau_1 = 86, \theta_0 = 550, \theta_1 = 16, \gamma_0 = 1$
- ❑ Applied velocity gradient: plane strain:

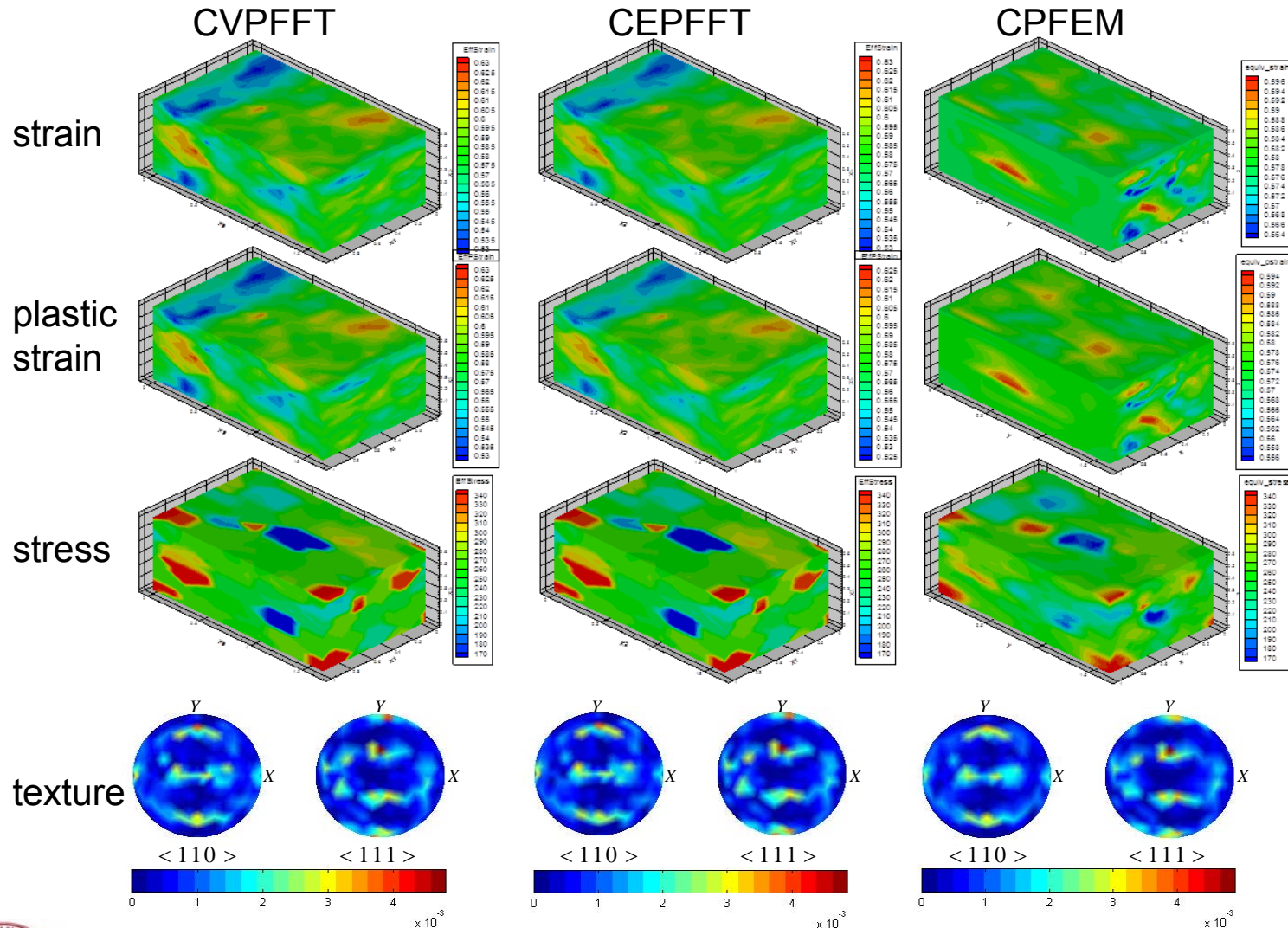
$$\mathbf{L} = \nabla \mathbf{V} = 10^{-3} \times \begin{bmatrix} 0 & 0 & 0 \\ 0 & 1 & 0 \\ 0 & 0 & -1 \end{bmatrix}$$

$$\mathbf{M}_s^p = \dot{\gamma}_0 \sum_{\alpha=1}^{N_s} \frac{\mathbf{m}^\alpha(\mathbf{x}) \otimes \mathbf{m}^\alpha(\mathbf{x})}{g^\alpha(\mathbf{x})} \left(\frac{|\mathbf{m}^\alpha(\mathbf{x}) : \boldsymbol{\sigma}(\mathbf{x})|}{g^\alpha(\mathbf{x})} \right)^{n-1}$$



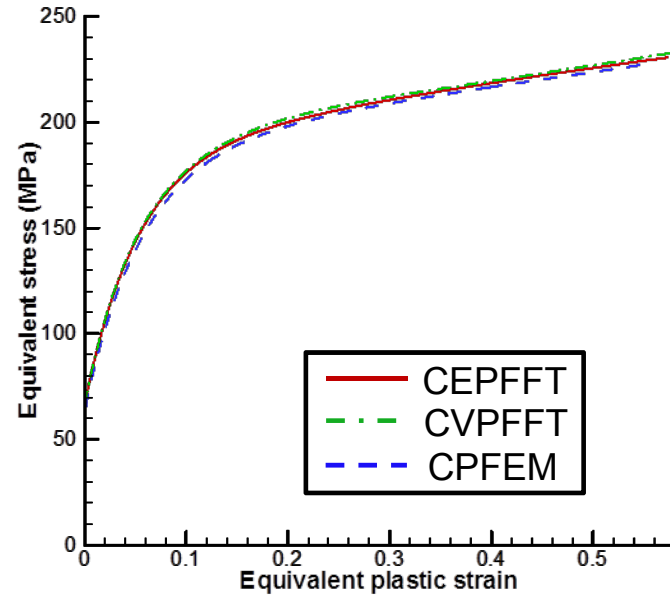
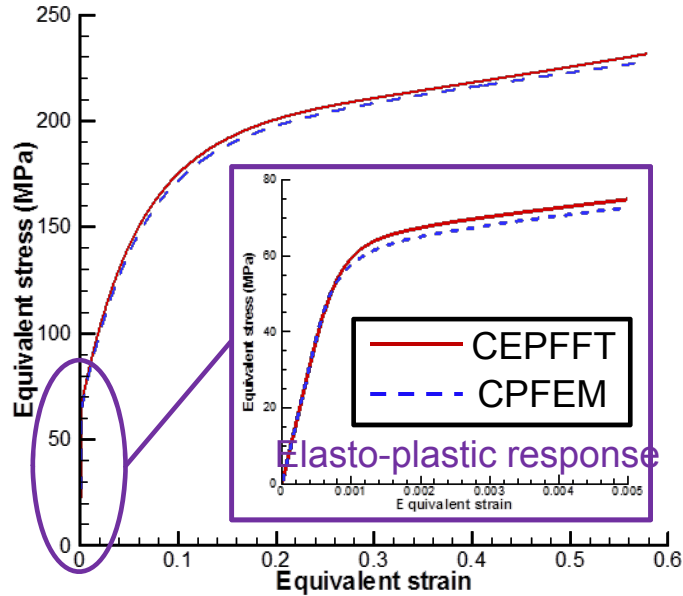
Micromechanical Response

- Strain, plastic strain, stress fields, and texture (single grid):



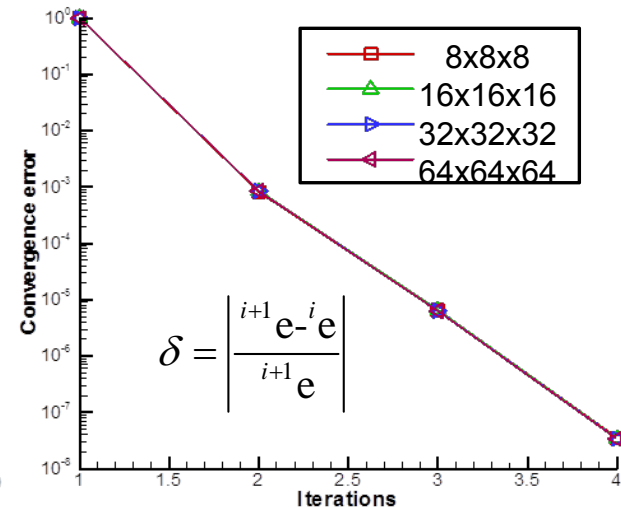
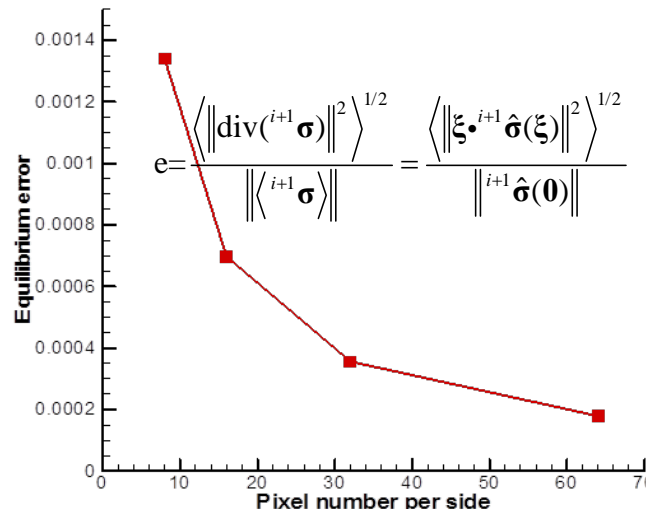
Homogenized Mechanical Response

□ effective stress – strain curve of the microstructure



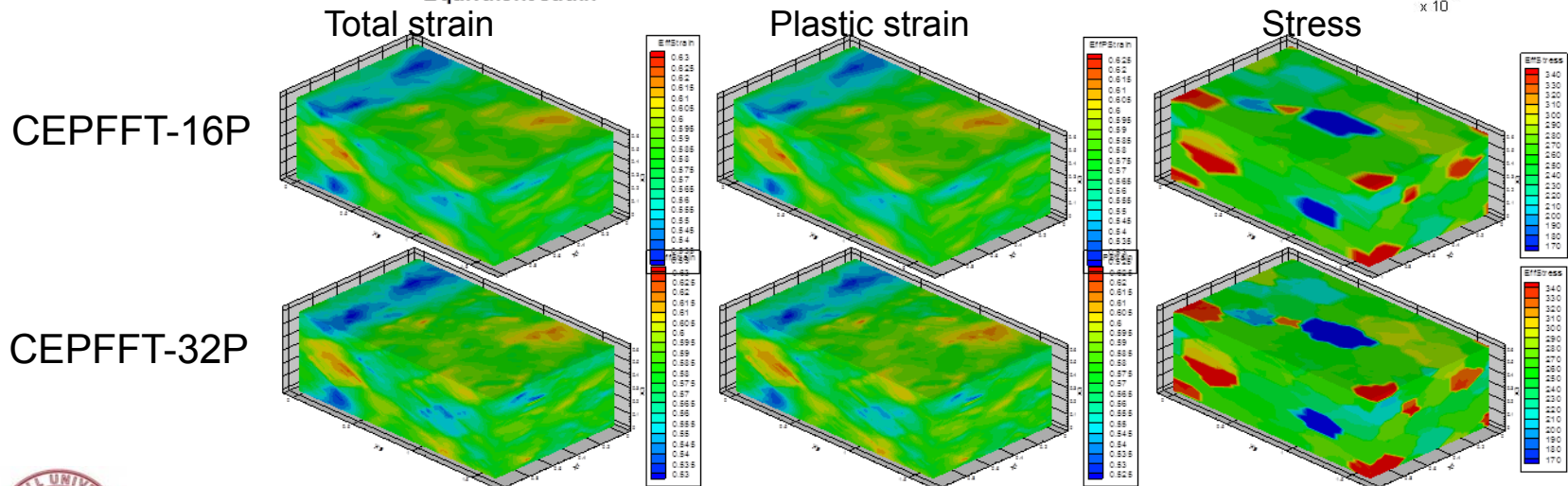
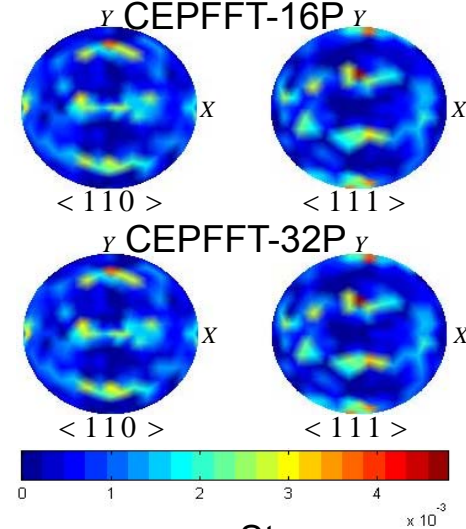
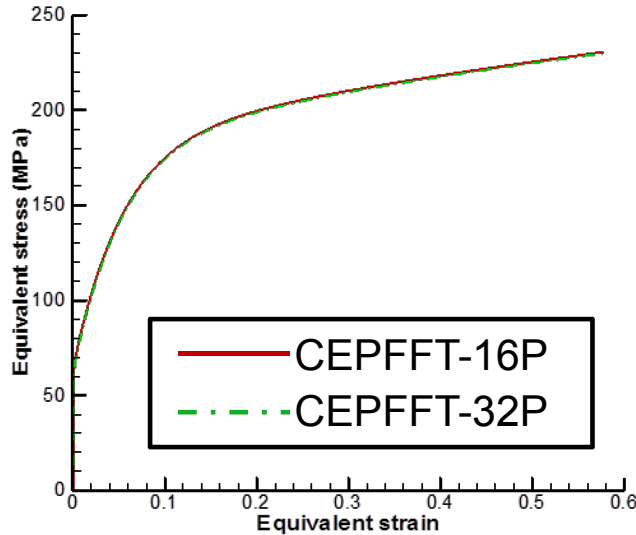
□ Error analysis

Pixel number per side	Equilibrium error
8	1.339737e-03
16	6.971389e-04
32	3.562514e-04
64	1.789642e-04



Convergence with Resolution

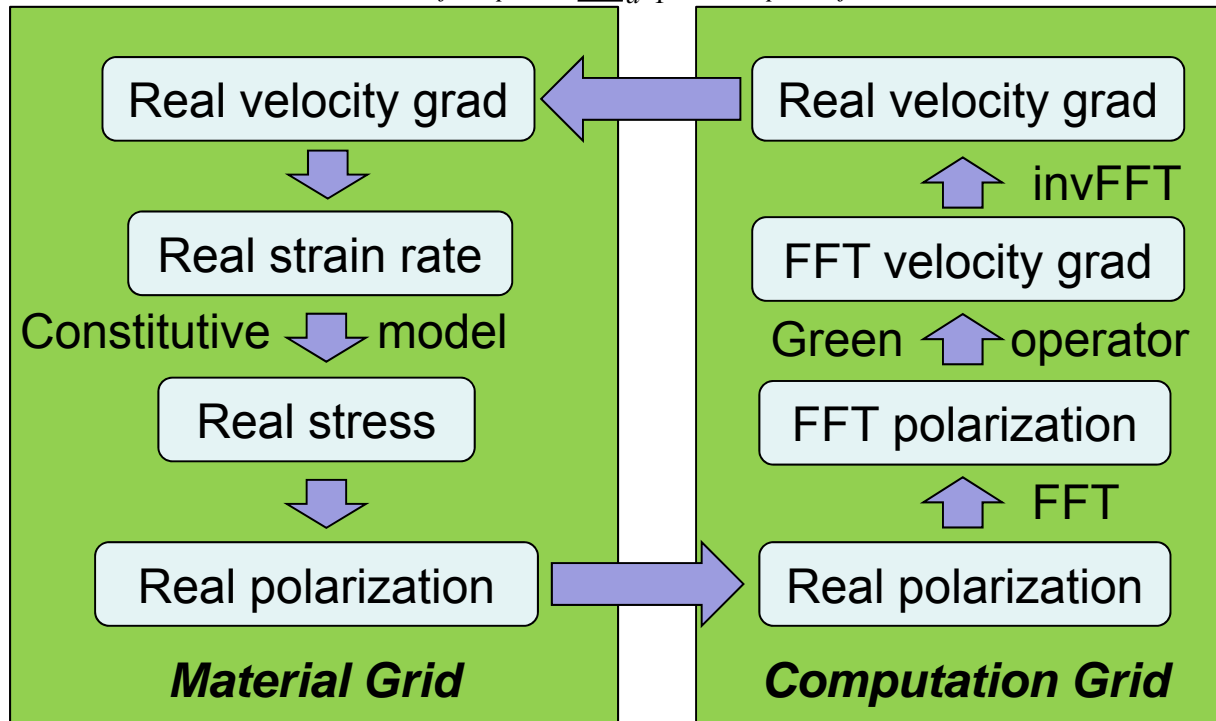
- An example of the same microstructure discretized by 32x32x32 voxels is also conducted to show the convergence with finer grid.



Multigrid Strategy

- ❑ The strain related fields are computed through FFT on computation grid.
- ❑ The stress related fields are updated according constitutive model on material grids.

$$v_{i,j}(\mathbf{x}_p) = \sum_{a=1}^A N^a(\mathbf{x}_p) v_{i,j}(\mathbf{x}_c^a)$$



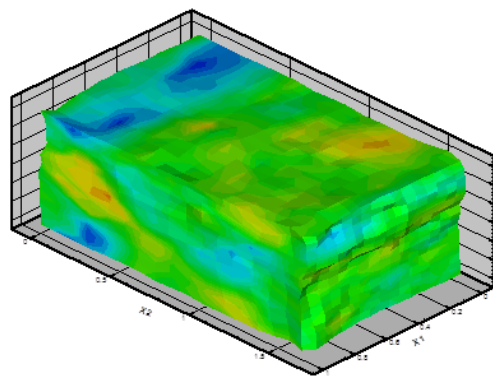
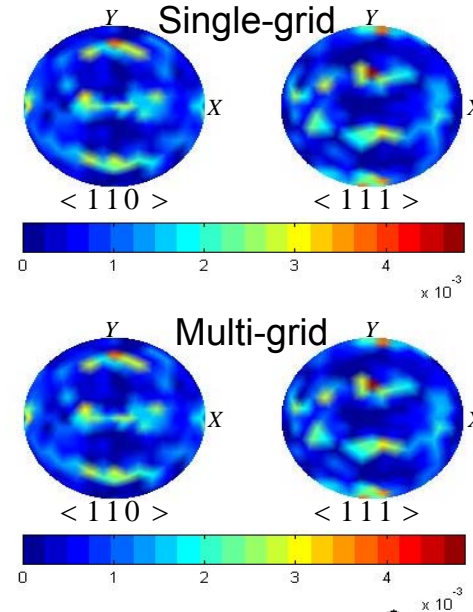
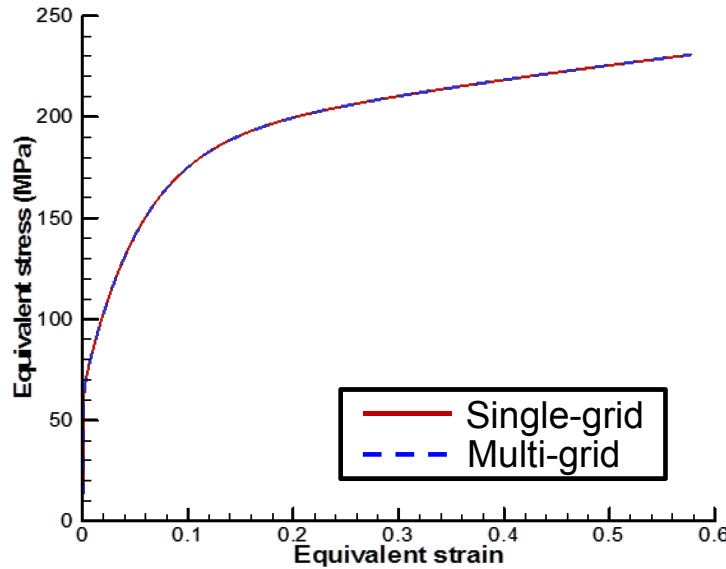
$$\phi_{ij}(\mathbf{x}_c) = \frac{1}{m(\mathbf{x}_c)} \sum_{k=1}^K m_p^k N^a(\mathbf{x}_p^k) \phi_{ij}(\mathbf{x}_p^k)$$

(N. Lahellec, J.C. Michel, H. Moulinec and P. Suquet, 2001)

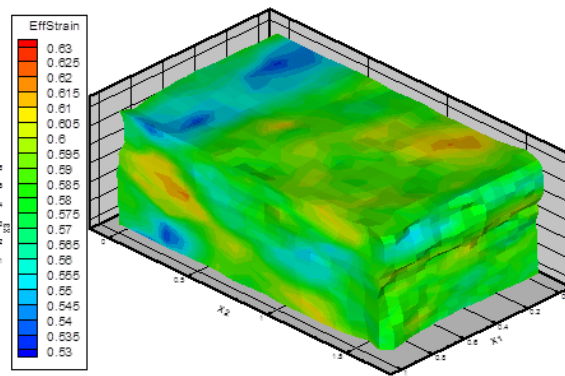


Mechanical Response and Texture

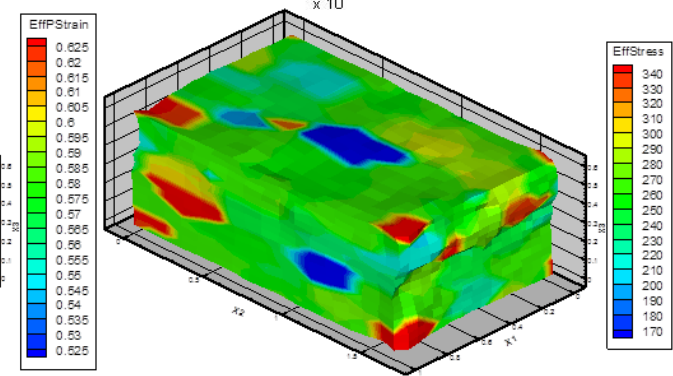
- Effective stress-strain response and orientation distribution predicted by CEPFFT.



Total strain



Plastic strain

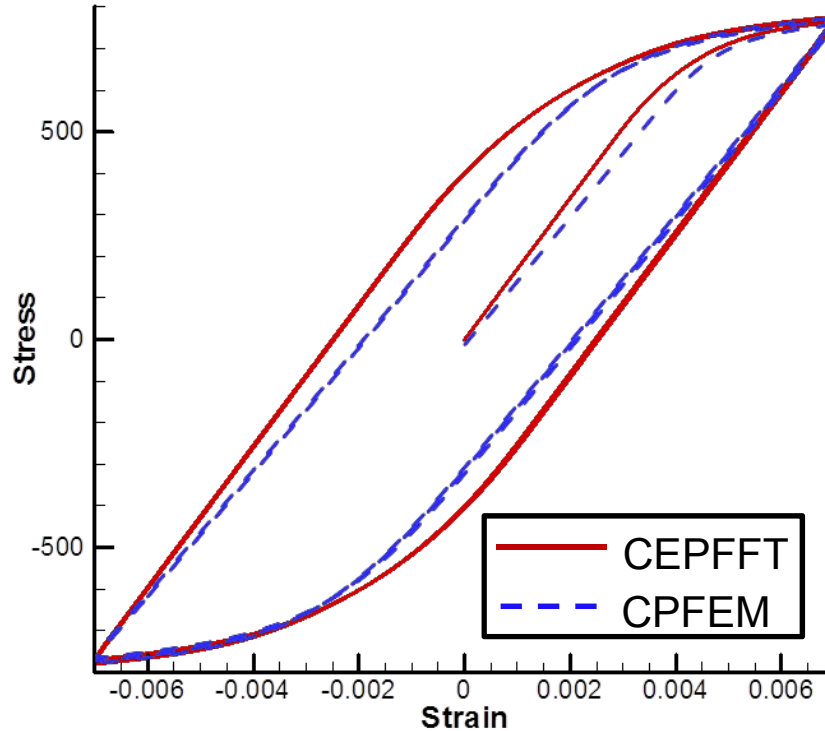


stress



A Fatigue Example

- Stress – strain response in the z-direction under cyclic loading.



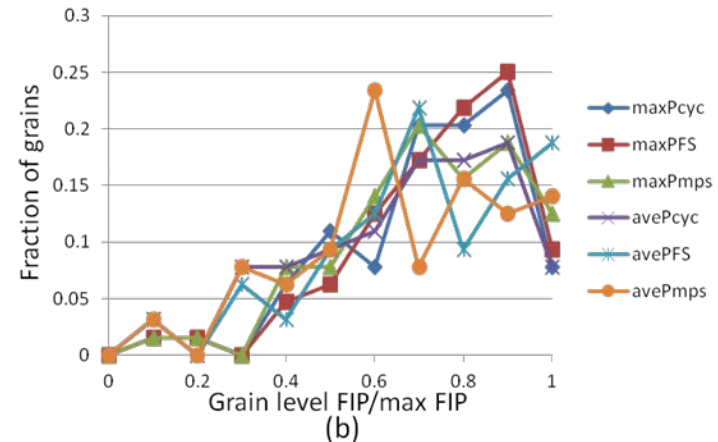
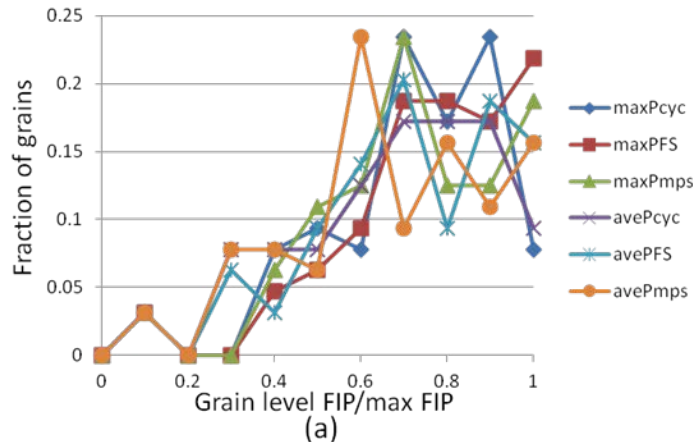
The same IN100 superalloy as used in the FIPs study.

$$\mathbf{M}_t^p = \sum_{\alpha}^{N_s} \mathbf{m}^{\alpha}(\mathbf{x}) \otimes \mathbf{m}^{\alpha}(\mathbf{x}) \left[\dot{\gamma}_1 \frac{n_1}{D_{\lambda}^{\alpha}} \left\langle \frac{|\tau_{\lambda}^{\alpha} - \chi_{\lambda}^{\alpha}| - g_{\lambda}^{\alpha}}{D_{\lambda}^{\alpha}} \right\rangle^{n_1-1} + \dot{\gamma}_2 \frac{n_2}{D_{\lambda}^{\alpha}} \left\langle \frac{|\tau_{\lambda}^{\alpha} - \chi_{\lambda}^{\alpha}|}{D_{\lambda}^{\alpha}} \right\rangle^{n_2-1} \right]$$



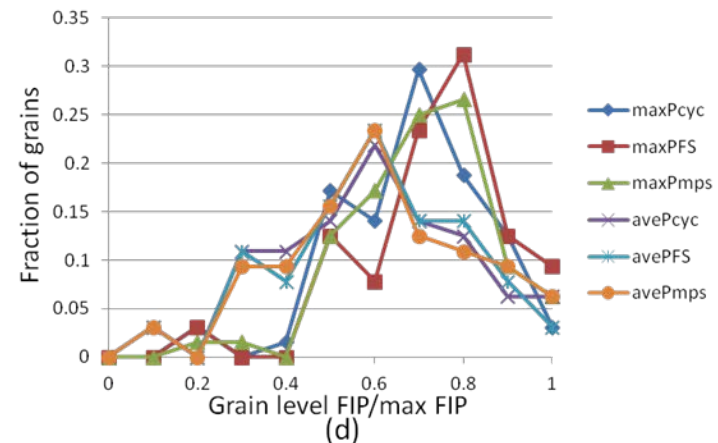
Distribution of Grain Level FIPs

- The distribution of FIPs among grains. maxP means the maximum FIP of an individual grain and aveP means the average value of the FIP in a grain.



(a) CEPFFT, 16x16x16 voxels
(b) CEPFFT, 32x32x32 voxels
(d) CPFEM, 16x16x16 elements

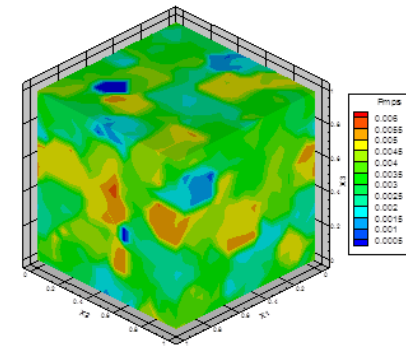
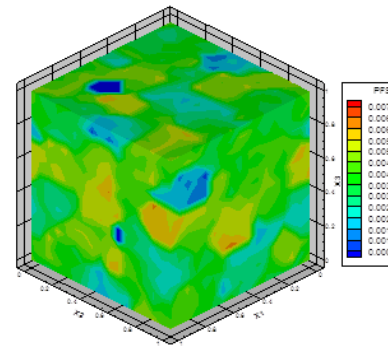
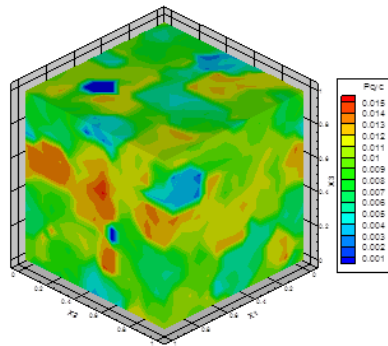
The FIPs predicted by CEPFFT are more spread than CPFEM.



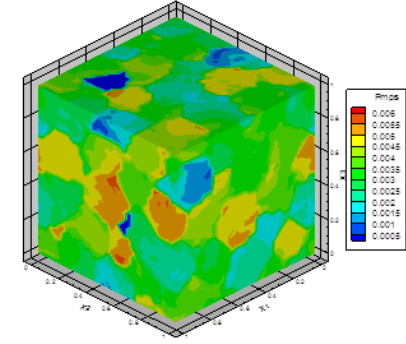
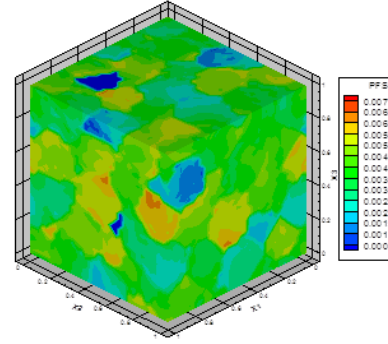
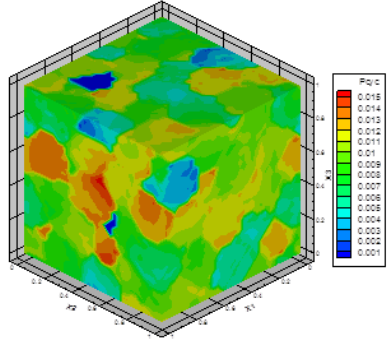
Fields of FIPs

- Contour plots of FIPs over the microstructure.

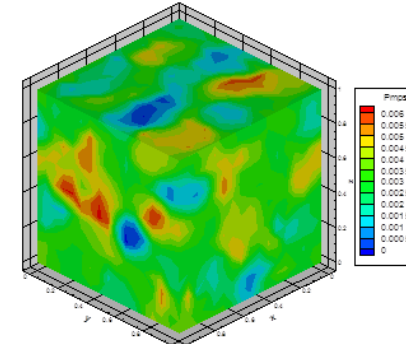
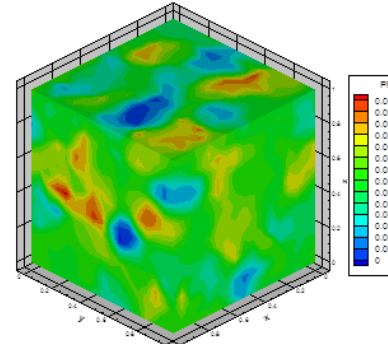
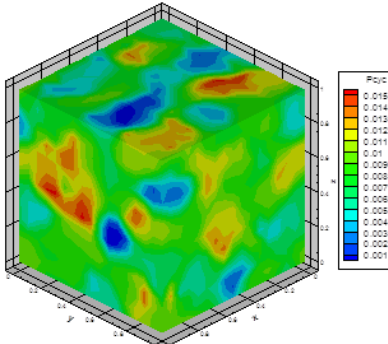
CEPFFT 16P



CEPFFT 32P



CPFEM 16E



Pqc

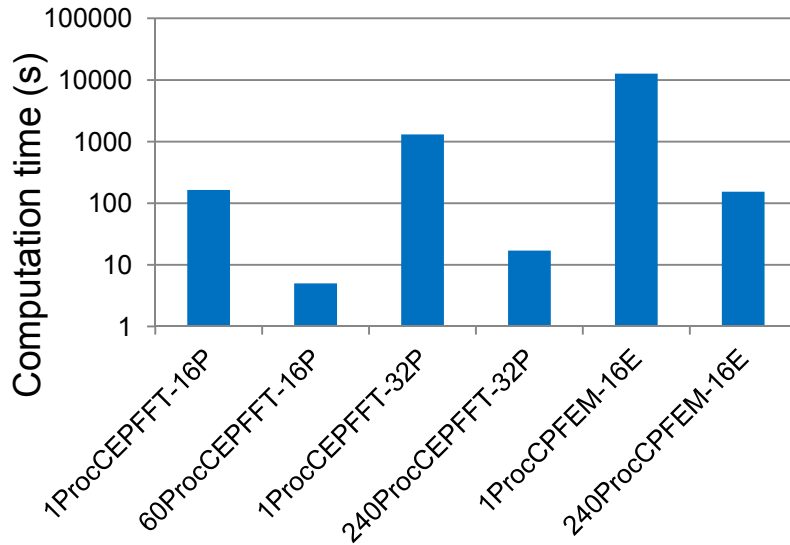
PFS

Pmps

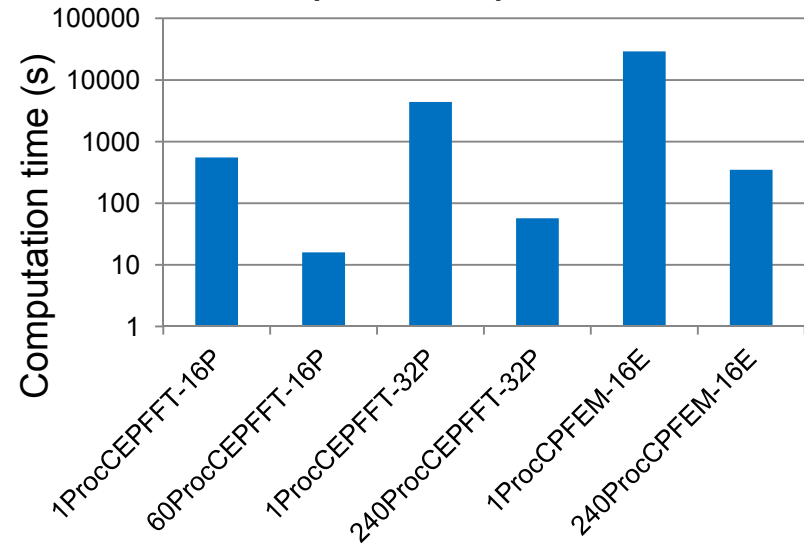


Computation Efficiency

Plane strain:
Strain=0.1, $\delta < 10^{-4}$



Fatigue:
1 complete loop, $\delta < 10^{-4}$



1-Processor, CEPFFT, 16x16x16-Pixel	60-Processors, CEPFFT, 16x16x16-Pixel	1-Processor, CEPFFT, 32x32x32Pixel	240-Processor, CEPFFT, 32x32x32Pixel	1-Processor, CPFEM, 16x16x16Element	240-Processor, CPFEM, 16x16x16Element
164	5	1309	17	12687	154
554	16	4385	57	29026	348



Outline

- ❑ Introduction and motivation
- ❑ Uncertainty quantification at a single material point
 - Investigating mechanical response variability of single-phase polycrystalline microstructures
 - Investigating variability of fatigue indicator parameters of two-phase nickel-based superalloy microstructures
- ❑ Uncertainty quantification of multiscale deformation process
- ❑ An efficient image-based method for modeling the elasto-viscoplastic behavior of realistic polycrystalline microstructures
- ❑ Conclusion and future research

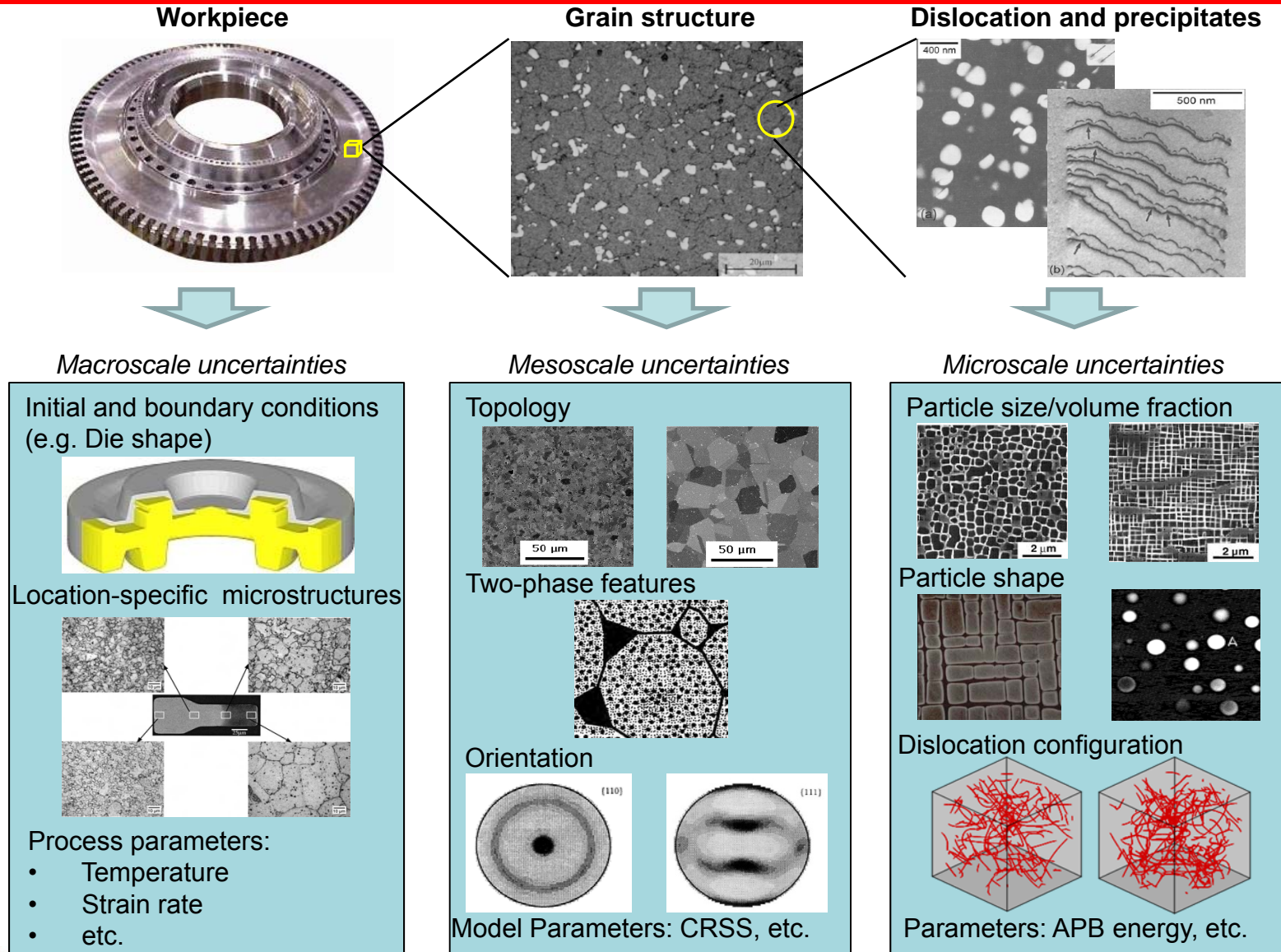


Conclusion

- ❑ Model reduction tools are developed to build the stochastic input based on a given dataset of random microstructures.
- ❑ Physics-based deterministic simulators are developed to evaluate material properties/responses according to underlying microstructures.
- ❑ Variability of material properties/responses induced by microstructure variation is studied. The uncertainty quantification is performed for microstructures at a single material point and for an entire workpiece, respectively.

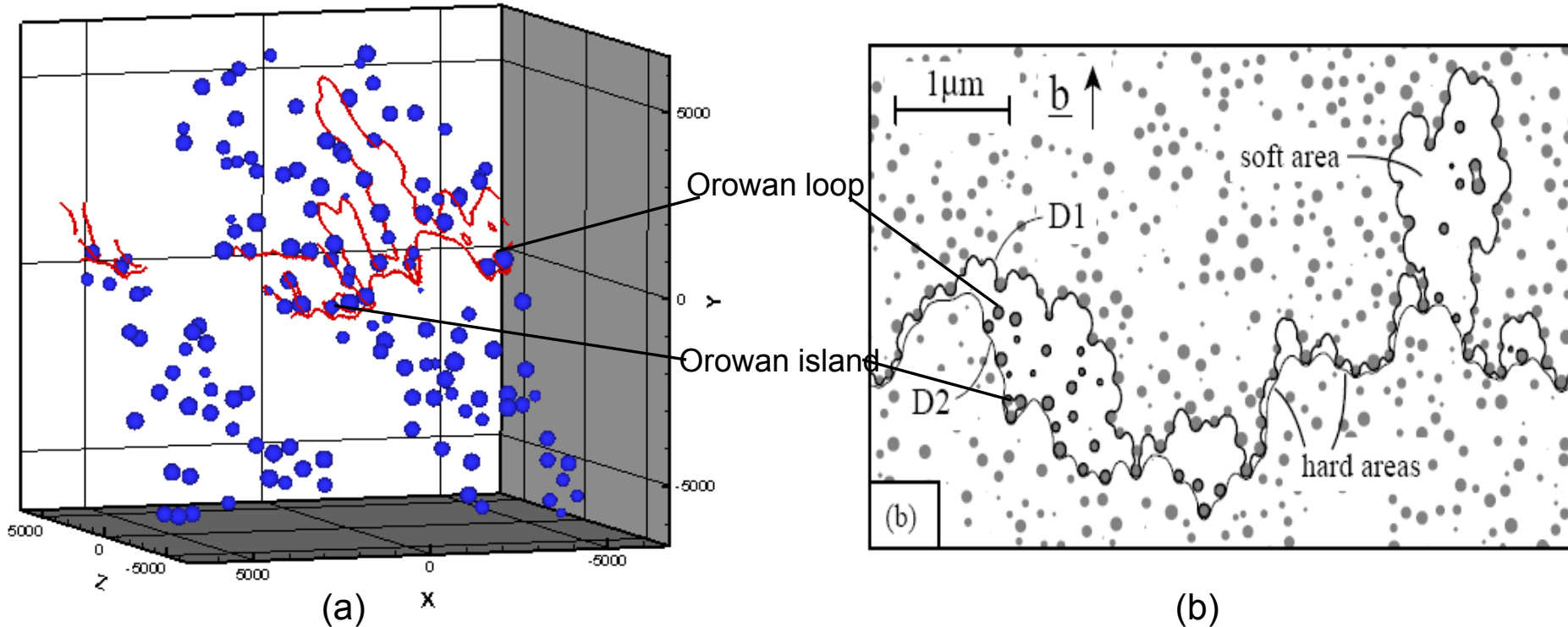


Multiscale Modeling of Superalloy Systems



Discrete Dislocation Dynamics in Superalloys

$r_m=200b$, APB energy density=200 mJ/m², volume fraction =10%.



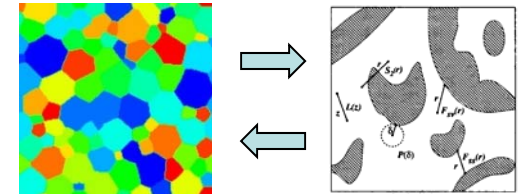
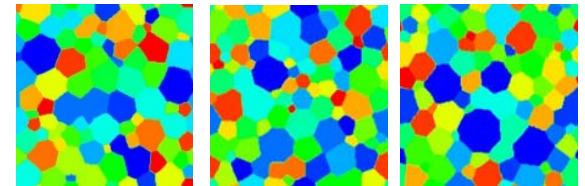
Dislocations in the nickel-base superalloy containing large particles. (a) Simulated dislocation configuration interacting with precipitates having large radius ($200b$) in current 3D DD framework. (b) Simulated dislocation configuration in 2D DD framework (Mohles, 2004).

Future focus: massive dislocation dynamics in precipitation hardened alloys.
Multiscale linking.



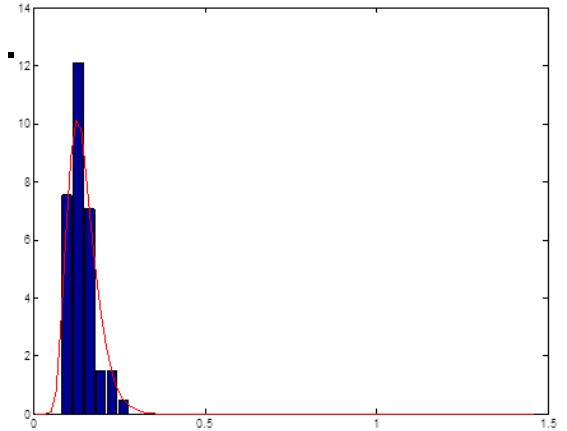
Uncertainty Quantification with Realistic Polycrystalline Microstructures

- ❑ Introduce realistic polycrystalline microstructures into uncertainty quantification.
- ❑ Provide more reliable prediction to material properties.
- ❑ Account for higher order spatial correlation of the microstructure.
- ❑ Efficient physics-based deterministic solver: CEPFFT.
- ❑ Stochastic microstructure input:
 - Pixelized models
 - Dimensionality depends on resolution
 - Need preprocessing on input data
 - Sampling of new samples
 - Statistical features
 - Physical constraints
 - Microstructure reconstruction

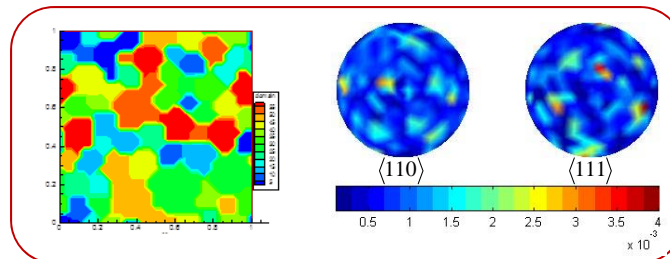


A Preliminary Example

- ❑ Grain size distribution: Lognormal distribution.
 - Mean grain size (diameter) = 0.1457
 - Standard deviation = 0.0437
 - Grain number = 60
 - Assume spherical/round grains
- ❑ Random crystallographic texture generation.



32x32 pixels



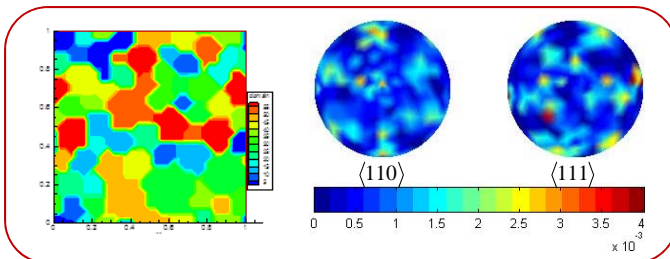
$t=300s$

$$\alpha_1, \alpha_2, \alpha_3 \sim U(-0.001, 0.001)$$

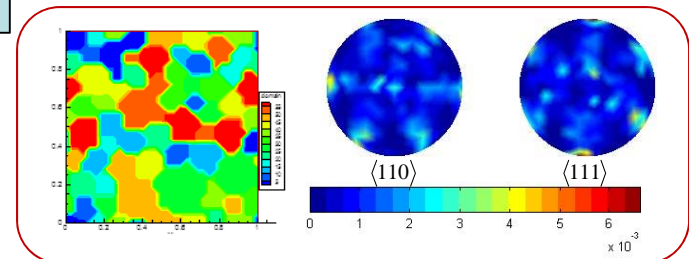
Deterministic solver:
CEPFFT

Random
deformation
process

$$\mathbf{L} = \alpha_1 \begin{bmatrix} 1 & 0 & 0 \\ 0 & -1 & 0 \\ 0 & 0 & 0 \end{bmatrix} + \alpha_2 \begin{bmatrix} 0 & 1 & 0 \\ 1 & 0 & 0 \\ 0 & 0 & 0 \end{bmatrix} + \alpha_3 \begin{bmatrix} 0 & 1 & 0 \\ -1 & 0 & 0 \\ 0 & 0 & 0 \end{bmatrix}$$



• • •



500 samples



Mixture of PPCA

- ❑ The mixture of PPCA (MoPPCA) is a combination of local PPCAs for the data that is approximately piece-wise linear.
- ❑ Two steps (the two steps are interactive):
 - A partition of data into classes.
 - Fitting local PPCA models within each class.
- ❑ The overall model distribution: $p(\mathbf{y}) = \sum_{j=1}^M \pi_j p(\mathbf{y} | j)$
- ❑ Local PPCA model: The data \mathbf{y} is generated by a linear combination of latent variables \mathbf{z} :
$$\mathbf{y} = \mathbf{W}\mathbf{z} + \boldsymbol{\mu} + \boldsymbol{\varepsilon}$$

$$\mathbf{z} \sim N(\mathbf{0}, \mathbf{I}) \quad \boldsymbol{\mu}: \text{mean of the data model} \quad \boldsymbol{\varepsilon} \sim N(\mathbf{0}, \sigma^2 \mathbf{I})$$

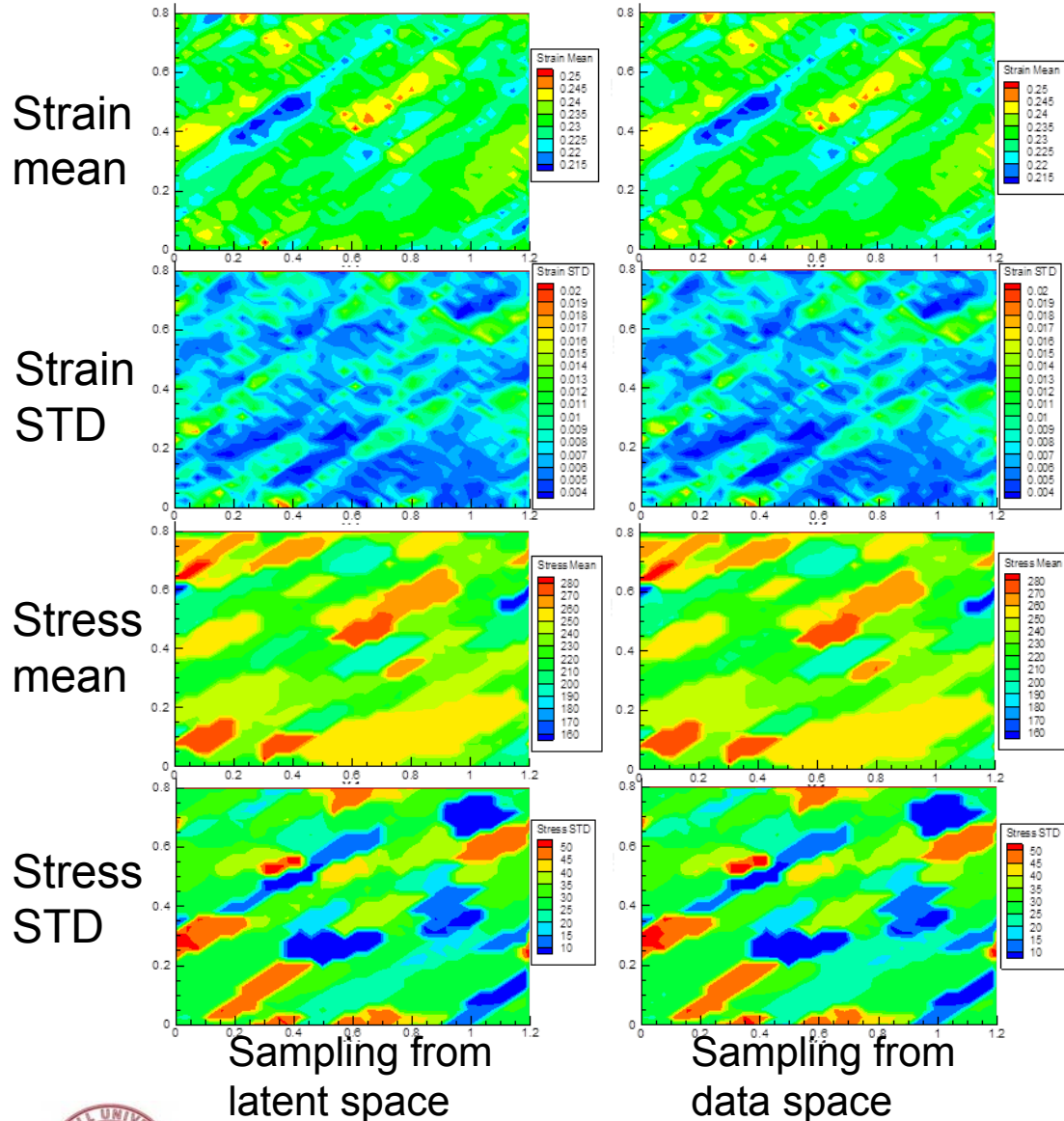
- ❑ An iterative EM algorithm can be designed to find the optimization of all model parameters:

$$\pi_j, \boldsymbol{\mu}_j, \mathbf{W}_j, \sigma_j^2$$

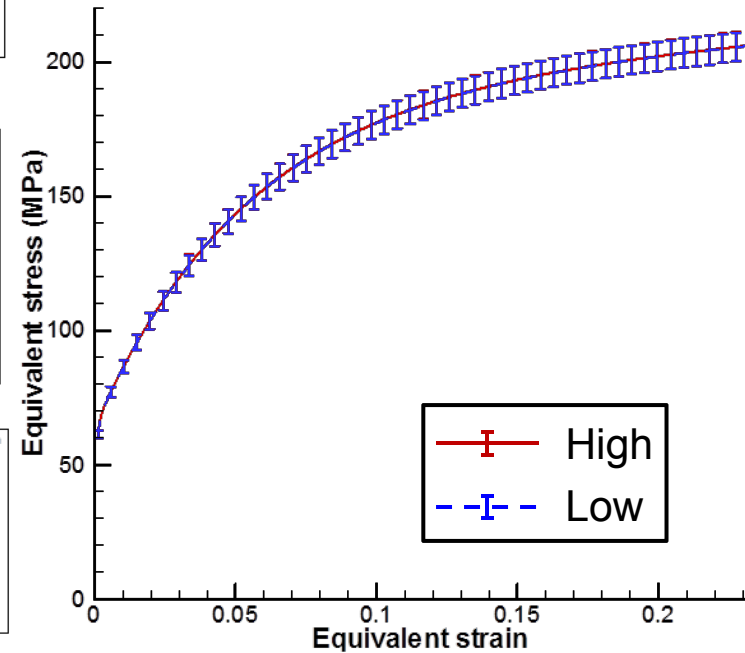
- Generation of new sample \mathbf{y} requires the random choice of a local model according to π_j , followed by sampling as in single PPCA.
- Two ways to generate new data samples in PPCA:
 - Generate from the marginal distribution of data \mathbf{y} directly:
$$p(\mathbf{y}) = N(\mathbf{y} | \boldsymbol{\mu}_{ML}, \mathbf{C}_{ML}) \quad \text{Sampling from high-dimensional data space}$$
 - Generate from both the distribution of latent variable \mathbf{z} and noise $\boldsymbol{\varepsilon}$:
$$p(\mathbf{z}) = N(\mathbf{z} | \mathbf{0}, \mathbf{I}) \quad p(\boldsymbol{\varepsilon}) = N(\mathbf{0}, \sigma_{ML}^2 \mathbf{I}) \quad \text{Sampling from low-dimensional latent space}$$
- Determination of intrinsic dimension: Maximum likelihood estimation.



Variability of Mechanical Responses



Equivalent stress-strain response with error bars.

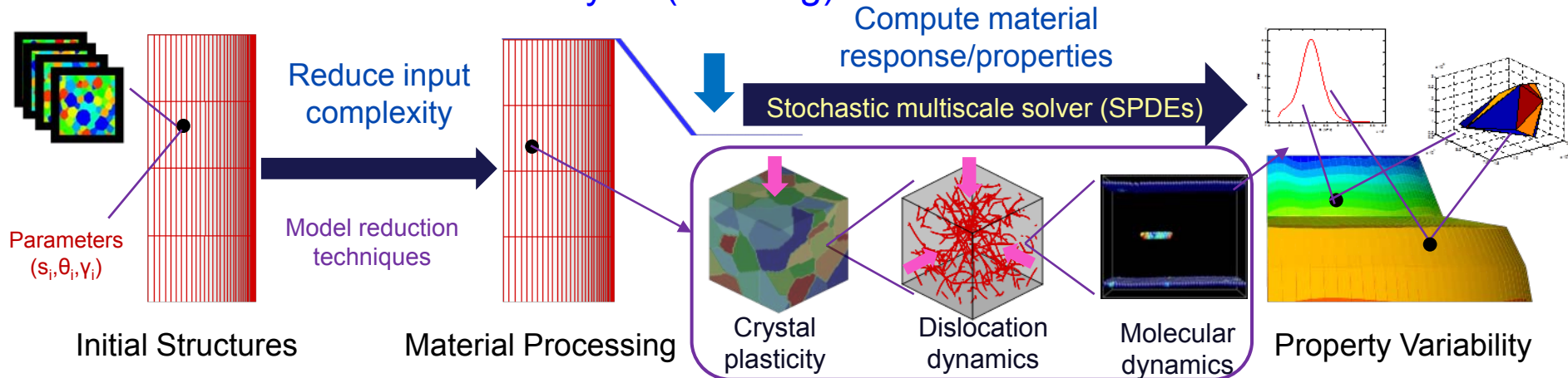


- The number of PPCA components is chosen to be 3.
- The ML estimation of the dimension of the latent space is 3.



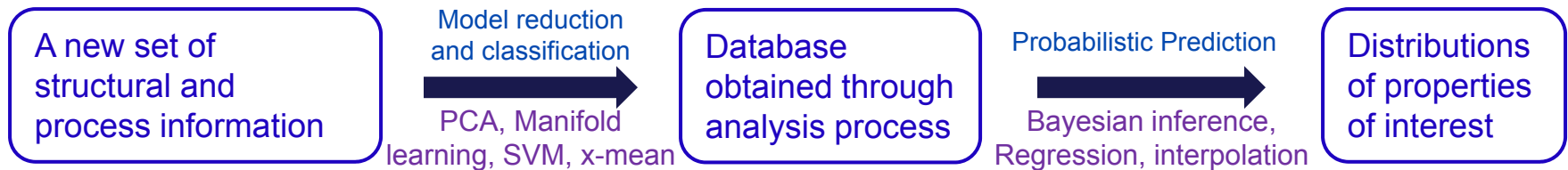
Advanced Methodology, Property Prediction & Material Design

Stochastic Multiscale Analysis (Training):

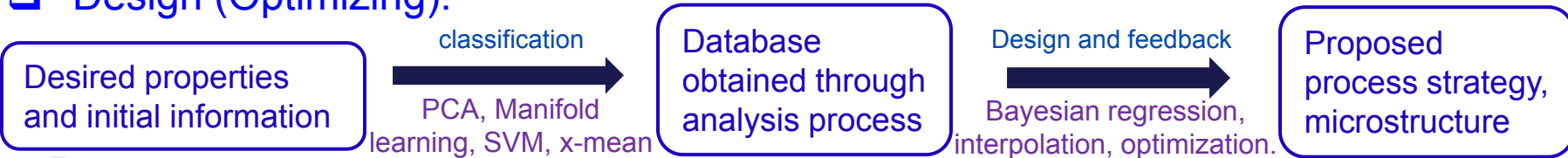


SPDE solver: Bayesian regression, HDMR+ASGC.

Prediction:



Design (Optimizing):



Publications

- ❑ Zheng Li, Bin Wen and N. Zabaras, "Computing mechanical response variability of polycrystalline microstructures through dimensionality reduction techniques", Computational Materials Science, Vol. 49, Issue 3, pp. 568-581, 2010.
- ❑ Bin Wen, Zheng Li and N. Zabaras, "Thermal response variability of random polycrystalline microstructures", Communications in Computational Physics, Vol. 10, No. 3, pp. 607-634, 2011.
- ❑ Bin Wen and N. Zabaras, "Investigating Variability of Fatigue Indicator Parameters of Two-phase Nickel-based Superalloy Microstructures", Computational Materials Science, 51 (1), pp. 455-481, 2012.
- ❑ Bin Wen and N. Zabaras, "A Multiscale Approach for Model Reduction of Random Microstructures", Computational Materials Science, Vol. 63, pp. 269-285, 2012.
- ❑ Bin Wen and N. Zabaras, "An image-based method for modeling the elasto-viscoplastic behavior of polycrystalline microstructures using the Fast Fourier Transform", Int Journal of Plasticity, under review.



Conference Presentations

- ❑ Bin Wen and Nicholas Zabaras, "Grain-size effect in 3D polycrystalline microstructure including texture evolution", 10th U.S. National Congress in Computational Mechanics, Columbus, OH, July 16-19, 2009.
- ❑ Bin Wen and Nicholas Zabaras, "Stochastic Multiscale Modeling of Two-Phase Superalloys for the Design of Engine Disks", NSF-CMMI, 2011 NSF Engineering Research and Innovation Conference, Atlanta, GA, January 4-7, 2011.
- ❑ Nicholas Zabaras and Bin Wen, "On the design of polycrystalline materials with an integration of multiscale modeling and statistical learning", NSF-CMMI, 2011 NSF Engineering Research and Innovation Conference, Atlanta, GA, January 4-7, 2011.
- ❑ Bin Wen and Nicholas Zabaras, "Uncertainty Quantification in Multiscale Deformation Processes", the 11th U.S. National Congress on Computational Mechanics, Minneapolis, MN, July 25-29, 2011.
- ❑ Bin Wen and Nicholas Zabaras, "Computing fatigue properties of polycrystalline Ni-based superalloy microstructures using an image-based computational approach", 1st International Conference on 3D Materials Science, Seven Springs Mountain Resort, Seven Springs, Pennsylvania, July 8-12, 2012.
- ❑ Nicholas Zabaras and Bin Wen, "Model Reduction and Reconstruction of Realistic Microstructures for Computing Property Variability", 1st International Conference on 3D Materials Science, Seven Springs Mountain Resort, Seven Springs, Pennsylvania, July 8-12, 2012.



Acknowledgement

- ❑ Special Committee:
 - Prof. Nicholas Zabaras, MAE, Cornell University
 - Prof. Christopher Earls, CEE, Cornell University
 - Prof. Derek Warner, CEE, Cornell University

- ❑ Funding Sources:
 - Air Force of Scientific Research (AFOSR)
 - National Science Foundation (NSF)
 - Office of Naval Research (ONR)
 - Sibley School of Mechanical & Aerospace Engineering

- ❑ Materials Process Design and Control Laboratory



Thank you very much!

